



Development of an Integrated Thermal Hydrolysis Process - Anaerobic Digestion (THPAD) Model

Prepared by:

Alexander Olando

Supervised by:

A/Prof. David Ikumi

Co-Supervised by:

Dr. Chris Gaszynski

Dissertation submitted in fulfilment of the requirements for the degree of
"MSc in Civil Engineering specializing in Water Quality"

Department of Civil Engineering
University of Cape Town, Private Bag Rondebosch, 7700
South Africa 7700

The copyright of this thesis vests in the author. No quotation from it or information derived from it is to be published without full acknowledgement of the source. The thesis is to be used for private study or non-commercial research purposes only.

Published by the University of Cape Town (UCT) in terms of the non-exclusive license granted to UCT by the author.

PLAGIARISM DECLARATION

1. I know the meaning of plagiarism and declare that all the work in the document, save for that which is properly acknowledged, is my own.
2. This thesis/dissertation has been submitted to the Turnitin module (or equivalent similarity and originality checking software) and I confirm that my supervisor has seen my report and any concerns revealed by such have been resolved with my supervisor
3. I have used the Harvard Convention for citation and referencing. Each significant contribution to and quotation in this report from the work or works of other people has been attributed and has been cited and referenced.
4. I have not allowed and will not allow anyone to copy my work with the intention of passing it as his or her own Work.

Signed:

Signed by candidate

Date: 8th February 2022

ABSTRACT

Historically, anaerobic digestion is one of the most common processes used to treat sludge generated from wastewater treatment plant (WWTP) processes. However, with the exponential increase in populations, which implies an increase in WWTP loads, the amount of waste generated poses an imminent problem to the handling capacity of current anaerobic digesters. Subsequently, there has been a lot of research into various physical and chemical processes that would allow for a more efficient sludge handling mechanism. Studies have reported various advantages associated with digesting sludge at higher temperatures known as thermophilic temperatures. These advantages include increased sludge handling capacity, a higher degree of sludge biodegradability and subsequently increased methane production and better sludge dewatering characteristics implying cheaper sludge transportation costs just to mention a few. However, despite the advantages associated with thermal treatment, this technology has not yet been proven in a South African context.

This project involved the development of an integrated thermal hydrolysis process (THP) and anaerobic digestion (AD) model capable of simulating these processes at elevated temperatures. A comparative desktop case study of the existing AD facility at the Cape Flats wastewater treatment works (CFWWTW) in Western Cape, South Africa was investigated following the City of Cape Town's (CCT) initiative to retrofit a THP unit to the anaerobic digesters to help deal with the increase in sludge handling capacity. A comparison was therefore carried out, investigating the base case scenario of maintaining the existing conventional mesophilic anaerobic digesters (MAD) and retrofitting a THP unit to the conventional anaerobic digesters (THPAD).

A steady-state THP and AD model was developed and used in conjunction with an integrated dynamic THP and modified AD (termed as the Extended-UCTSDM3P) model for simulating both the conventional MAD and THPAD processes. This allowed for a comparison of results not only between the two processes, but also the two types of models.

These models were then used to simulate the treatment of a mixture of primary sludge (PS) and waste activated sludge (WAS) at a ratio of 60:40 with the WAS obtained from a Nitrification-Denitrification Biological Excess Phosphorus Removal (NDBEPR) activated sludge treatment. The AD models, therefore, accounted for the increased phosphorus concentration as a result of

polyphosphates (PP) breakdown and consequently the possible precipitation of struvite (MgNH_4PO_4) from the AD liquor.

The results showed that the THPAD configuration allowed the digesters to process 2.3 times more sludge than with the conventional mesophilic anaerobic digesters. Furthermore, the methane production in the THPAD was conservatively calculated to be 2.5 times higher than the MAD. This implied an increased potential for use of the methane gas as an alternative source of energy in the wastewater treatment plants.

Given that no laboratory experiments were carried out, the results were based on theoretical scenarios and knowledge collected from an extensive literature review. However, given the capacity, flexibility and detail the model has been developed to, different scenarios in the anaerobic digestion process can be investigated and valuable practical insight extracted. Furthermore, through calibration with accurate meaningful data from a pilot or full-scale plant, the developed model is a tool that could be used in predicting digester performance.

ACKNOWLEDGEMENTS

God Almighty – All praise is due to the most High for carrying me through this trying period and giving me the energy and hope to see this project through. Without Him none of this would be possible.

A/Prof. David Ikumi – Many thanks for all the help and assistance in all its forms that you provided to me. You were always available whenever I needed assistance with areas and concepts that I struggled to grasp. Working with you on this project has been an absolute honour. May you stay blessed.

Dr. Chris Gaszynski – Thank you so much for all the support and advice that you afforded me during this entire journey. Thank you specifically for all the help with understanding and developing the THP model. Your assistance was really appreciated. Working with you was an honour. May you stay blessed.

Chris Brouckaert – Thank you for your assistance, advice, and input especially when working on the WEST® model

My parents Gordon and Jayne Olando – Thank you so much for the numerous sacrifices that I know you have both made, so that I may get a quality education. I could not have asked God for more supportive, understanding, and loving parents. May you continue to be blessed abundantly.

My sisters Adah and Abigail Olando – You are both my inspiration. Thank you for being the kind, supportive and positive energies that you are.

My late brother George Olando – Still making you proud Ikomo.

All my supportive friends – This project was not accomplished on my own. Thank you to my friends who opened their hearts and houses to me. Many thanks to Andrew, Rhonda, Chawezi, Edward, Marion, Tondani and Cungu. I am eternally grateful to you lot for all the support you gave me. None of it was taken for granted.

Table of Contents

Plagiarism Declaration.....	ii
Abstract	iii
Acknowledgements.....	v
1 Introduction	1
1.1 Background	1
1.2 Research problem	2
1.3 Research Questions.....	3
1.4 Objectives	3
1.5 Project Scope and Limitations	4
1.6 Overview of report	4
2 Literature Review	6
2.1 Anaerobic Digestion process	6
2.1.1 Hydrolysis	7
2.1.2 Acidogenesis	10
2.1.3 Acetogenesis.....	11
2.1.4 Methanogenesis	11
2.2 Anaerobic Digestion Treatment systems	12
2.2.1 Conventional Mesophilic Anaerobic Digester (MAD) system	12
2.2.2 Thermal Hydrolysis Process (THP) System	13
2.2.3 Thermophilic Anaerobic Digestion (TAD) System.....	16
2.3 History of Anaerobic Digestion Modelling	18
2.3.1 Introduction	18
2.3.2 ADM1 Model	18
2.3.3 UCTADM1 Model	19
2.3.4 UCTSDM3P Model.....	20
2.3.5 THPAD and TAD modelling	21
2.4 Closure.....	24
3 Development of the THPAD model	26
3.1 Plant Layout and Model Setup	27
3.1.1 Cape Flats Wastewater Treatment Works (CFWWTW) Plant Layout.....	27
3.1.2 Model Setup	30

3.1.3	Feed.....	31
3.2	Steady State AD Model	36
3.2.1	Component Characterization and Elemental Composition	37
3.2.2	Stoichiometric Model for the Steady State AD	38
3.2.3	Weak Acid/Base Chemistry	39
3.3	Dynamic Extended UCTSDM3P model	44
3.3.1	Model description of the Extended-UCTSDM3P	45
3.3.2	PWM_SA Physico-Chemical Model Framework	46
3.3.3	Ionic Speciation Routine.....	47
3.3.4	Processes	49
3.4	THP Model	52
3.4.1	Pasteurization	54
3.4.2	Activation	57
3.4.3	Solubilization	58
3.5	Analytical Procedures.....	62
3.6	Model evaluation	63
3.7	Closure.....	64
4	Results and Discussions	65
4.1	Influent Composition	65
4.2	THP Model Results	66
4.3	AD Model Results.....	69
4.3.1	Nutrient removal (and Methane Production)	69
5	Conclusions and Recommendations	74
6	References	76
7	Appendix	83
7.1	Influent Component Composition	83
7.2	Mass Balance Verification Spreadsheets	90
THP Model Verification.....		90
Extended-UCTSDM3P Model Verification		90
7.3	Dynamic Model Description	94
Terminology		94

List of Figures

Figure 1.1: A mind map showing an overview of the project report, including the main components of each chapter and their respective associations with each other	5
Figure 2.1: Diagram showing the phases of the Anaerobic Digestion process	7
Figure 3.1: Flow diagram of Cape Flats WWTW (adapted from Google Earth) : 1) influent / raw wastewater, 2 and 3) effluent of primary clarification, 4-7) effluent of secondary clarification, 8-15) outflow of activated sludge section, 16) underflow of primary clarification, 17) underflow of primary sludge thickener, 18) overflow of secondary sludge dissolved air flotation unit, 19) influent of anaerobic digestion, 20-22) effluent of anaerobic digestion, 23) mechanical dewatering overflow (non-active), 24) mechanical dewatering underflow to sludge drying beds, 24) sludge to disposal and 25) reject water to pond (Flores-Alsina et al., 2021)	28
.....	29
Figure 3.2: Conventional AD schematic (Potts, 2021)	29
Figure 3.3: THPAD schematic (Potts, 2021)	29
Table 3.1: Cape Flats Wastewater Treatment Works Anaerobic Digester Operating Parameters	30
Figure 3.4: Virtual Setup of AD configurations	31
Table 3.2: Influent Wastewater Component Compositions.....	33
Table 3.3: Elemental Composition Equations.....	37
Table 3.4: Equilibrium Equations	40
Table 3.5: Mass Balance Equations.....	40
Figure 3.5: Physico-Chemical Modelling Framework (Ghoor, 2020)	47
Table 3.6: THPAD Ionic Species.....	48
Table 3.7: Processes included in the dynamic extended UCTSDM3P model	51
Table 3.7: THP Model Parameters	53
Table 3.8: Electron Donating Capacities	55
Table 3.9: Pasteurization Kinetic and Stoichiometric Equations	56
Table 3.10: Pasteurization Resultant Masses	57
Table 3.11: Activation Kinetic and Stoichiometric Equations	57

Table 3.12: Activation Resultant Masses	58
Table 3.13: Solubilization Kinetic and Stoichiometric Equations	59
Table 3.14: Solubilization Resultant Masses	61
Table 3.15: Final THP component masses.....	62
Table 4.1: Influent Component Compositions.....	65
Figure 4.1: Graphs showing Wastewater composition changes through different THP temperatures	67
Table 4.2: Steady State and Dynamic AD results with and without THP at infinite solubility	70
Table 4.3: Steady State and Dynamic AD Model Results accounting for Struvite Precipitation...	71
Table 4.4: Methane production	73

List of Tables

Table 3.1: Cape Flats Wastewater Treatment Works Anaerobic Digester Operating Parameters.	30
Table 3.2: Influent Wastewater Component Compositions	33
Table 3.3: Elemental Composition Equations.....	37
Table 3.4: Equilibrium Equations.....	40
Table 3.5: Mass Balance Equations	40
Table 3.6: THPAD Ionic Species	48
Table 3.7: Processes included in the dynamic extended UCTSDM3P model.....	51
Table 3.7: THP Model Parameters	53
Table 3.8: Electron Donating Capacities	55
Table 3.9: Pasteurization Kinetic and Stoichiometric Equations	56
Table 3.10: Pasteurization Resultant Masses	57
Table 3.11: Activation Kinetic and Stoichiometric Equations	57
Table 3.12: Activation Resultant Masses	58
Table 3.13: Solubilization Kinetic and Stoichiometric Equations.....	59
Table 3.14: Solubilization Resultant Masses.....	61
Table 3.15: Final THP component masses	62
Table 4.1: Influent Component Compositions.....	65
Table 4.2: Steady State and Dynamic AD results with and without THP at infinite solubility.....	70
Table 4.3: Steady State and Dynamic AD Model Results accounting for Struvite Precipitation	71
Table 4.4: Methane production	73

List of Symbols and Abbreviations

A	Composition subscript for nitrogen in organics empirical formulation
Ac	Dissociated Acetic Acid
ACOX	Acetate Oxidizing Bacteria
AD	Anaerobic Digestion
ADM1	Anaerobic Digestion Model number 1
ADM-3P	Three-phase Anaerobic Digestion Model
ANO	Autotrophic Nitrifying Organism
AS	Activated Sludge
B	Composition Subscript for Phosphorus in organics empirical formulation
BPO	Biodegradable Particulate Organics
BSO	Biodegradable Soluble Organics
BNR	Biological Nutrient Removal
C	Carbon
CFWWTW	Cape Flats Wastewater Treatment Works
CHON	Carbon, Hydrogen, Oxygen and Nitrogen
CH ₄	Methane
C _x H _y O _z N _a P _b	Biomass empirical composition
CO ₂	Carbon dioxide
COD	Chemical Oxygen Demand
CSTR	Continuously Stirred Tank Reactor
d	Day
°C	Degrees Celsius
fS'up	Fraction of unbiodegradable particulate COD in the influent wastewater
fS'us	Fraction of unbiodegradable soluble COD in the influent wastewater
H ⁺	Hydrogen ion
H ₂	Hydrogen molecule

HAc	Undissociated acetic acid (mg/l)
HCO_3^-	Bicarbonate ion
VFA	Volatile Fatty Acid
IC	Inorganic Carbon
ISS	Inorganic Settleable Solids
IWA	International Water Association
K_a	Dissociation constant for weak acid/base
K_H	Henry's Law Constant
k_{cambi}	Calibration parameter in thermophilic anaerobic digestion modelling
l	Litre
LI_{NH_3}	Free ammonia sigmoidal inhibition term
Mg	Elemental Magnesium
MI_{O_2}	Oxygen Monod Inhibition Term
MI_{NO_2}	Nitrite Monod Inhibition Term
MI_{NO_3}	Nitrate Monod Inhibition Term
MM	Molar mass
MS_{Sac}	Total acetate Monod inhibition term
MS_{Hac}	Undissociated acetate Haldane Term
N	Elemental Nitrogen
NDEBPR	Nitrification Denitrification Excess Biological Phosphorus Removal
NH_4^+	Ammonium ion
O	Elemental Oxygen
Orgs	Organisms
P	Elemental Phosphorus
pH	Activity of hydrogen ions
RBCOD	Readily Biodegradable COD
R _{hn}	Hydraulic retention time

r_g	Acetate oxidizers growth rate
r_{\max}	Maximum hydrolysis rate
R_s	Sludge age
SBCOD	Slowly biodegradable COD
S_b	Biodegradable organics in the reactor
S_{bp}	Biodegradable Particulate Organics
SCFA	Short-Chain Fatty Acid
SF	Fermentable soluble organics
SRT	Solids Retention Time
SS	Steady state
SAOB	Syntrophic Acetate Oxidizing Bacteria
SU	Unbiodegradable soluble organics
THP	Thermal Hydrolysis Process
UPO	Unbiodegradable Particulate Organic
USO	Unbiodegradable Soluble Organic
VFA	Volatile Fatty Acids
VS	Volatile Solids
VSS	Volatile Suspended Solids
WAS	Waste Activated Sludge
WWTP	Wastewater Treatment Plant
WWTW	Wastewater Treatment Works
X	Composition subscript for carbon in organics empirical formulation
X_{acox}	Acetate oxidizers
XBOrg	Activated Sludge biodegradable particulate organics
XBIInf	Primary sludge biodegradable particulate organics
XUIInf	Primary sludge biodegradable particulate organics
XUOrg	Activated sludge unbiodegradable particulate organics

X_s	Slowly biodegradable organic material
Y	Composition subscript for hydrogen in organics empirical formulation
Z	Composition subscript for oxygen in organics empirical formulation
Z_{AD}	Biomass concentration in the AD reactor
μ_{max}	Maximum specific growth rate
f_{cv}	COD/VSS ratio
f_p	P/VSS ratio
f_n	N/VSS ratio
f_c	C/VSS ratio

1 INTRODUCTION

The goal of this project is to develop an integrated Thermal Hydrolysis Process Anaerobic Digestion (THPAD) model. The project is funded by the Water Research Group (WRG) at the University of Cape Town and conducted under the supervision of A/Prof. David Ikumi and co-supervised by Dr. Chris Gaszynski. This research aims to provide a better understanding of the THPAD process through a comprehensive review of the available literature, verification of the developed model, as well as a comparative study of the Cape Flats wastewater treatment works (CFWWTW) facility.

1.1 BACKGROUND

Environmental pollution is one of the most serious global challenges. It is defined as the contamination of biological and physical components of the earth or atmosphere. These contaminants vary in their nature and are responsible for the cause of adverse change in the environment. Water bodies make up a huge fraction of our environment. With rapid growth in human population and increased urbanization, the amount of waste we produce has also increased. Due to inappropriate management of this waste, a significant amount ends up in our water streams and is eventually discharged into larger water bodies causing pollution in our hydrological cycle. In response to this, innovative methods of wastewater (WW) treatment have been investigated and developed over the years.

Anaerobic digestion is one of the oldest methods for treating sewage sludges. However, with the exponential increase in populations, the amount of sludge waste generated renders some of the currently standing anaerobic digesters insufficient in handling capacity. Subsequently, there has been a lot of research into various physical and chemical processes that would allow for a more efficient sludge handling mechanism. Over the years, various advantages have been reported from digesting sludge at higher temperatures known as thermophilic temperatures (Gavala *et al.*, 2003; Valo *et al.*, 2004). These advantages include increased sludge handling capacity, a higher degree of sludge biodegradability and subsequently increased methane production and better sludge dewatering characteristics implying cheaper sludge transportation costs just to mention a few. However, despite the advantages associated with treatment at these elevated

temperatures, there have been a number of studies that have associated compromised performance with the operation of these digesters (e.g., excessive ammonia discharge with the effluent) (Gebreyessus and Jenicek, 2016; Westerholm *et al.*, 2016).

This project involves a comparative desktop case study of the existing anaerobic digestion (AD) facility at the Cape Flats WWTW in Western Cape, South Africa following the City of Cape Town's initiative to install an improved process to help deal with the increase in sludge handling capacity. A comparison was done between the base case scenario of maintaining the existing conventional mesophilic anaerobic digesters (MAD) and retrofitting a thermal hydrolysis process (THP) unit to the conventional anaerobic digesters (THPAD).

The steady-state model developed by Potts (2021) was used in conjunction with the dynamic model developed in this project for both the conventional MAD and integrated THPAD. This allowed for a comparison of results not only between the two processes, but also the two types of models.

1.2 RESEARCH PROBLEM

Studies on the effects of various environmental conditions (e.g., increased ammonia and VFA concentration, change in the methanogenic community structure, etc.) on digester operations reveal a shift in the biological processes and microbial populations with application of temperature (Zinder and Koch, 1984; Westerholm *et al.*, 2016). An understanding of how these interact is essential to addressing the issue of failing digesters.

Over recent years, modeling has been used to simplify and understand complex processes. Earlier models were empirical in nature following a black box approach. Over time, and with a better understanding of treatment processes, models began to adopt a glass-box approach where an attempt was made to understand the processes that take place at a microscopic level (Ikumi, 2011). Such models include the International Water Association (IWA) anaerobic digestion model no.1 ADM1 (Batstone *et al.*, 2002) and the subsequent development of the first family of models. The deliverable for this project is therefore the development of an integrated THPAD model equipped to account for processes resulting from operation at these elevated temperatures and capable of virtually simulating the anaerobic digestion of a full-scale plant. Additionally, through the development of a steady state and dynamic THPAD model, a better understanding of the

processes in the anaerobic digestion process, as well as the limitations of the different models could be gained.

1.3 RESEARCH QUESTIONS

In order to address the aforementioned research problem, this dissertation looks to explore the following research questions.

- Can a thermal hydrolysis process (THP) unit be modelled and incorporated into the anaerobic digestion (UCTSDM3P) model?
- Is it possible to develop models that can reasonably simulate and subsequently predict the performance of integrated THP -AD unit operations of a wastewater treatment plant (WWTP)?
- Are there any limitations in modelling the THPAD with simplified steady state excel-based tools versus more sophisticated dynamic simulation models?

1.4 OBJECTIVES

In response to the questions mentioned stated above, the following are the objectives for this dissertation.

- Determination of the relevant processes for modelling THP and AD that is fed substrate pre-treated using THP, through a comprehensive literature review.
- Development of a thermal hydrolysis process (THP) unit model in MS Excel (simplified version) and in WEST®, as a sub model of the PWM_SA plant wide model of Ikumi *et al.*, (2015).
- Extension of the dynamic UCTSDM3P model developed by Ikumi (2011) to include the processes resulting from AD at elevated temperatures and also AD-fed sludge effluents from a THP unit process.
- Integration of the THP model (developed in objective 2) and the extended AD model (from objective 3) to simulate a full-scale system as a case study to showcase the application of the THP using both simplified steady state tools and more complex dynamic simulation software (WEST®). The Cape Flats wastewater treatment works (CFWWTW) sludge digestion scheme

was selected for this case study because its future proposed upgrade includes addition of THPAD. The outputs from the steady state MS excel spreadsheet model is compared to the complex WEST® model to check for possible limitations in utilizing the simplified MS Excel model.

1.5 PROJECT SCOPE AND LIMITATIONS

The following are the scope and limitations for this research project:

- This thesis involves the development of an integrated THPAD model. To adequately evaluate the model, a verification process as well as a rigorous calibration process involving uncertainty and sensitivity analyses would need to be carried out. However, due to project load and time constraints, only a model verification process was carried out.
- Availability of data: The model uses an algebraic converter for the THP-treated substrate that simply converts one compound to another. Due to limited experimental data on the THP processes, the conversion of compounds was based on values and fractions found in literature.

1.6 OVERVIEW OF REPORT

This dissertation comprises various sections that have been subdivided into five main chapters. The report begins with a background to the problem and sets out the questions and objectives to be met in this thesis as well as the scope and limitations of the research project (Chapter 1). This is followed by a comprehensive literature review (Chapter 2) that consolidates the literature regarding the anaerobic digestion process at elevated temperatures and highlights relevant research gaps. Chapter 3 involves a description of the methodology followed to develop the steady state and dynamic thermal hydrolysis process of pre-treatment to anaerobic digestion (THPAD) model followed by a discussion of the results (Chapter 4) obtained. The report will then conclude (Chapter 5) with a section discussing the results obtained and their implications with respect to the research questions laid out above as well as recommendations for further research. Figure 1.1 gives a figurative overview of the report.

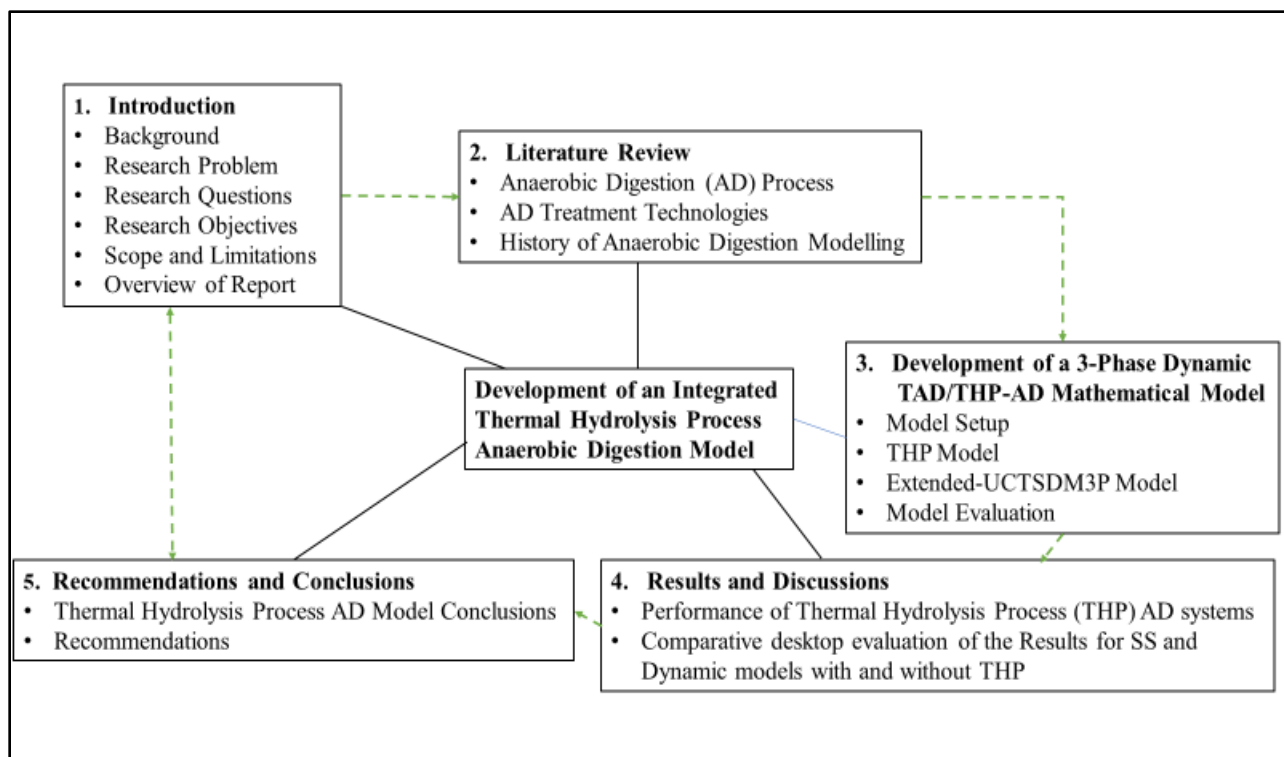


Figure 1.1: A mind map showing an overview of the project report, including the main components of each chapter and their respective associations with each other

2 LITERATURE REVIEW

The literature review looks at the work and ideas conveyed by previous researchers in contribution to understanding the topic of anaerobic digestion. Consequently, this chapter is subdivided into sections highlighting the key concepts involved in the conventional anaerobic digestion (AD) process, the intricacies involved in alternative treatment technologies, the challenges associated with these treatment technologies and consequently highlighting the areas that need further research. The chapter is then concluded with a brief discussion on the history of AD modelling.

2.1 ANAEROBIC DIGESTION PROCESS

Anaerobic digestion is a sequence of processes through which microorganisms break down biodegradable matter in the absence of oxygen. Given the numerous microbial communities present and the various substrate compositions, anaerobic wastewater treatment is a complex process that is consequently sensitive to digester disturbances. In order to understand and model the AD process, it is important to understand the microorganisms that are responsible for the processes that make up the AD process. In order to ensure a stable anaerobic digestion process, specific substrate use is reliant on the growth and metabolism of different groups of organisms that are very different in terms of their physiology, nutritional needs, individual growth capabilities and responses to environmental stresses (Demirel *et al.*, 2002). Based on their functions and processes, the major groupings of bacteria and the reactions they represent are as follows: (i) fermentative bacteria (i.e., acidogens), (ii) hydrogen-producing acetogenic bacteria (acetogens), (iii) hydrogen-consuming acetogenic bacteria (i.e., acetogens), (iv) carbon-dioxide-reducing methanogens, and (v) acetoclastic methanogens (i.e., methanogens). The anaerobic digestion process can therefore be broken down into the following four phases: 1) *Hydrolysis*, 2) *Acidogenesis*, 3) *Acetogenesis*, and 4) *Methanogenesis*. These phases are summarized as shown in Figure 2.1. Efficient operation of the AD process requires that the “acid-forming” organisms grow in harmony with the “methane-formers” because any loss in the balance of activities between the two groups of organisms, usually in favor of the relatively faster-growing acid-formers, could result in an upset in digester conditions (Ghosh *et al.*, 1975).

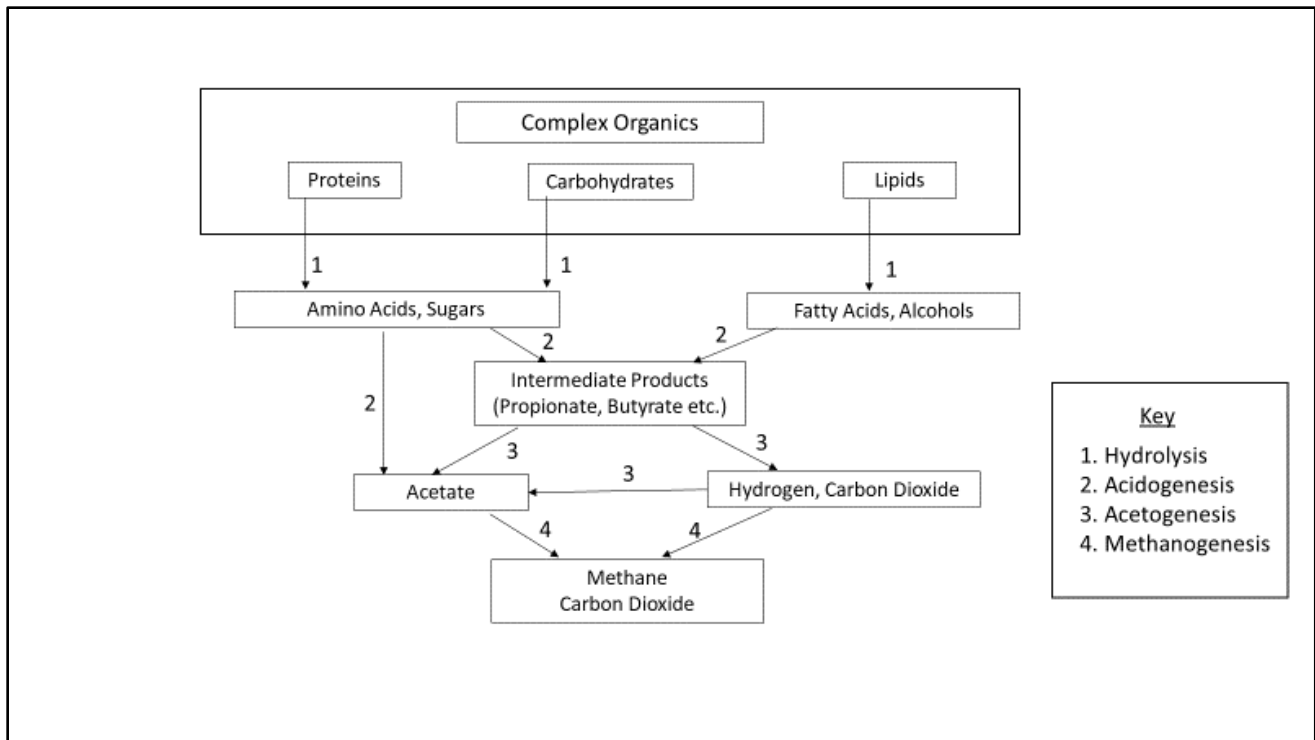


Figure 2.1: Diagram showing the phases of the Anaerobic Digestion process

2.1.1 Hydrolysis

Hydrolysis is the process mediated by acidogens and is responsible for the breakdown of complex organics (i.e., proteins, carbohydrates, and lipids) to short-chain fatty acids (SCFA) acetic and propionic (HAc, HPr), carbon-dioxide and hydrogen (van Lier *et al.*, 2008). This is done through the degrading action of exo-enzymes to produce smaller molecules (van Lier *et al.*, 2008). In mesophilic conditions (i.e., temperatures around 37°C), hydrolysis is considered the rate-limiting step in the anaerobic digestion of complex substrates. This implies that it is considered to be the slowest of the processes in the entire anaerobic digestion process (Vavilin *et al.*, 2001). At elevated temperatures (i.e., thermophilic conditions) however, an accelerated hydrolysis rate has been reported and methanogenesis becomes the rate-limiting step (Wilson *et al.*, 2008; Westerholm *et al.*, 2016). The following sub-section describes the various hydrolysis kinetics that have been investigated by various researchers.

2.1.1.1 Process Kinetics

As described in Section 2.1.1, under mesophilic conditions the hydrolysis process is the rate-limiting step in the biological process and subsequently all the processes that proceed it are

assumed to take place instantaneously, and hence determined through stoichiometry. However, under thermophilic conditions the hydrolytic process is hastened making methanogenesis the rate-limiting process.

It is therefore important to ensure that the biological process and kinetic constants chosen to represent hydrolysis are appropriately selected. Various studies have been carried out to investigate which kinetic mechanism best describes the hydrolytic process that takes place in the AD (O'Rourke, 1968; Izzet *et al*, 1992; Sötemann *et al*, 2005; Ikumi, 2011). There are four kinetic equations that have been widely proposed to express the hydrolysis process namely: First order kinetics, specific first order kinetics, Monod kinetics and saturation kinetics.

2.1.1.2 First Order Kinetics

First order kinetics has a simple formulation where the rate of hydrolysis is directly proportional to the concentration of available substrate as shown in Equation (2-1).

$$r_{HYD} = k_h S_{bp} \quad (2 - 1)$$

Where:

r_{hyd} refers to the volumetric hydrolysis rate in gCOD/l.d

and

k_h is the first order kinetic rate constant (1/d)

2.1.1.3 First Order Specific Kinetics

This formulation models the hydrolysis rate as being proportional to the residual biodegradable particulate COD concentration (S_{bp}) and the acidogen biomass (Z_{AD}) concentration.

$$r_{HYD} = k_H S_{bp} Z_{AD} \left[\frac{gCOD}{l.d} \right] \quad (2 - 2)$$

Where k_H refers to the specific first order kinetic rate constant [$l/(mgZ_{AD}.d)$]

This kinetic expression was used to model the conversion of readily biodegradable organics into short chain fatty acids (Wentzel *et al.*, 1998). Furthermore, this kinetic expression might be preferred to the first order kinetics as it dependent on the substrate concentration as well as the organism group (Z_{AD}) which mediates the process.

2.1.1.4 Monod Kinetics

The kinetic equation by Monod (1951) estimates the growth rate of an organism dependent on a specific limiting substrate by relating the rate of uptake of that substrate to its concentration in the growth medium. All other substrates and nutrients are assumed to be available in excess such that the products of reaction do not accumulate sufficiently enough to inhibit the hydrolysis reaction (McCarty and Mosey, 1991). Hence the Monod equation describes the relationship between the specific hydrolysis rate (r_{HYD}/Z_{AD}) and concentration of the growth limiting substrate (S_{bp}) as shown in Equation (2-3) below:

$$r_{HYD} = \frac{k_m S_{bp}}{K_s + S_{bp}} \cdot Z_{AD} \quad \left[\frac{gCOD}{l.d} \right] \quad (2-3)$$

Where k_m refers to the maximum specific hydrolysis rate and K_s the substrate concentration at which the specific hydrolysis rate is half k_m .

The Monod equation is used in many bioprocess applications due to its mathematical stability, simplicity, and functionality as a switching factor between zero and first order kinetics when dealing with low or high substrate concentrations respectively.

2.1.1.5 Saturation kinetics

Similar to Monod kinetics, the saturation kinetic formulation includes the acidogenic biomass concentration (Z_{AD}) and incorporates the maximum rate of hydrolysis under conditions of high substrate concentration. Unlike Monod kinetics, the saturation kinetics is not dependent on the bulk liquid residual biodegradable COD concentration (S_{bpe}) but rather dependent on its concentration with respect to the acidogenic biomass concentration (Z_{AD}). This implies that the rate of hydrolysis operates at a maximum when all the active sites available on the acidogenic organism are saturated regardless of how much excess substrate is available for consumption by the acidogenic organisms. Thus, the saturation kinetic formulation is as shown in Equation (2-4) below:

$$r_{HYD} = \left(\frac{k_m \cdot \frac{S_{bp}}{Z_{AD}}}{k_m \cdot \frac{S_{bp}}{Z_{AD}}} \right) \cdot Z_{AD} \quad \left[\frac{gCOD}{l.d} \right] \quad (2-4)$$

Where K_s is the substrate and acidogenic biomass concentration ratio, at which the specific hydrolysis rate is half its upper limit (k_M) at saturation.

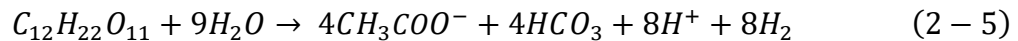
This kinetic formulation has been used to model the utilization of slowly biodegradable organics in activated sludge models (Dold *et al.*, 1981; Henze *et al.*, 1987) and the hydrolysis of sewage sludge (McCarty, 1976).

In order to use any of the aforementioned kinetic formulations, the kinetic constants (k_h , k_H , k_m , K_s , k_M and K_S) need to be determined for the different sludge types. The procedure to calculate this can be found in works by Ikumi, (2011).

The hydrolysis kinetics therefore determines the concentration of biodegradable COD utilized in the AD and converted to AD products. Stoichiometric equations on the other hand, were then used to determine the concentration of these respective AD products. The products of the hydrolysis step are the substrates for acidogenesis, the next phase in the process.

2.1.2 Acidogenesis

The products from hydrolysis (i.e., amino acids, sugars, alcohols, fatty acid, etc.) which are relatively small compounds are taken up into the bacteria cell through the membrane and subsequently fermented or anaerobically oxidized (Lier *et al.*, 2008). This step is referred to as acidogenesis/fermentation. The products of this process consist of a variety of small organic acids such as acetate and in the case of high hydrogen partial pressure, higher organic acids including propionate, butyric- and valeric-acid. Given acetate and carbonic acid are the main end products, this process is commonly referred to as the acidifying phase. The following Equation (2-5) is an example of a typical acidogenic process starting from sucrose to yield acetate, hydrogen gas, hydrogen ions and bi-carbonate ions.



The operations in an anaerobic digester are sensitive to the operating conditions. For example, an increased hydrogen gas pressure above 10 Pa has been reported as a characteristic in failed anaerobic digesters (Wilson *et al.*, 2008). It is therefore critical to ensure effective removal of H_2 concentration in order to maintain acetate as the main end product of the acidogenic process. Under stable conditions, this role is fulfilled by methanogenic bacteria.

2.1.3 Acetogenesis

In instances where high hydrogen partial pressures result in the generation of higher organic acids, the acidogenic step is followed by the acetogenic process where the short-chain fatty acids besides acetate (i.e., propionate, butyric- and valeric- acid) are converted to acetate, hydrogen, and carbon-dioxide by the acetogenic bacteria. Key substrates of the acetogenic process are propionate and butyrate. Alcohols, hydrogen, and carbon dioxide are also converted to acetate by the acetogens. Studies on the acetogenic conversion processes have shown the close relationship between the H₂-producing acetogenic bacteria and the H₂-consuming methanogenic bacteria. As previously mentioned, under stable conditions, methanogenic bacteria usually utilize molecular hydrogen rapidly so that the partial pressure in the digester drops below 10⁻⁴ atmospheres, enough to ensure occurrence of the acetogenic reaction. Under such low hydrogen concentrations, the degradation of ethanol, butyrate or propionate becomes exergonic and will yield energy for acetogens (van Lier *et al.*, 2008).

2.1.4 Methanogenesis

Methanogenesis is the final step in the anaerobic process. Up to this point, none of the influent chemical oxygen demand (COD) has been stabilized, it has only taken up different forms. It is through the methanogenic process that influent COD gets stabilized through the conversion to methane and carbon dioxide gases that automatically exit the reactor. During this conversion process, there are two groups of methanogenic bacteria that are involved. Whereas the hydrogen-utilizing or the hydrogenotrophic methanogens reduce carbon-dioxide to methane using hydrogen as the electron donor, the acetate-converting or acetoclastic methanogens use acetate as the electron donor. In mesophilic conditions (i.e., 35-38°C), about 70% of the methane produced originates from acetate (Parkin and Owen, 1986). The rest mainly originates from H₂ and CO₂ in a process that has come to be known as syntrophic acetate oxidation. The selected pathway is dependent on the digester operating conditions.

Within the acetate-conversion process, two methanogenic pathways from acetate have been reported. The first methanogenic pathway involves direct cleavage of acetate in acetoclastic methanogenic archaea such as *Methanosarcinaceae* and *Methanosaetaceae* whereas the second methanogenic pathway involves the syntrophic association of acetate-oxidizing organisms and

hydrogenotrophic methanogens such as *Methanobacteriales* (Ho *et al.*, 2013). The species *Methanosarcinaceae*, however, has been observed as capable of both acetoclastic methanogenesis and acetate oxidation and dominant even in thermophilic conditions (Ho *et al.*, 2013). Westerholm *et al.*, (2016) observed that the species *Methanosarcinaceae* is less sensitive to the ammonia concentration compared to *Methanosaetaceae* with the latter dominating at lower acetate concentration ranges due to a higher affinity for acetate.

The selected pathway is dependent on the environmental factors influencing methanogenesis. These factors include volatile fatty acids, ammonia concentrations, pH, temperature and even solid retention times (Fotidis *et al.*, 2013; Westerholm *et al.*, 2016). For instance, the dominance of syntrophic acetate oxidizing bacteria (SAOB) over acetoclastic methanogens (AM) is dependent on the ammonia concentrations that would inhibit AMs, hence SAOBs do not usually occur in conventional AD systems. However, when the ammonia concentration is high, they may be significant enough to be included.

Various configurations have been investigated in order to attempt to optimize the environmental conditions required to enhance operation efficiency in an anaerobic digester. The following section concerns a discussion of these configurations and their respective literature.

2.2 ANAEROBIC DIGESTION TREATMENT SYSTEMS

Numerous studies have been carried out attempting to maximize the energy recovered from organic matter degradation. In this regard various technologies have been proposed in order to improve the digestion process. In this sub-section three treatment technologies shall be discussed, the conventional mesophilic anaerobic digestion (MAD) system, the thermal hydrolysis process (THPAD) anaerobic digestion system and the thermophilic anaerobic digestion (TAD) system.

2.2.1 Conventional Mesophilic Anaerobic Digester (MAD) system

This treatment process is commonly used to stabilize primary sludge and waste activated sludge of high concentration. This process is often favored over aerobic sludge treatment because it includes a lower energy requirement (as no oxygen is required), lower biomass production and ability to degrade certain pollutants that cannot be aerobically removed (Gebreeyessus and

Jenicek, 2016). The anaerobic digestion process occurs as has been described in sub-section 2.1. Conventional mesophilic anaerobic digesters are operated at a temperature of 35°C and hydraulic retention times between 20 – 30 days. The relatively long retention times are a key disadvantage of these systems as long retention times imply that more wastewater is contained in the reactor tanks. Consequently, this means that an increased reactor capacity is required and hence high initial costs. Furthermore, the larger the reactor tanks the higher the cost required to ensure optimal mixing. This implies an increase in the maintenance costs. (Ho *et al.*, 2013).

2.2.2 Thermal Hydrolysis Process (THP) System

Thermal hydrolysis process is a pre-treatment that involves the physical breakdown of cells of organics through the application of high temperatures of about 140 – 200°C at a corresponding pressure of 6-25 bars (Phothilangka *et al.*, 2008) in a separate unit before release into an anaerobic digester operated at mesophilic conditions. During digestion, only the biodegradable portion of the organics fed into the digester are converted to methane. In primary sludge, this portion could make up to 65% of the total sludge whereas in waste activated sludge (WAS), studies show that it is much lower and dependent on the respective solid retention time of the activated sludge system (Ikumi *et al.*, 2014). Elliott and Mahmood (2007), estimated the fraction of WAS that is biodegradable to be about 50% with the remaining fraction remaining as unbiodegradable, either due to being inorganically bound to carbon or forming part of the slowly biodegradable organics.

As mentioned earlier, in mesophilic conditions, it has been observed that hydrolysis is the rate-limiting process. It follows that the process of hydrolysis is dependent on the physical characteristics (shape, size etc.) of the influent organics. Therefore, the rate at which higher particulate organics are broken down to smaller sizes and utilized for fermentation determines the overall rate of the digestion process. Various studies (Ge *et al.*, 2011) have shown that this digestion process can be improved if the slowly degradable material can be degraded faster or if the 'unbiodegradable' material can be made available for digestion. For instance, the intercellular components of WAS are biodegradable. However, due to the unbiodegradable cross-linked D-amino polysaccharide chains that make up the cell wall to protect the cellular contents from physical and chemical stress, this biodegradable part remains inaccessible (Neyens and Baeyens,

2003) hence making it all effectively 'unbiodegradable'. Consequently, numerous studies have been carried out to investigate the application of different pre-treatment technologies in a bid to break down this protective cell layer and avail the previously inaccessible and hence 'unbiodegradable' part for the process (Neyens and Baeyens, 2003; Elliott and Mahmood, 2007; Phothilangka, *et al.*, 2008). This process is referred to as solubilization. Some of the investigated pre-treatment technologies include the use of exposure to high frequency ultrasound, use of high temperatures and pressure, dosing of alkali, application of ozone oxidation and mechanical disintegration by cavitation. This section focuses on the use of high temperature and pressure in a process known as thermal hydrolysis process (THP). THP is a high-rate pre-treatment process that is widely applied in the disintegration of WAS to allow for the biodegradation of the intercellular content.

Experiments by Brooks (1970) revealed an increase in the solubilization of organic matter from samples of a mixture of WAS and primary sludge and WAS alone in the order of 40-60% and 20-35% respectively, at a treatment temperature of 170°C. Similarly, studies (Li and Noike, 1992; Valo, *et al.*, 2004) showed a progressive increase in solubilization with increase in thermophilic temperatures between 120-180°C. However, above 180°C further increase in temperature was observed to have an inhibitory effect on digestion presumably due to formation of refractory compounds (Li and Noike, 1992).

In addition to increased solubilization rates, the methane production and methane production rates have been observed to generally increase with THP temperatures until a certain point beyond which the gas production decreases presumably due to the formation of refractory compounds (Li and Noike, 1992; Phothilangka *et al.*, 2008; Abelleira-Pereira *et al.*, 2015; Higgins *et al.*, 2017; Choi *et al.*, 2018). Though not clear, the reported varied increase in the gas production (between 20 to 120% relative to the control) for THP could be due to different sludge properties and specific testing conditions (batch vs continuous tests) (Abelleira-Pereira *et al.*, 2015).

Besides the advantages of increased solubilization, and subsequently increased biogas production, implementation of the thermal hydrolysis process leads to better dewatering characteristics of the sludge as a result of the heat, leading to a higher breakdown of the cell

structure and subsequent release of the intracellular bound water. This results in a sludge cake higher in concentration and consequently much smaller in volume resulting in cost savings. Furthermore, given the increasing pressure on sludge production and handling capacity at wastewater treatment plants, this process would help save on the size of the reactor and consequently the high initial and maintenance costs associated with the conventional mesophilic digestion process.

Despite the advantages associated with thermal hydrolysis process pre-treatment, studies have shown that as a result of high temperatures, there exists instances of process disturbances during the digestion process. Because thermal disintegration improves the biological accessibility of compounds, more nitrogen gets released into solution in the form of ammonium-nitrogen (NH_4^+) from the breakdown of the N-containing organic matter (Phothilangka, *et al.*, 2008). The digestion of THP sludge with feed of higher total solids concentrations produces higher alkalinity and produces free ammonia. An increase in alkalinity results in further increase in the pH resulting in higher concentrations of free ammonia. The prevailing conditions are not optimal for acetoclastic methanogens as under high ammonia concentrations, studies have shown the activity of these methanogens to be inhibited (Ho *et al.*, 2013; Westerholm *et al.*, 2016).

In mesophilic conditions where inhibition due to ammonia is minimal, up to 70% of the methane is formed through acetoclastic methanogenesis (Parkin and Owen, 1986). For THP sludge, following the inhibition of the acetoclastic methanogens, with the exception of the *Methanosarcinaceae* species, syntrophic acetate oxidation to H_2 and CO_2 by the Acetate-oxidizing organisms (ACOX) predominantly occurs. ACOX and hydrogenotrophic organisms are relatively more resistant to ammonia inhibitions and thus become the dominant contributors to methane production in the THP process (Westerholm *et al.*, 2016).

Despite this information, there is still limited knowledge on how this organism shift affects the efficiency of biogas production and possibility of causing process failure. Additionally, the presence of higher H_2 concentrations both in the headspace and in solution, could indicate a possible increase in the H_2 partial pressure which is known to inhibit the activity of acid forming organisms and consequently the methanogenic process. Hence through the development of a

model, insight can be gained on the stability of the AD process as well as identification of parameters that would assist in monitoring and controlling the digestion process.

2.2.3 Thermophilic Anaerobic Digestion (TAD) System

Thermophilic Anaerobic Digestion (TAD) on the other hand, involves the operation of anaerobic digesters at a temperature usually in the range of 55-65°C (Gavala *et al.*, 2003; Westerholm *et al.*, 2016). In contrast to the THPAD process, the TAD process occurs in a single reactor as with the conventional AD process. Numerous studies have been carried out on the high-rate process and the use of elevated temperatures in order to improve the digestion process and enable higher loading rates in anaerobic digesters (Angelidaki and Ahring, 1993; Han and Dague, 1997; Bolzonella *et al.*, 2007). In this regard there have been some contradictory findings. Nges and Liu (2009), evaluated the effect of temperature on digester performance and reported that the digestion performance of mixed primary sludge and activated sludge is not influenced by thermophilic temperatures as the same volatile solids (VS) destruction of 42% was achieved at the thermophilic temperature of both 50 and 70°C at a retention time of 2 days. However, this result was still greater than the VS destruction of 39% achieved in the single-stage mesophilic control reactors. Investigations by Ho *et al.*, (2013) yielded results with thermophilic digesters operated at 55°C and a retention time of 3-4 days comparable to mesophilic digesters operated at a solid retention time of 15 to 20 days reported by Ge *et al.*, (2011) and Bolzonella *et al.*, (2004). At shorter retention times (i.e., 2 days and lower), investigations by Ho *et al.*, (2013) noted the failure of digesters due to loss of methanogenesis as opposed to primary hydrolysis, evidenced by a decrease in the gas produced and accumulation of acetate. This washout of methanogens could be the reason for the results obtained by Nges and Liu (2009) where their digesters were operated at a retention time of 2 days. Investigations (Han and Dague, 1997; Bolzonella *et al.*, 2007; Ho *et al.*, 2013) show that thermophilic anaerobic digestion offers higher destruction of pathogens and organic solids as well as potentially increasing the methane production.

Various studies attribute the improved performance of thermophilic anaerobic digesters to increased hydrolysis rates reported to be as high as 2 to 3 times the hydrolysis coefficient in conventional mesophilic conditions (Ge *et al.*, 2011; Ho *et al.*, 2013). As a result of the significantly

increased hydrolysis rates, methanogenesis becomes the rate-limiting step and system failure could occur as a result of accumulation of intermediate products such as ammonia and acetate. Hansen *et al.*, (1998) and Hejnfelt and Angelidaki, (2009) noted that digestion of protein-rich substances like animal products, caused instability in anaerobic digesters indicated by decreased steady state methane production rates and increased intermediate products. Other studies into the process have investigated the effect of accumulation of intermediate products in the cause of failure in digesters especially at elevated temperatures (Hansen *et al.*, 1998; Chen *et al.*, 2007; Hejnfelt and Angelidaki, 2009). Rajagopal *et al.*, (2013) and Westerholm *et al.*, (2016) noted that the inhibitory effects of ammonia had a pronounced effect on the later stages of the digestion process involving non-acclimatized hydrogen/formate-utilizing organisms and acetoclastic methanogens. Acclimatization of the microbial community has been proposed to cope with the inhibitory effects of excess ammonia. However, investigations by Fotidis *et al.*, (2013) led to observations of limited diversity in methanogens under high ammonia concentrations for both thermophilic and mesophilic conditions. The acclimatized *Methanosarcinaceae* was found to be the dominant species. Studies have shown the versatility of *Methanosarcinaceae* with respect to substrate utilization for methane formation where the species is able to utilize not only acetate but also CO₂ and H₂ which would explain its presence in thermophilic conditions. Essentially, *Methanosarcinaceae* can facilitate both methanogenic pathways. This limited diversity of methanogens however, implies the inability to cope with ammonia toxicity compared to a more diverse consortium of organisms (Fotidis *et al.*, 2013).

As mentioned in Section 2.1 of this literature review, various studies (Ho *et al.*, 2013) report the occurrence of two potential methanogenic pathways from acetate; (i) direct acetate cleavage facilitated by acetoclastic methanogens and (ii) non-acetoclastic methanogenesis or syntrophic acetate oxidation facilitated by syntrophic acetate-oxidizing bacteria (SAOB) (which convert acetate into H₂ and CO₂) and hydrogenotrophic organisms (which convert H₂ and CO₂ into CH₄). At elevated temperatures (thermophilic conditions) and in non-acclimatized cultures, investigations show non-acetoclastic methanogenesis as the dominant pathway (Ho *et al.*, 2013; Westerholm, *et al.*, 2016) while at mesophilic conditions, acetoclastic methanogenesis has been observed to be the dominant pathway. This is because in thermophilic conditions, Zinder and

Koch (1984) demonstrated that the syntrophic acetate-oxidizing bacteria (SAOB) display significantly shorter doubling times indicating that their growth rates can exceed that of obligate acetoclastic methanogens. Hence high temperatures and short retention times lead to the washout of the acetoclastic methanogens as observed by Nges and Liu, (2009).

A better understanding of the role that digestion temperature plays in the accumulation of intermediates is critical to the design of high-temperature digestion systems. Considering the functional importance of SAOBs, increased knowledge of these populations and factors influencing their behavior in ecosystems is critical for predicting process failures and devising strategies for process optimization (Westerholm *et al.*, 2016).

2.3 HISTORY OF ANAEROBIC DIGESTION MODELLING

2.3.1 Introduction

Until the late 20th century, in comparison to the Activated Sludge (AS) reactor, little modelling had gone into the Anaerobic Digestion (AD) reactor. The International Water Association (IWA) Task Group formed in 1997 was tasked with the objective to develop a generalized anaerobic digestion model (ADM1). Gathering from a large body of knowledge through research and experience, key topics of concern were identified and a model structure, kinetic rate equations and implementations were presented in a paper (Batstone *et al.*, 2002). The task group adopted the philosophy of process and component inclusion to maximize on applicability while maintaining the simplicity of the model.

2.3.2 ADM1 Model

The reaction system in ADM1 is represented as biochemical and physico-chemical reactions. The biochemical reactions involve the processes mediated by micro-organisms. The model structure comprises three general biological steps (acidogenesis, acetogenesis and methanogenesis), an extra-cellular disintegration step (partly non-biological) and an extra-cellular hydrolysis step (Batstone *et al.*, 2002). The extra-cellular disintegration step involves the breakdown of complex particulates into carbohydrates, proteins, and lipid particulates. The disintegration step, as well as the subsequent hydrolytic step, was assumed to follow first-order kinetics which is based on empiricism, reflecting the cumulative effect of a multi-step process (Eastman and Ferguson,

1981). The intra-cellular biological steps on the other hand, are described by the uptake of substrates and biomass growth i.e., Monod kinetics.

The physico-chemical reactions involved processes that are not mediated by micro-organisms.

These included:

- Liquid-liquid reactions i.e., ion association/dissociation
- Gas-liquid reactions e.g., gas transfer and ammonia stripping
- Liquid-solid exchanges i.e., precipitation and solubilization of ions

The ADM1 task group did not model the effects of precipitation even though the process is likely to occur in anaerobic digester reactors. Furthermore, the shortcomings of ADM1 are as listed as follows:

- It has a non-aligned input set that characterizes influent into carbohydrates, lipids and proteins as opposed to the routinely measured COD, TKN, VSS, etc.
- As mentioned, it only considers 2-phases and so does not include mineral precipitation and therefore, it does not (i) accurately predict digester pH when mineral precipitation takes place, (ii) include the effects of gas partial pressure in the aqueous and headspace, and (iii) include the effects of high hydrogen partial pressures on the acid-forming bacteria.

2.3.3 UCTADM1 Model

Investigations by Sötemann *et al.*, (2005) led to the development of UCTADM1, an integrated 2-phase (aqueous-gas) mixed weak acid/base chemical, physical and biological process kinetic model for AD of sewage sludge. Sötemann *et al.*, (2005) also compared the different kinetic relationship in order to determine the most suitable hydrolytic equation. Through the incorporation of COD, C and N mass balances and the interrelation of physical, chemical, and biological processes, the relationship between the compounds involved was determined. In this model, the sewage sludge was characterized in terms of total COD, particulate COD fraction, the short-chain fatty acid (SCFA) COD and the CHON content of the particulate organics (Sötemann *et al.*, 2005). This characterization allowed for linkages to upstream unit processes in some Activated Sludge (AS) system models such as that by Batstone *et al.*, (2002) through mass

balances over the primary settling tank (PST). This was a significant contribution to the subsequent development of a plant-wide mass-balanced model (PWM_SA) by Ekama *et al.*, (2006) and Nopens *et al.*, (2009).

Following characterization, the feed sludge goes through hydrolysis which is considered the slowest process and hence critical in steady state model development. In contrast to the ADM1 process which involves disintegration of carbohydrates, proteins, and lipids, the UCTADM1 hydrolysis process was modelled to act on a single generic organic compound i.e., $C_xH_yO_zN_A$ to yield the idealized carbohydrate, glucose. Glucose was modelled as an intermediate product and was directly converted to acetate and propionate through the process of acidogenesis. The effect of high hydrogen partial pressure as proposed by Sam-Soon *et al.*, (1991) was included in the model.

2.3.4 UCTSDM3P Model

A 3-phase (aqueous-gas-solid) full element (C, H, O, N, P, S), charge and mass-balanced plant-wide AD model (UCTSDM3P) was developed by (Ikumi *et al.*, 2015). This AD model is a subset of the University of Cape Town (UCT)/University of Kwa-Zulu Natal (UKZN) plant-wide model (PWM_SA) based on the supermodel approach of Jones and Takacs (2004). This approach differed from the transformation approach in that it did not require the use of a transformation matrix through the various unit processes. The physico-chemical states were expressed globally, and the biological components linked through the respective models. The choice of components was done to represent all the unit operations within the plant. Just as in Sötemann *et al.*, (2005) UCTADM1, the organics and biomass involved were expressed through parameterized stoichiometry based on measurements from wastewater. Each component was parameterized based on its COD and molar concentration (Molality) (Brouckaert *et al.*, 2010). Additionally, the dissolved ionic species were represented in the stoichiometric process as the total concentration of the ionic states of the related species. This was useful in determining the pH of a digester by considering the undissociated H^+ ions as opposed to the total H^+ ion concentration. This approach resolved the problems Musvoto *et al.*, (2000) identified and was incorporated into on-going stoichiometric process calculations that simultaneously acted on the various weak acid/base species. The ionic species concentrations are fast and assumed to be in equilibrium allowing them

to be instantaneously determined by algebraic equations in an external speciation routine. The differential kinetic bioprocess mass balanced equations were used to determine changes in the ionic species composition. Like UCTADM1, UCTSDM3P assumed a single hydrolysis process for the particulate feed sewage sludge organics into an idealized intermediate product, glucose. Furthermore, the model included the effects of high hydrogen pressure on the acidogenic process to produce acetate, propionate, and hydrogen and on the acetogenic process where the high hydrogen partial pressure prohibited the conversion of propionate to acetate. This is critical in predicting the stability of the digestion process.

2.3.5 THPAD and TAD modelling

By the late 20th century, few attempts had been made to model the AD process at thermophilic temperatures. The role of free ammonia (NH₃) as an active component in ammonia inhibition had already been observed. This followed from experiments to anaerobically digest livestock waste and manure that contained compounds that readily released ammonia upon breakdown e.g. urea and proteins (Angelidaki and Ahring, 1993; Hansen *et al.*, 1998).

2.3.5.1 TAD Modelling

Studies by Angelidaki and Ahring (1993) observed the inhibition effect of ammonia on anaerobic digestion at a thermophilic temperature of 55°C. These studies included investigations into corresponding activities such as increased VFA concentration and the effect of acclimatization of the organisms to higher ammonia concentrations. Based on these studies (Angelidaki and Ahring, 1993), Angelidaki *et al.*, (1999) developed a comprehensive model of anaerobic bioconversion of complex substrates into biogas. The model involved two enzymatic processes and eight bacterial groups. The hydrolytic steps were expressed in terms of first-order kinetics with inhibition because of the sum of VFA taken on a molar basis, whereas the bacterial steps were based on Monod kinetics with respect to their primary substrate. This model identified the sigmoidal pattern of inhibition in acetoclastic methanogens because of ammonia. It did not, however, consider the alternative process of syntrophic oxidation in the high-rate process. While the model was successful in simulating the process, given that it was developed prior to the ADM1, it contained the same limitations as those highlighted in ADM1.

2.3.5.2 THPAD Modelling

As a result of the simplification of ADM1, the model contained deficiencies from an engineering perspective that restricted it from accurately simulating high-rate digestion processes. Recognizing the inhibitory impact of ammonia at a concentration of 2500 mgNH₄-N/l and a pH above 7.5, Wett *et al.*, (2014) proposed the addition of an ACOX model that:

- Adds acetate oxidation to model high loaded and high temperature anaerobic systems.
- Relates metabolic activity to un-ionised species such as undissociated acetic acid as substrate and un-ionised ammonia as inhibitor.
- Incorporates all chemical species and their activity coefficients allowing for an accurate prediction of pH crucial for CO₂ and NH₃ ionization and gas transfer.

From previous research, it was observed that acetoclastic methane generation was mildly inhibited at low unionised ammonia concentrations whereas a logistic reduction in methanogenesis was observed with increase in the ammonia concentration (Angelidaki and Ahring, 1993).

Using the Activated Sludge Digestion Model (ASDM) as a starting point, and using BioWin™ as a platform, Wett *et al.*, (2009) extended the model to include the Cambi heat treatment step and digestion of the heat-treated sludge. The extensions included the addition of two new processes to the heat treatment step, namely, solubilization of the particulate COD and pasteurization of biomass. Solubilization involves conversion of the slowly biodegradable material (X_s) into readily degradable counterparts i.e., soluble COD content. This step is described empirically by high-rate first-order kinetics as shown in Equation (2-6).

$$r_{max} = k_{Cambi} \cdot X_s \quad (2 - 6)$$

Where:

r_{max} = maximum hydrolysis rate

k_{Cambi} = calibration parameter

X_s = slowly biodegradable organics

The solubilized slowly degradable substrate is directed towards acetate (40%) and readily biodegradable organics (60%) with the N and P fractions being solubilized in parallel kinetic

expressions. The k_{cambi} rate constant is a calibration parameter, and must be selected such that the measured amount of soluble COD (30-40%) is generated in the model (Wett *et al.*, 2009).

For the pasteurization process, 77% of the active biomass is converted to particulate substrate, 20% to endogenous residue and 3% to inert material before feeding the heat-treated sludge into the digester.

Digestion of high concentration heat-treated sludge tends to run at higher pH values which affect ammonia inhibition and kinetics of methanogenesis. Monod inhibition terms were used to describe acetoclastic methanogenesis with proposals for the substitution of the total acetate inhibition term (MS_{Sac}) with the undissociated acetic acid Haldane term (MS_{HAc}) and the addition of a sigmoidal inhibition to describe the inhibition effect as a result of free ammonia concentration increase. The maximum growth rate is dependent on temperature and is first order relative to the active biomass concentration. This gives the following growth rate function as shown in Equation (2-7):

$$r_g = \mu \cdot \theta^{T-20} \cdot X_{ACO} \cdot MS_{HAc} \cdot MI_{O_2} \cdot MI_{NO_2} \cdot MI_{NO_3} \cdot LI_{NH_3} \quad (2-7)$$

The Monod Inhibition (MI) terms as shown in the rate equation above are used to ascertain that the obligate anaerobic biomass only grows in the lack of oxygen, nitrite, and nitrate (i.e., true anaerobic conditions).

The Monod inhibition terms are of the form $MI = K_i/(K_i + S)$. The Haldane term form applied to undissociated acetic acid (HAc) as the substrate is as shown in Equation (2-8):

$$MS_{HAc} = \frac{[HAc]}{K_{Ac} + [HAc] + \frac{[HAc]^2}{K_{i,HAc}}} \quad (2-8)$$

The sigmoidal inhibition as a result of ammonia is represented by the logistic curve as described in Equation (2-9) below:

$$LI_{NH_3} = \frac{1}{1 + e^{(-I_{NH_3} \text{ slope} (I_{NH_3} \text{ halfval} - [NH_3]))}} \quad (2-9)$$

Based on experiments carried out by Wett *et al.*, (2009), the following values were selected for the corresponding parameters:

- $I_{\text{NH}_3 \text{ slope}} = 338$
- $I_{\text{NH}_3 \text{ halfval}} = 12 \text{ mmol}$ (in terms of free ammonia, where 50% inhibition occurs)

The observed ammonia concentrations were observed by the model simulations which included gas transfer and ammonia stripping. In this regard the model developed by Wett *et al.*, (2009) could be used as a tool to evaluate digester configurations (e.g. 2-stage vs single stage) and measures to relieve ammonia inhibition.

2.4 CLOSURE

Anaerobic digestion is one of the oldest methods of treating wastewater. Renewed interest over recent years as a result of the methane recovery potential has led to an increase in research into this treatment method. This literature review outlines the generic processes that take place in anaerobic digestion. This is done with particular reference to technological configurations that have shown an improvement in the generated methane potential as well as enhanced performance with regard to dewaterability and sludge quality, namely thermophilic anaerobic digestion (TAD) and thermal hydrolysis process (THP).

Particular attention is drawn to the problems of instability associated with these high-rate digestion processes. A review of the consortia of microorganisms involved in the AD process, gives better insight into the effect of various products such as high concentrations of ammonia and hydrogen on the process. An understanding of these interactions allows for the opportunity to model this process and thereby draw associations between the different parameters involved. In this regard, various models have been developed in a bid to simulate this high temperature and high-rate process. This literature review gives a comprehensive description of the models developed, highlighting the weaknesses associated with them. Progressive development has been made in the development of thermophilic digestion models with notable changes to inhibition terms leading to a better simulation of the actual AD process.

Comparing the TAD and the THPAD models, it is observed that both configurations undergo the same processes with variations in the extent of exposure to high temperature and pressures and the respective retention times. Similar bio- and physico-chemical processes apply to both

configurations. Of note is that previous models, while able to accurately predict the high-rate processes, did not consider the resultant syntrophic acetate oxidation process that dominates at these higher temperatures. This thesis looks to incorporate the process of syntrophic acetate oxidation along with the organisms that facilitate it in a bid to better simulate the process.

3 DEVELOPMENT OF THE THPAD MODEL

This Chapter describes the development of the steady state and integrated dynamic THPAD model. The chapter begins with (Section 3.1) an overview of the context in which the developed models will be applied. This entails a description of the Cape Flats Wastewater Treatment Works (CFWWTW) detailing not only the process train followed, but also the parameters and measurements of relevant to the development of the integrated THPAD model (e.g., feed characteristics). Additionally, Section 3.1 describes the model setup applied to both the steady state and dynamic AD model as well as the characterization of the influent feed that goes into both models. This is followed by a description of the steady state AD model (Section 3.2) where the characterization of the components of the influent organics are discussed followed by a description of the kinetic equations considered, the stoichiometry and finally the weak acid/base chemistry. Section 3.3 details a description of the counterpart dynamic AD model along with an explanation of the physico-chemical framework, ionic speciation routine and the processes incorporated. This is followed by Section 3.4 where a detailed description of the THP model and the equations that describe the various processes are laid out and explained. Finally, Sections 3.5 and 3.6 conclude the chapter by looking at the analytical procedures that will be used to evaluate the model performances and a brief description of the processes used to evaluate the steady state and dynamic models.

To concisely describe the development of the integrated THPAD model, it is imperative to nominally distinguish the different modelling aspects that make up this model. Following the literature review discussion in Section 2.2 on the different innovations meant to improve anaerobic digestion, the UCTSDM3P model developed by Ikumi (2011) was extended to cater for the thermophilic anaerobic digestion (TAD) pathways primarily facilitated by syntrophic acetate oxidizing bacteria (SAOB). This was done by incorporating the TAD stoichiometry and kinetics into the UCTSDM3P model. This modified AD model will from henceforth be referred to as the 'extended UCTSDM3P model'. Additionally, to account for the thermal hydrolysis process (THP) as described in Section 2.2.2, both a steady state and dynamic THP model were developed and will from henceforth be referred to as the 'THP model'. Once developed, these 2 models were integrated such that the THP model outputs fed into the extended UCTSDM3P model to establish

the integrated THPAD model. This integration followed from speculation that because of the high temperatures and pressures associated with the thermal hydrolysis process pre-treatment, the accelerated breakdown of organics would result in an increased ammonia concentration (as NH_3) that would result in a deterred action by the acetoclastic methanogens and prevalence of the SAOBs, like what would have occurred in a TAD.

Given no experimental data for the integrated THPAD model was available, the parameters adopted for the development of this model were obtained from literature. Hence, while the THPAD model was developed to a rudimentary stage, the main objective of this model was to integrate the THP model and the extended UCTSDM3P model and verify the model through mass balance checks. Additionally, the development of this model would allow for an impact assessment of the inclusion of the THP unit to the AD through a case study of the Cape Flats Wastewater Treatment Works (CFWWTW) allowing for a better-informed decision by stakeholders. As stated in Sub-Section 1.5 of this report, the scope of this project did not include a calibration process.

3.1 PLANT LAYOUT AND MODEL SETUP

As highlighted above and in the objectives in Chapter 1, the primary objective of this project is to develop unit process models for THP and AD, with an approach that allows for their integration to allow for the simulation of THPAD conditions and virtual simulation of the CFWWTW. This Section describes the plant layout of the CFWWTW and model setup for both the WEST- and Excel-based Thermal Hydrolysis Process (THP) and Anaerobic digestion (AD) units.

3.1.1 Cape Flats Wastewater Treatment Works (CFWWTW) Plant Layout

The Cape Flats Wastewater Treatment Works (CFWWTW) is located adjacent to, and south of the Zeekoevlei Nature Reserve, adjoining the suburb of Muizenberg in the south of Cape Town. The WWTW primarily treats wastewater of domestic origin, with a small portion of commercial/industrial wastewater (ca. 5%). The treatment facilities are owned and operated by the City of Cape Town (CCT) where the plant currently handles a total influent wastewater flow of 200,000 m^3/d .

The CFWWTW was designed for nitrification, denitrification, and biological phosphorus removal. The treatment process in the WWTW comprises of primary sedimentation, aerobic digestion, anaerobic digestion, a maturation pond for effluent from the aerobic digesters, and sludge drying beds for effluent from the anaerobic digesters. The thickened primary and activated sludge are anaerobically digested.

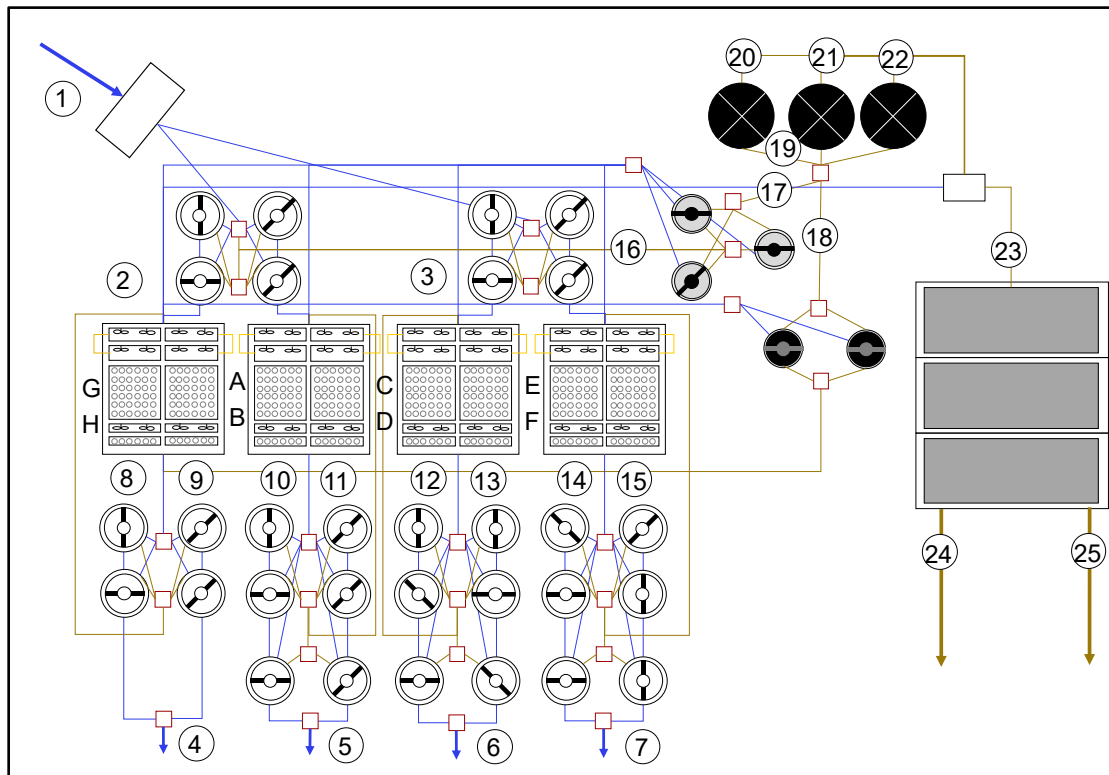


Figure 3.1: Flow diagram of Cape Flats WWTW (adapted from Google Earth) : 1) influent / raw wastewater, 2 and 3) effluent of primary clarification, 4-7) effluent of secondary clarification, 8-15) outflow of activated sludge section, 16) underflow of primary clarification, 17) underflow of primary sludge thickener, 18) overflow of secondary sludge dissolved air flotation unit, 19) influent of anaerobic digestion, 20-22) effluent of anaerobic digestion, 23) mechanical dewatering overflow (non-active), 24) mechanical dewatering underflow to sludge drying beds, 24) sludge to disposal and 25) reject water to pond (Flores-Alsina et al., 2021)

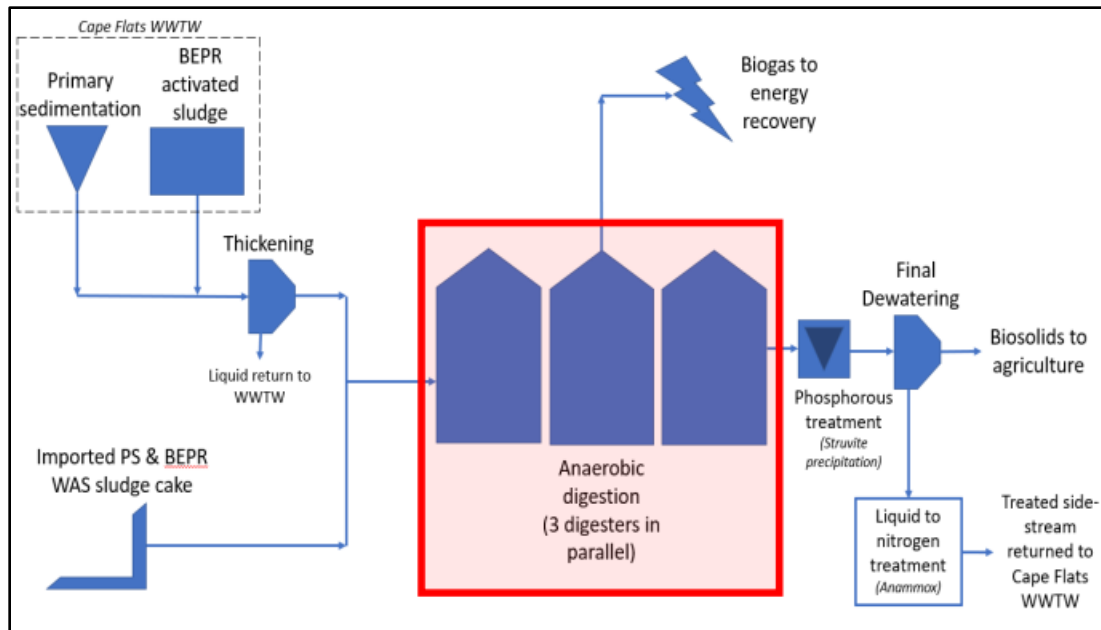


Figure 3.2: Conventional AD schematic (Potts, 2021)

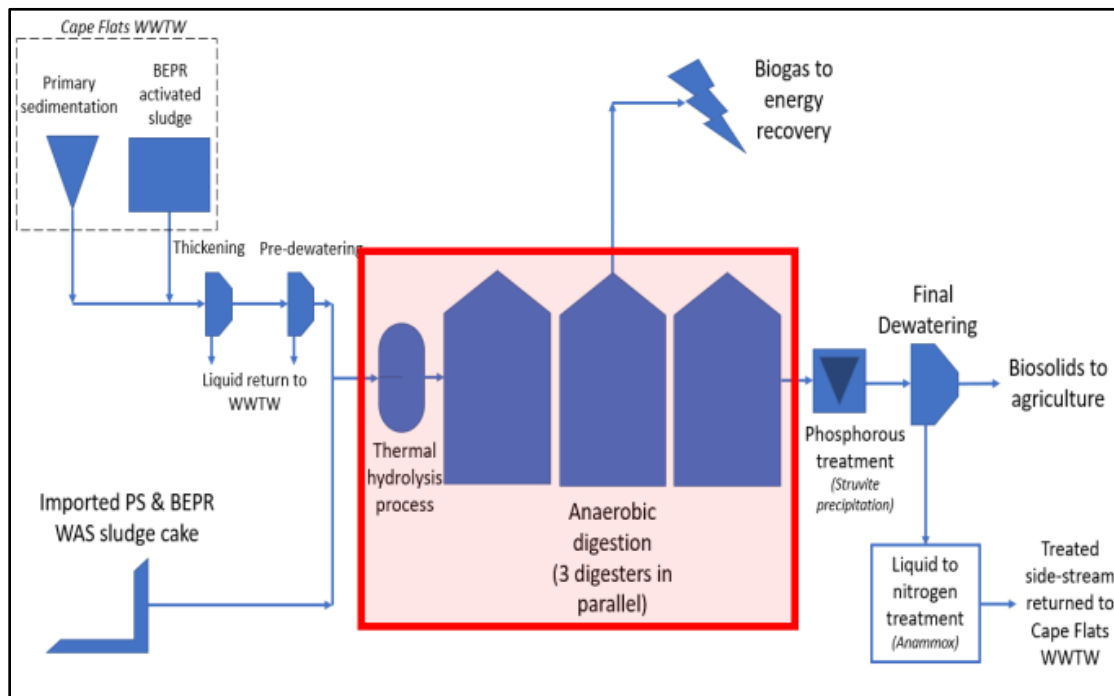


Figure 3.3: THPAD schematic (Potts, 2021)

Figure 3.1 depicts the flow diagram of the overall plant layout, with Figure 3.2 and 3.3 displaying a schematic of the conventional AD and THPAD layout respectively. The following Table 3.1 summarizes the main design characteristics of the CFWWTW AD.

Table 3.1: Cape Flats Wastewater Treatment Works Anaerobic Digester Operating Parameters

AD Operating Parameters		
Parameters	Conventional	THP
Retention time	15	15
WAS in Feed (%)	60	60
PS in Feed (%)	40	40
Sludge age (days)	15	15
Flowrate (m ³ /d)	1257	1257
Solid Concentration (TSS g/l)	47	110
Solid Concentration (VSS g/l)	36.0	84.2
Solid Concentration (ISS g/l)	11.0	25.8
Loading Rate (kgVSS/m ³ /d)	2.4	5.6
No. of Anaerobic Digesters	3	3
Operating Temperature (°C)	37	37
Total Reactor Volume (m ³)	18850	18850

3.1.2 Model Setup

The developed AD model (extended UCTSDM3P) was used to virtually replicate the Cape Flat's Wastewater treatment Works (CFWWTW) AD system and to simulate the impact of including THP in its operation. Figure 3.4 depicts the setup of virtual AD configurations in WEST®. The same virtual replication of the integrated THPAD in CFWWTW that was simulated in WEST® was also used in the simplified Excel steady state model and the two models were run in parallel.

The unit labelled 'Municipality_1' contained the influent concentration into the configuration containing a THP unit. This influent component concentration values are already adjusted for thickening before input into the model. 'Municipality_2' on the other hand, also contained influent component concentrations. The only difference is that these values were for the mesophilic conditions.

For the thermal hydrolysis process (THP) case, in addition to the same AD configurations, a thermal hydrolysis process pre-treatment unit labeled 'THP_1' preceding the AD unit was modelled to operate between 150 – 180°C.

The units labeled 'Sensor_1' and 'Sensor_2' were added onto the WEST® model in order to be able to track the concentrations in Chemical Oxygen Demand (COD) equivalents from the influent or the THP unit into the anaerobic digesters. The function of the sensors was therefore to convert the incoming concentrations from the mass equivalent concentration to the COD equivalent concentration.

The units labeled 'AD_1' and 'AD_2' represent the anaerobic digesters both operated at mesophilic conditions. These units were coded with the relevant parameters that enabled the simulation to replicate the CFWWTW anaerobic digesters.

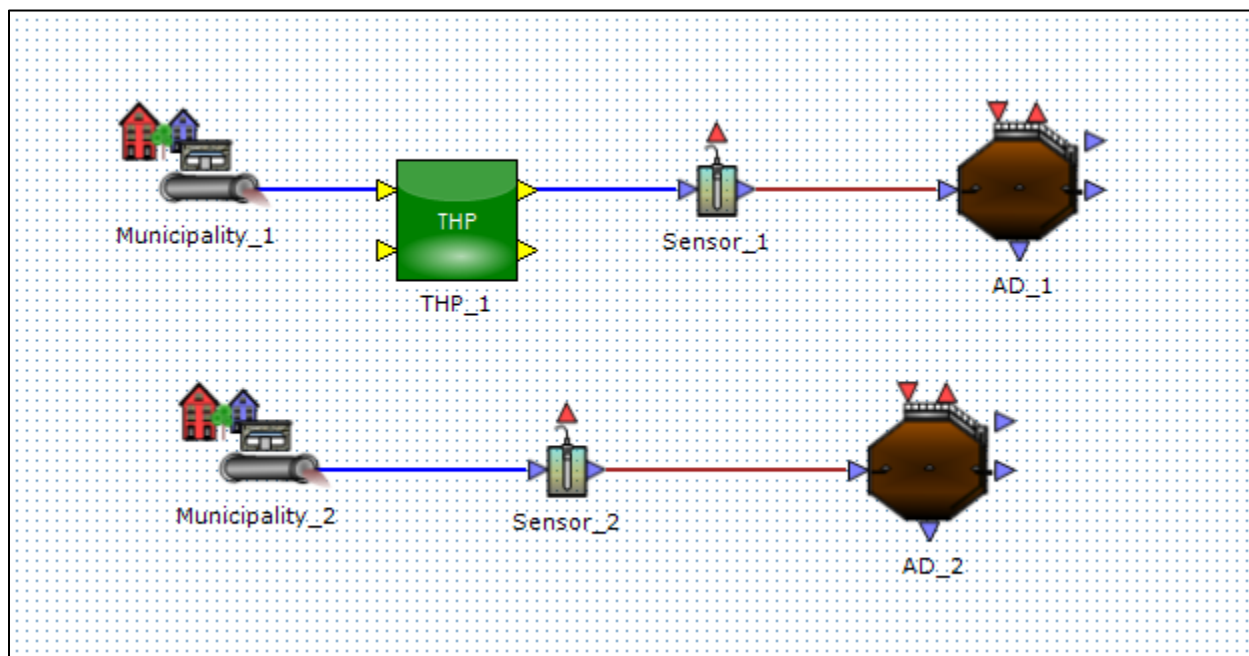


Figure 3.4: Virtual Setup of AD configurations

3.1.3 Feed

In order to successfully develop, compare and evaluate the anaerobic digestion models, a baseline influent wastewater composition was used for both models. Influent feed data was obtained from experiments carried out by Ikumi (2011) where he characterized PS sludge from Athlone Wastewater Treatment Plant and WAS from operating a Nitrification-Denitrification Excess Biological Phosphorus Removal (NDEBPR) system at a 10-day sludge age using settled

wastewater samples from Mitchell's Plain wastewater treatment plant. Using the wastewater characteristics from the works of Ikumi (2011), along with the Cape Flats AD design parameters depicted in Table 3.1 (Section 3.1.1), the influent wastewater composition and subsequent substrate flowing into the THP and AD unit was calculated. Since this was a desktop comparative study and no data directly from the CFWWTW influent sludge was available, Ikumi (2011) data was accepted as a significant portion of the sludge to be processed in the CFWWTW AD is from the Athlone WWTW transported to CFWWTW for processing.

In section 2.2.2 and 2.2.3 of the literature review section, we saw that incorporation of the THP unit resulted in 2-3 times increase in hydrolysis and subsequently loading rates into the anaerobic digesters (Ho *et al.*, 2013). Consequently, as can be seen from Figure 3.2 and 3.3, a thickening unit is provided after the primary settling tank and activated sludge reactor in order to thicken the influent sludge concentration into the anaerobic digesters. For the configuration without the incorporation of the THP unit (conventional setup), the influent wastewater was thickened to a concentration of 4.7% whereas the configuration involving the incorporation of a THP unit thickened the influent wastewater to a concentration of 11% as can be observed from Table 3.1 above.

The PS and WAS mixture was broken down and characterized into 8 groups: organisms (Orgs), fermentable soluble organics (SF), unbiodegradable soluble organics (SU), PS biodegradable particulate organisms (XBOrg), PS biodegradable particulate organics (XBInf), unbiodegradable particulate organics (XUInf), endogenous residue (XUOrg) and volatile fatty acids (VFA). Based off measurements taken and following procedures as laid out by Ikumi (2011), the elemental compositions (i.e., X,Y,Z,A,B corresponding to Carbon, Hydrogen, Oxygen, Nitrogen and Phosphorus, respectively) of the different groups in the wastewater were established with the carbon subscript X equal to 1. These elemental values were deemed acceptable as Ikumi (2011) obtained an acceptable mass balance over the AS and PST system for the WAS and PS elemental compositions respectively. The elemental composition for the different groups is as shown in Table 3.2.

Table 3.2: Influent Wastewater Component Compositions

Compositions		C	H	O	N	P	MM	COD	f _{cv}
Org	organisms	1	1.534	0.421	0.166	0.019	23.21	34.312	1.479
SF	fermentable soluble	1	1.942	0.681	0.030	0.008	25.53	36.240	1.419
SU	unbiodegradable soluble	1	1.833	0.600	0.086	0.000	24.66	35.000	1.419
XBInf	PS biodegradable particulate	1	1.623	0.577	0.032	0.008	25.57	35.304	1.498
XBOrg	biodegradable particulate	1	1.534	0.421	0.166	0.019	23.21	34.312	1.479
XUInf	unbiodegradable particulate	1	1.534	0.421	0.166	0.019	23.21	34.312	1.48
XUOrg	endogenous residue	1	1.534	0.421	0.166	0.019	23.21	34.312	1.479
VFA	Volatile Fatty Acids	2	3	2	0	0	59.04	63.996	1.084

Once the elemental compositions from the different groups were chosen, the mass of COD in a molecule was calculated as follows in Equation (3-1).

$$COD = 8 * (4X + Y - 2Z - 3A + 5B) \quad (3 - 1)$$

The molar mass for the various groups was calculated as shown in Equation (3-2).

$$MM = (12.011 * X) + (1.0079 * Y) + (15.999 * Z) + (14.007 * A) + (30.974 * B) \quad (3 - 2)$$

The mass of COD per mole (f_{cv}) for the different groups was calculated by the respective COD/MM ratio. Once the f_{cv} was established, the remaining molar ratios f_c, f_n, f_h and f_o were calculated as shown in Equations (3-3)-(3-7).

$$f_c = \frac{12.011 * X}{MM} \quad (3 - 3)$$

$$f_n = 14.007 * \frac{A}{MM} \quad (3 - 4)$$

$$f_p = 30.974 * \frac{B}{MM} \quad (3 - 5)$$

$$f_o = 15.99 * \frac{Z}{MM} \quad (3 - 6)$$

$$f_h = 1.0079 * \frac{Y}{MM} \quad (3 - 7)$$

Once obtained, the molar ratios were summed together to ensure they added up to a value of 1 as a check for all the groups.

The wastewater measurements such as the Chemical Oxygen Demand (COD), Volatile Suspended Solids (VSS), Nitrogen (N), Carbon and Phosphorus (P) concentrations for both the primary sludge and waste activated sludge could now be computed. The wastewater composition was subdivided into the biodegradable (BPO) and unbiodegradable particulates (UPO), the unbiodegradable soluble organics (USO), volatile fatty acids, fermentable soluble organics (F-BSO) and inorganics. Given the concentration of the soluble organics (VFA, USO and F-BSO) and inorganics (NH_4^+) do not change regardless of the reactor size, these were modelled to be input directly from measurements in the Excel-based model.

Employing the VSS/TSS ratio and the unbiodegradable fraction ($f_{s'up}$) for both PS and WAS from experimental works by Ikumi (2011), the UPO COD was calculated as shown in Equation (3-8).

$$UPO \text{ COD} = \frac{(-f_{cv} * X_v * 1000) - (USO + FBSO + VFA)}{\left(1 - \frac{f_{cv,BPO}}{f_{cv,UPO}} - \frac{1}{f_{s'up}}\right)} \quad (3 - 8)$$

Where:

X_v = volatile settleable solids (VSS) concentration for either the PS (3.8%) or WAS (3.5%) which can be calculated using the selected reactor total solids concentration and the VSS/TSS ratio and

$f_{s'UP} = 0.36$ for PS and 0.53 for WAS

Following the calculation of the PS and WAS UPO COD, it was then possible to compute the UPO VSS using $f_{cv,UPO}$ as follows in Equation (3-9).

$$UPO \text{ VSS} = \frac{UPO \text{ COD}}{f_{cv,UPO}} \quad (3 - 9)$$

Once the UPO VSS was established, it was possible to compute the BPO VSS as no soluble organics are contained in the VSS and therefore subtracting the UPO VSS from the total volatile settleable

solids would leave the BPO VSS as the resulting value. With the BPO VSS established, the BPO COD was obtained by multiplying the BPO VSS by the $f_{cv,BPO}$. The corresponding elemental concentrations for the nitrogen, phosphorus and carbon were then computed by use of the f_{cv} and the respective molar ratios.

For example, for the carbon content contained in the PS and WAS UPO, BPO, VFA, FBSO and USO, the following Equations (3-10)-(3-14) were used:

$$UPO\ C = UPO\ VSS * f_{c,UPO} \quad (3 - 10)$$

$$BPO\ C = BPO\ VSS * f_{c,BPO} \quad (3 - 11)$$

$$VFA\ C = VFA\ COD * \frac{f_{c,VFA}}{f_{cv,VFA}} \quad (3 - 12)$$

$$FBSO\ C = FBSO\ COD * \frac{f_{c,FBSO}}{f_{cv,FBSO}} \quad (3 - 13)$$

$$USO\ C = USO\ COD * \frac{f_{c,USO}}{f_{cv,USO}} \quad (3 - 14)$$

The same equations with the respective adjustments can therefore be used to calculate the concentration of the different elemental components in the different groups for both PS and WAS after which the total concentration can be added and obtained.

Following the calculation of the PS and WAS compositions, the influent feed characteristics for the blended sludge was calculated. A ratio of PS:WAS of 60:40 (same ratio as that used in CFWWTW) was selected for the simulations and so an example of the formula using BPO COD for the blended sludge computations is as shown in Equation (3-15).

$$BPO\ COD = (60\% * PS\ BPO\ COD) + (40\% * WAS\ BPO\ COD) \quad (3 - 15)$$

The same equation was applied to obtain the various blended concentrations of the different influent wastewater component compositions. A notable distinction was made in the biodegradable material from WAS and that from the PS (i.e., [X_B_Org] and [X_B_Inf], respectively as stated in Table 3.2). The biodegradable material from WAS is assumed to comprise the respective organism compositions as it was assumed that the sludge from WAS does not contain any biodegradable material from the wastewater besides that from the growth of the organisms that facilitate the breakdown of the organic material. Indeed, [X_OHO] and [X_PAO] were the only organism masses that were significant in the simulations tested in this project and consequently an OHO/PAO split ratio of 0.55 on the WAS BPO was selected.

Once the influent feed was established for both the conventional and THP AD case, a uniform input into both the steady state and dynamic model was guaranteed. A pre- and post-processor were used to convert between the excel-based model and the WEST-based model.

3.2 STEADY STATE AD MODEL

In developing the integrated dynamic THPAD model, a counterpart steady state model was developed in parallel in order to take advantage of the complementary uses of the excel-based model. Steady state models allow for the sizing of system design parameters such as reactor volumes and recycle flows to allow for sufficient digestion of the influent wastewater. These values could then be employed in the dynamic model dealing with varying flows and material loads. This avoids the need for tedious trial and error attempts that would have been required in dynamic models in order to optimize the design parameters.

A steady state model for the anaerobic digestion (AD) containing a blend of primary and secondary sludge is presented. The steady state model developed was an extension of the model developed by Ikumi (2011) and similar to that by Potts (2021). Consequently, similar to the modifications by Sötemann *et al.*, (2005) the biodegradable particulate organics were presented in a generic composition i.e. $C_xH_yO_zN_A P_B$. As described in Section 2.2.2 of this project, hydrolysis was identified as the rate-limiting step of the AD processes. Therefore, the AD processes that proceeded hydrolysis were calculated stoichiometrically to yield the digester end products i.e., CH_4 , CO_2 and water. The steady state AD model as explained by Ikumi (2011) contains 3 sequential parts:

1. A COD based kinetic part from which the concentration of biodegradable COD utilization, methane and sludge production are determined for a given AD sludge age
2. A COD, C, H, O, N, P and charge mass balance stoichiometry part from which gas production and composition, NH_4 released, biomass produced, and alkalinity generated are calculated from the biodegradable COD removed.
3. A 3-phase mixed inorganic carbon and ortho-phosphate weak acid/base chemistry from which the digester pH and mineral precipitation are calculated.

3.2.1 Component Characterization and Elemental Composition

Prior to inputting the influent flow into the steady state model, the wastewater components and elemental compositions had to be determined. The wastewater components comprised biodegradable and unbiodegradable particulate and soluble organics with the biodegradable soluble organics further differentiated into volatile fatty acids (VFAs) and fermentable readily biodegradable organics (F-RBCOD). The detail on the characterization procedure of the wastewater can be obtained in the Appendix 7.1 at the end of this report. The blend of sludge from the primary settling tank and waste activated sludge was then computed as elaborated in Section 3.1.3 on feed.

Following the characterization of the blend, the wastewater elemental composition was then carried out as explained in the works of Ikumi (2011). The mass ratios (f_{cv} , f_n , f_p , f_o and f_h) for both the PS and WAS sludge were obtained from experimental works of Ikumi (2011). Assuming the hydrogen elemental ratio (Y) was set to 7, the influent characteristic components (BPO, UPO, USO, VFA and RBCOD) were transformed into the carbon (C), hydrogen (H), nitrogen (N), oxygen (O) and phosphorus (P) elemental compositions (X, Y, Z, A and B) using the respective mass ratios as shown in Table 3.3.

Table 3.3: Elemental Composition Equations

Elemental Denotation	Elemental Expression
X	$= \frac{C}{MM} \frac{(Y + 16Z)}{12. [1 - (\frac{C}{MM}) - (\frac{N}{MM}) - (\frac{P}{MM})]}$
Z	$= \frac{y [1 - (\frac{COD}{8.MM}) - (\frac{8.C}{12.MM}) - (\frac{17N}{14.MM}) - (\frac{26.P}{31.MM})]}{2 [1 + (\frac{COD}{MM}) - (\frac{44.C}{12.MM}) + (\frac{10.N}{14.MM}) - (\frac{71.P}{31.MM})]}$
A	$= \frac{N}{MM} \frac{(Y + 16Z)}{14. [1 - (\frac{C}{MM}) - (\frac{N}{MM}) - (\frac{P}{MM})]}$

B	$= \frac{P}{MM} \frac{(Y + 16Z)}{31. [1 - (\frac{C}{MM}) - (\frac{N}{MM}) - (\frac{P}{MM})]}$
---	---

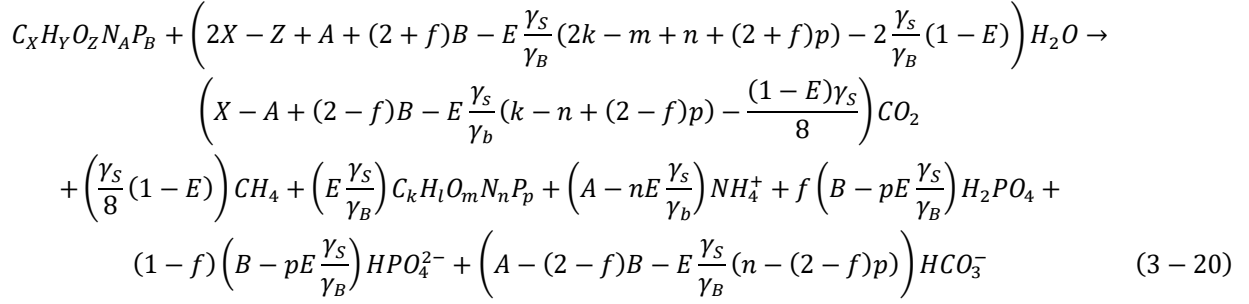
The determination of the influent PS and WAS elemental compositions is required for the CHONP, COD and charge mass balance in the AD model.

3.2.2 Stoichiometric Model for the Steady State AD

The stoichiometric equations used in the model are derived from the electron donors and acceptors involved in the AD bioprocess as was investigated by McCarty (1975). Sötemann *et al.*, (2005) used the method described by McCarty (1975) to develop a two-phase (aqueous-gas) steady state model to describe the AD of organics based on the C, H, O, N, P and COD mass balanced stoichiometry. Harding (2009) then extended the steady state model to include biomass P and polyphosphate (PP) in NDBEPR WAS and so included P and metals (magnesium, potassium, and calcium) mass balanced stoichiometry.

Given the stoichiometry is based on the balance of the electrons donated by the organics and the electrons accepted by the AD products, it was important to determine the elemental composition of the organics going into the AD and that of the organism mass as a result of cell growth (anabolism). As described in Section 3.2.1 on component characterization and elemental composition, it was possible to determine the wastewater blend elemental composition going into the AD. Additionally, based on the mass ratios for the biomass as obtained from the experimental works of Ikumi (2011), it was possible to derive the elemental composition of the organism mass formed through anabolism.

Now, if a fraction E of the electrons donated are captured in sludge mass, then the fraction that is used in the formation of methane is (1-E). Subsequently, the generic expression of the mass balanced stoichiometric equation for the AD process could be described as follows in Equation (3-20):



Where:

- X, Y, Z, A and B refer to the influent organic elemental compositions as calculated from Table 3.3.
- k, l, m, n, and p refer to the AD biomass elemental composition as calculated from the mass ratios obtained experimentally, and in this case taken from investigations carried out by Ikumi (2011)
- f refers to the fraction of $H_2PO_4^-$ in the total phosphate species (mainly $H_2PO_4^-$ and HPO_4^{2-}) in equilibrium and dependent on the pH
- Y_S and Y_B refers to the electron donating capacity of the organics and the AD biomass respectively and is calculated as follows:

$$Y_S = 4X + Y - 2Z - 3A + 5B$$

$$Y_B = 4k + l - 2m - 3n + 5p$$

And

- E is the fraction of biodegradable COD that is converted to biomass (Z_{AD})

$$E = \frac{Z_{AD}}{S_{bpi} - S_{bpe}} = \frac{Y_{AD}(1 + b_{AD}R_s)}{[1 + b_{AD}R_s(1 - Y_{AD})]}$$

Where:

- Y_{AD} is the yield coefficient (gCOD biomass formed/ gCOD organics utilized)
- b_{AD} is the acidogen endogenous respiration rate (/d)
- R_s is the digester sludge age (days)

3.2.3 Weak Acid/Base Chemistry

From the stoichiometry, it can be observed that while the anaerobic digestion process is primarily facilitated by the organics and organisms present in the bulk medium, they are not the only

participants that have an effect on the process. Some of the chemical species involved belong to one of the many weak acid/base systems that exist simultaneously in solution. Loewenthal *et al.*, (1994) and Musvoto *et al.*, (2000) described the influence of the digester pH on the molar concentrations of the chemical species within each of these sub-systems using a set of equilibrium and mass balance equations as shown in the following Tables 3.4 and 3.5:

Table 3.4: Equilibrium Equations

Sub-system	Equilibrium Equations
Carbonate sub-system (C_T)	$K'_{c1} = \frac{(H^+)[HCO_3^-]}{[H_2CO_3^*]}$
	$K'_{c2} = \frac{(H^+)[CO_3^{2-}]}{[HCO_3^-]}$
Ammonia sub-system (N_T)	$K'_N = \frac{(H^+)[NH_3]}{[NH_4^+]}$
Phosphate sub-system (P_T)	$K'_{p1} = \frac{(H^+)[H_2PO_4^-]}{[H_3PO_4]}$
	$K'_{p2} = \frac{(H^+)[HPO_4^{2-}]}{[H_2PO_4^-]}$
	$K'_{p3} = \frac{(H^+)[PO_4^{3-}]}{[HPO_4^{2-}]}$
Acetate sub-system (A_T)	$K'_{A1} = \frac{(H^+)[Ac^-]}{[HAc]}$
Water sub-system	$K_w = (H^+)(OH^-)$

Where (H^+) is the hydrogen ion activity, $[X]$ the molar concentration of the species 'X' and K_X the thermodynamic constant for the species X adjusted for Debye-Huckel effects to account for ion activity in solutions higher concentrations.

Table 3.5: Mass Balance Equations

Mass Balance Equations	
C_T	$[H_2CO_3] + [HCO_3^-] + [CO_3^{2-}]$
N_T	$[NH_4^+] + [NH_3]$
P_T	$[H_3PO_4] + [H_2PO_4^-] + [HPO_4^{2-}] + [PO_4^{3-}]$

A_T	$[HAc] + [Ac^-]$
-------	------------------

The AD stoichiometric and kinetic model as described in Sections 3.2.2 and 3.2.3 above were used to determine the aqueous concentrations of the weak acid/base species as final AD products (HCO_3^- , HPO_4^{2-} , NH_4^+ , Ac^- , etc.). These aqueous concentrations were then employed to obtain the total species concentrations as shown in Table 3.5 above. This is in accordance with investigations by Loewenthal *et al.*, (1994), where they noted that the total species of the various weak acid/base sub-systems (C_T , P_T , N_T and A_T) had to be determined before speciation could be carried out.

Depending on the nature of the sludge to be treated, specific weak acid/base sub-systems play a more significant role in determination of the system pH. For example Sötemann *et al.*, (2005) noted that the pH established in an AD system treating PS and ND WAS is primarily affected by the inorganic carbon system. Although other weak acid/base systems are present such as the phosphate, ammonia and SCFA sub-systems, they do not significantly affect the pH either because their concentration in the system is too low or their pK values do not fall within the normal pH range of AD systems (for VFA $pK_a = 4.7$ and ammonia $pK_n = 9.1$ sub-systems).

For the inorganic carbon system, while the stoichiometric AD model can be used to determine the bi-carbonate concentration generated, the H_2CO_3 species exists at equilibrium in both the gaseous CO_2 and aqueous ($H_2CO_3^*$) phase. Additionally, investigations by Moosbrugger *et al.*, (1993) revealed that the gas-liquid equilibrium within the AD is dependent on the partial pressure of the gas phase. This CO_2 partial pressure is calculated as shown in Equation (3-21) below using the molar concentrations of CO_2 and CH_4 which can be obtained from the stoichiometric model as shown in Section 3.2.3 above. CH_4 is insoluble and so does not participate in the aqueous phase reactions

$$p_{CO_2} = \frac{[CO_2]_g}{[CO_2]_g + [CH_4]_g} \quad (3 - 21)$$

Since in the steady state the dissolved CO_2 species in the aqueous phase [$H_2CO_3^*$] is in equilibrium with the partial pressure p_{CO_2} in the headspace, it can be determined using Henry's Law expression as follows in Equation (3-22) (Loewenthal *et al.*, 1994).

$$[H_2CO_3^*] = k_{HCO_2} \times p_{CO_2} \quad (3 - 22)$$

Where:

K_{HCO_2} = Henry's Law constant which is 1.59 at 37°C

Given the aqueous and gas phases of CO_2 can be determined, and the HCO_3^- concentration through the stoichiometric model, the (H^+) and subsequently the pH of the system can be determined using the known kinetic (K'_H) and thermodynamic (K'_{c1} and K'_{c2}) constants as well as the mass balance and equilibrium equations.

Where the phosphate species are included in the AD stoichiometry such as for the NDBEPR WAS system used in this project, the P_T system is included as it significantly affects the AD pH through the second dissociation constant $pK_{p2} = 7$. As can be seen from the general stoichiometric model in Section 3.2.3 and the equilibrium equations in Table 3.4, the f value that fractionates the phosphate species as AD products is required for the AD pH calculation (Harding, 2009). Accepting that $P_T = [H_2PO_4^-] + [HPO_4^{2-}]$ i.e. $[H_3PO_4]$ and $[PO_4^{3-}]$ are insignificant within the pH range of 5 – 9, then the f value can be related to the pH and second dissociation constant pK_{p2} as shown in Equations (3-23) – (3-25):

$$[H_2PO_4^-] = fP_T = f \left[B + q - pE \frac{\gamma_s}{\gamma_B} \right] \quad (3 - 23)$$

And

$$[H_2PO_4^-] = \frac{P_T}{1 + 10^{pH - pK_{p2}}} \quad (3 - 24)$$

So:

$$f = \frac{1}{1 + 10^{pH - pK_{p2}}} \quad (3 - 25)$$

As noted by Ikumi (2011) and Harding (2009), this iteration procedure for calculating pH can be used when predicting the AD pH for systems where precipitation takes place but the mineral that is precipitated must be included in the stoichiometry as part of the AD products. This is because the precipitation would cause a change in some of the AD products as they change state from liquid to solid phase and hence influence the final digester pH and p_{CO_2} .

In order to have a convenient way to deal with these state changes due to chemical changes, Loewenthal *et al.*, (1991) used proton donating and accepting capacity parameters termed as

alkalinities and acidities respectively. The following Equations (3-26)-(3-30) below describe the total alkalinity, where the proton balance is based on the weak acid reference species in the most protonated form. Following the nomenclature by Loewenthal *et al.*, (1989), where Alk as a suffix includes the water species and Alk as a prefix excludes the water species then:

- Inorganic Carbon:

$$H_2CO_3^* Alk = [HCO_3^-] + 2[CO_3^{2-}] + [OH^-] - [H^+] \quad (3-26)$$

- Phosphate:

$$Alk H_3PO_4 = [H_2PO_4^-] + 2[HPO_4^{2-}] + 3[PO_4^{3-}] \quad (3-27)$$

- Ammonia:

$$Alk NH_4^+ = [NH_3] \quad (3-28)$$

- Acetate:

$$Alk HAc = [Ac^-] \quad (3-29)$$

Therefore, for a mixture of inorganic carbon, phosphate, ammonia, and acetate weak acid/base subsystems:

$$\begin{aligned} Total Alk &= [HCO_3^-] + 2[CO_3^{2-}] + [H_2PO_4^-] + 2[HPO_4^{2-}] + 3[PO_4^{3-}] + [NH_3] + [Ac^-] + [OH^-] - [H^+] \\ &= [HCO_3^-] + 2[CO_3^{2-}] + [H_2PO_4^-] + 2[HPO_4^{2-}] \text{ for the pH range between 6 - 8} \end{aligned} \quad (3-30)$$

3.2.3.1 Struvite precipitation in an Anaerobic Digester

During the hydrolysis of BEPR WAS, metals such as magnesium, potassium, calcium and even phosphates from polyphosphates are released into the AD liquor along with the other species (ammonia and inorganic carbon species) as part of the AD products. Under certain conditions when the dissolved concentrations in the AD are significantly high mineral precipitation begins to occur in the AD liquor. In this project, the main mineral precipitate that was focused on was struvite ($MgNH_4PO_4$). The determination of the amount of precipitate formed is dependent on the comparison of the ionic product of the soluble AD products with the thermodynamic solubility product (K_{spm}) of the struvite in this case.

Therefore, struvite precipitation occurs when the ionic product of the molar activity of Mg^{2+} , NH_4^+ and PO_4^{3-} in solution exceeds the thermodynamic solubility product of struvite ($K_{spm} = 12.6$ at $25^\circ C$) in the aqueous phase (Loewenthal *et al.*, 1994).

$$[Mg^{2+}][NH_4^+][PO_4^{3-}] = \frac{K_{spm}}{f_d f_m f_t} = K'_{spm} \quad (3 - 31)$$

Where f_m , f_d and f_t , are the activity coefficients of mono-, di- and tri-valent ionic species. The equation above shows that struvite will continue to dissolve into or precipitate out of solution until equilibrium exists between the aqueous Mg^{2+} , NH_4^+ and PO_4^{3-} concentrations in the aqueous phase and the ionic product K_{sp} .

3.3 DYNAMIC EXTENDED UCTSDM3P MODEL

Dynamic models are tools that are used to establish relationships between plant inputs (influent wastewater) and the observed outputs (treated effluent) using ordinary and partial differential equations which seek to mimic the reaction mechanisms (Ikumi, 2011). In this way, they complement steady state models. Their uses include:

- Forecasting wastewater treatment plant performance
- Explaining behavioural performances that occur within a treatment plant and hence train operators on the effects various decisions have on the plant's performance.
- Evaluation of the system responses to dynamic conditions.
- To establish better design and operational procedures through trying out various configurations that may result in cost savings.
- To assess the components and parameters that are of significance to the dynamic model through a rigorous sensitivity analysis (Ikumi, 2011).

The development of dynamic model involves ensuring that the fundamental system processes are represented and coded in a mathematically tractable manner such that the model is capable of providing realistic predictions (Ikumi, 2011). The Gujer matrix provides a flexible system into which the kinetics and stoichiometry of the system processes can be captured. The matrix is comprised of rows and columns, where each row represents a process and each column a component. The relevant kinetic rates are displayed to the right-end of the matrix on the same row as the coefficients of the respective process. Negative coefficients represent utilization of the respective component whereas positive coefficients represent generation of the respective

component. Therefore, the summation of the stoichiometric coefficients across all components and along any selected process would result to a total of zero, ensuring continuity in the respective equations representing the various processes.

This Section hereby gives insight into the development of the model through a model description where the modelling framework, the ionic speciation routine as well as the processes added to the Extended-UCTSDM3P model were discussed. A comprehensive description of the terminologies used in this dynamic model as well as the components, parameters and variables employed can be found in Appendix 7.3 at the end of this report.

3.3.1 Model description of the Extended-UCTSDM3P

The Extended-UCTSDM3P model developed in this project accounted for the inclusion of processes due to thermophilic conditions and was a modification of the UCTSDM3P subset model of the PWM_SA model developed by Ikumi *et al.* (2015) and Ghoor (2020). Consequently, the model components were selected such that all the features of the PWM_SA model were present. All components in the model have distinctive chemical composition formulations allowing for the direct calculation of the molar and material (COD, C, H, O, N and P) balances. The inorganic and some organic (VFA) component compositions are known whereas other organic components such as the organism and sewage components (i.e., USO, UPO, FBSO, BPO and BSO) were given parameterized compositions in their generalized form in order to allow for their compositions to be entered as model inputs (Ikumi, 2011). For example, all organism groups were given the same elemental formulation of $C_{x_o}H_{y_o}O_{z_o}N_{A_o}P_{B_o}$ (where 'o' denotes the various organism material elemental formulation) with each organism component coded to carry out its respective function. The elemental molar ratios (i.e., X, Y, Z, A and B) for the sewage compositions were expressed as model parameters in order to cater for the variable nature of the sewage. Additionally, these elemental molar ratios were obtained by use of empirically formulated relationships and routinely taken measurements at a treatment plant i.e., COD, TKN, TOC, TP and VSS which is an advantage of this model (Sötemann *et al.*, 2005).

Through the use of an external algebraic equation equilibrium speciation sub-routine, issues of model stiffness associated with the incorporation of fast and slow bioprocesses are alleviated. The model developed by Brouckaert *et al.*, (2010) allows for the calculation of pH, gas partial

pressure and ionic concentrations for wastewater of high ionic strength. It uses non-ideal determination of dissociation constants which allows for the modelling of physical, chemical, and biological processes of systems at high ionic strength.

Lastly, given the model is a 3-phase model, it contains the effects of mineral precipitation on the pH and ionic strength of the system as a result of phosphate, ammonia, and inorganic carbon releases in the AD.

Generally speaking, the model seeks to simulate a combination of physical, chemical, and biological processes that occur at different rates. Essentially, the model allows us to replicate the processes by determining the amount of materials at a particular time in the system and determining the physical state that it will take on at that point (Ghoor, 2020; Brouckaert *et al.*, 2010). The hierarchical approach in the processes and entities and their interrelationships is described in the physicochemical framework shown in Figure 3.5.

3.3.2 PWM_SA Physico-Chemical Model Framework

The underlying objective of this approach is to incorporate the different rates of reactions that take place in the anaerobic digestion process. The PWM_SA model and its subset, the UCTSDM3P, incorporate a framework that enables a model to separate the fast and slow biological processes.

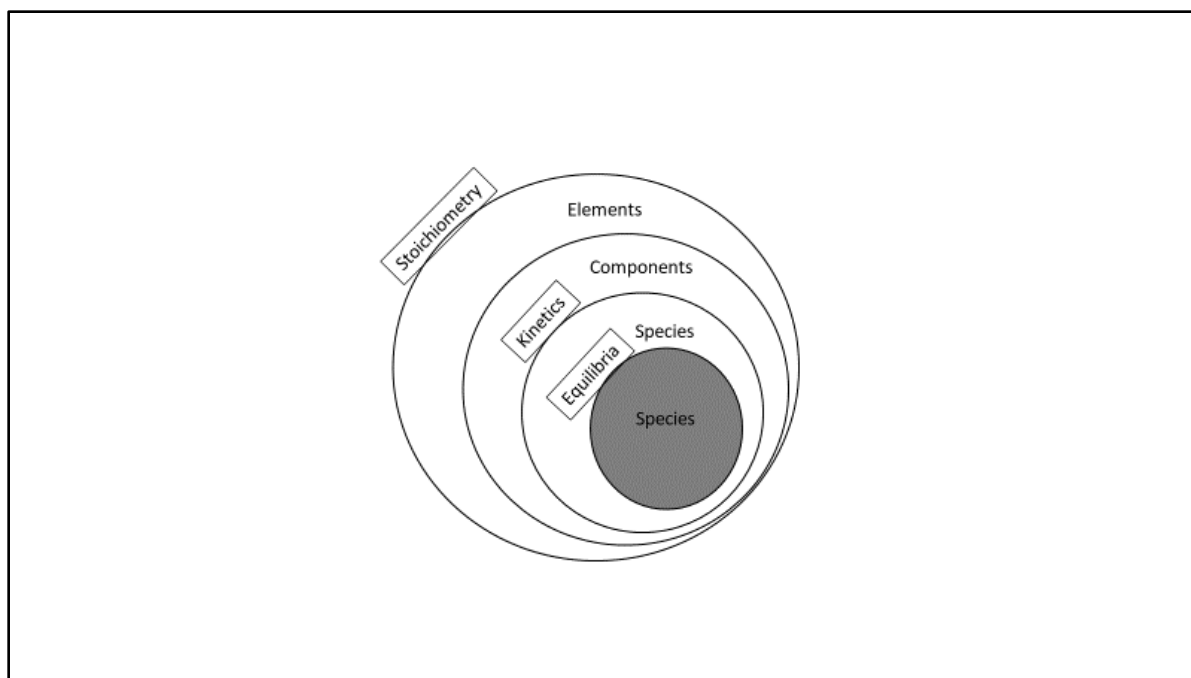


Figure 3.5: Physico-Chemical Modelling Framework (Ghoor, 2020)

The Figure 3.5 above shows that the mass balance of the material content (stoichiometry) applies throughout with the mass elements (C, H, O, N, P & charge) representing this material content. Species are the material entities that describe the actual physical state of the material content. This is carried out either through the algebraic equilibrium equations governed by the thermodynamic behavior of the species or through the use of kinetic constants that are used to define the endpoint for processes that do not reach equilibrium. The processes that do not reach equilibrium require calibration of the kinetic constants. As for the processes that do reach equilibrium, no calibration is required as the endpoints are defined by relatively fast equilibrium processes well defined by their thermodynamics.

3.3.3 Ionic Speciation Routine

As mentioned in the physico-chemical framework sub section, through the incorporated model developed by Brouckaert *et al.* (2010), the rapidly occurring ionic speciation reactions were separated from the slower bioprocesses governed by process kinetics. Brouckaert *et al.* (2010) expressed the model components as the total concentrations of the respective reference species used to define the material balances. Employing sets of aqueous phase equilibrium dissociation and mass balance equations, the detailed speciated equilibrium position of the solution is

obtained relatively instantaneously for every time step in the dynamic simulation. The ion pairs that can be formed from the aqueous ionic concentrations are as listed in Table 3.6.

Table 3.6: THPAD Ionic Species

Ionic Species Selected for THPAD Modelling					
1	H ⁺	Hydrogen ion	23	NH ₄ SO ₄	Ammonium sulphate
2	Na ⁺	Sodium	24	MgPO ₄	Magnesium phosphate
3	K ⁺	Potassium	25	CaCH ₃ COO ⁺	Calcium acetate
4	Ca ²⁺	Calcium	26	CaCH ₃ CH ₂ COO ⁺	Calcium propionate
5	Mg ²⁺	Magnesium	27	CaHCO ₃ ⁻	Calcium bicarbonate
6	NH ₄ ⁺	Ammonium	28	NaSO ₄	Sodium sulphate
7	Cl ⁻	Chlorine	29	MgHPO ₄	Magnesium hydrogen phosphate
8	CH ₃ COO ⁻	Acetate	30	CH ₃ COONa	Sodium acetate
9	CH ₃ CH ₂ COO ⁻	Propionate	31	H ₂ CO ₃	Di-hydrogen carbonate
10	CO ₃ ²⁻	Carbonate	32	MgSO ₄	Magnesium sulphate
11	SO ₄ ²⁻	Sulphate	33	HPO ₄ ⁻	Hydrogen phosphate
12	PO ₄ ³⁻	Phosphate	34	NH ₃	Ammonia
13	NO ₃ ⁻	Nitrate	35	MgCO ₃	Magnesium carbonate
14	OH ⁻	Hydroxide ion	36	ACPO ₄	Calcium Phosphate
15	CH ₃ COOH	Acetic acid	37	MgHCO ₃ ⁺	Magnesium hydrogen carbonate
16	CH ₃ CH ₂ COOH	Propionic acid	38	CaHPO ₄ ⁻	Calcium hydrogen phosphate
17	HCO ₃ ⁻	Bi carbonate	39	NaCO ₃	Sodium carbonate
18	CaSO ₄	Calcium sulphate	40	MgH ₂ PO ₄	Magnesium di-hydrogen phosphate
19	H ₂ PO ₄ ⁻	Dihydrogen Phosphate	41	NaHCO ₃	Sodium hydrogen carbonate
20	MgCH ₃ COO	Magnesium acetate	42	NaHPO ₄ ⁻	Sodium hydrogen phosphate
21	MgCH ₃ CH ₂ COO	Magnesium propionate	43	CaOH ⁺	Calcium hydroxide
22	CaCO ₃	Calcium carbonate	44	MgOH ⁺	Magnesium hydroxide

The 14 ionic components (Appendix 7.3) are therefore total solution concentrations as sums of their respective species as shown in Table 3.6 and are used for determination of the material balances in the model. Ionic speciation involves determination of the species within the weak acid/base sub systems existing in a solution, through the dissociation of total ionic concentrations. Given that the ionic aqueous phase reactions are solved algebraically, they are

assumed to reach equilibrium relatively instantaneously at each time step. Thus, the model instantly redistributes the weak acid/base species including the hydrogen ion (H⁺) for the direct calculation of pH while separating the slower processes to avoid model stiffness (Ikumi, 2011).

3.3.4 Processes

The processes coded into the Gujer matrix for the Extended-UCTSDM3P model are similar to those of the 3-phase anaerobic digestion model (UCTSDM3P) developed by Ikumi (2011). The biological reactions therefore include those prescribed by Ikumi (2011). Additionally, in order to simulate the thermophilic conditions, modifications were added to account for the TAD and THP pathways.

3.3.4.1 Extended UCTSDM3P Stoichiometric Modifications

Following the identification of acetate oxidation pathway from the literature review (Section 2.2.3) modifications were incorporated into the Extended UCTSDM3P model in accordance with McCarty (1975). Their approach, adopted by Ikumi and Ekama (2019) and Ghooor (2020) entails the formulation of an electron donor equation, an electron acceptor equation (catabolism) and an equation for biomass growth (anabolism). Equation (3-32) below is the general equation for any bioprocess as expressed by McCarty (1975).

$$R = R_d - f_e R_a - f_s R_c \quad (3 - 32)$$

Where:

R = overall equation

R_d = electron donor equation

R_a = electron acceptor equation

R_c = equation for bacterial cells

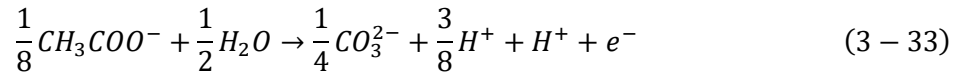
f_e = proportion of the electron donor that is coupled with the electron acceptor

f_s = proportional of the electron donor coupled with the cell formation

Ikumi and Ekama (2019) and Ghooor (2020) worked with equations expressed as biomass yield (i.e., the number of electrons conserved in biomass (anabolism) as a fraction of the electrons of the substrate utilized). For dynamic models, the biomass grown and the substrate utilized are

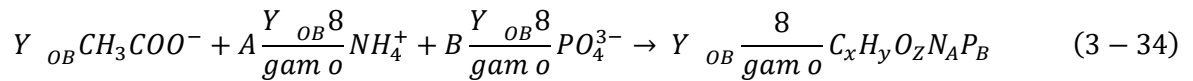
related through the biomass yield, Y . In contrast to the method employed by Sötemann *et al.* (2005), this model was expressed in terms of COD (gO/e^-) by multiplying the electron donating capacity by 8gO/e^- as has been detailed by Ghooor (2020).

For the acetate oxidation process the electron donor equation (R_d) is as shown in Equation (3-33) below:

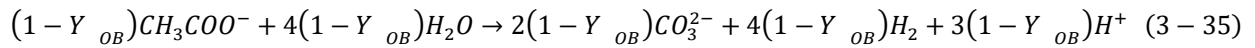


From Equation (3-33) above it can be noted that one-eighth of a mole of the acetate as substrate is required to release 1 mole of electrons. Conversely, 1 mole of acetate is oxidized to yield 8 moles of electrons. From the electrons donated, a fraction is utilized in the manufacture of organism mass in a process known as anabolism where the relationship between the substrate utilized and the mass of organism grown is described by the yield coefficient, Y_{OB} .

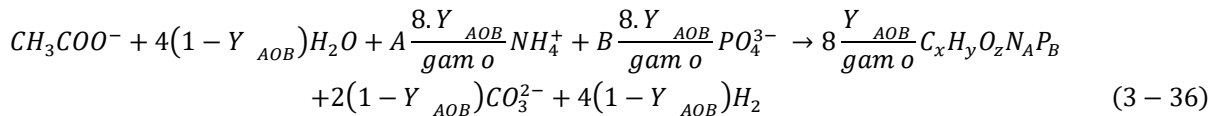
The biochemical reaction for anabolism (R_c) is represented by Equation (3-34) below:



The catabolic reaction for the respective process (R_a) is as shown in Equation (3-35) below.



From Equation (3-34) above, the acetate acts as a carbon source for biomass growth. This is in agreement with the studies carried out (Zinder and Koch, 1984; Schnurer *et al.*, 1994) where it was presumed from experimental results that the methyl group of acetate contributes to the biomass carbon source whereas the carboxyl group gets oxidized to CO_3^{2-} and H_2 as expressed in Equation (3-35). Adding both the catabolic and anabolic equations together, the overall equation representing syntrophic acetate oxidation is as shown in Equation (3-36).



Following the incorporation of the acetate oxidation process facilitated by SAOBs, a stoichiometric process catering for the degradation (lysis) of these organisms was also included.

The composition and molecular weight of these oxidizing bacteria was assumed to be equal to that of other organisms. The only differentiating factor being the rate at which the disintegration of the bacteria would take place. Like the degradation of the other organisms, the stoichiometric equation of the lysis process of these SAOBs was expressed as a first order kinetic rate. These processes are summarized in Table 3.7.

Table 3.7: Processes included in the dynamic extended UCTSDM3P model

Stoichiometric processes of the extended UCTSDM3P model	
1	Hydrolysis of fermentable soluble organics (FBSO)
2	Hydrolysis of biodegradable particulate organics (BPO) produced by dead biomass
3	Hydrolysis of BPO from primary sludge (PS)
4	Lysis of ordinary heterotrophic organisms (OHO)
5	Lysis of phosphorus accumulating organisms (PAOs)
6	Release of polyphosphate (PP) with uptake of poly-hydroxy-alkanoate
7	Release of PP in PAOs
8	Release of PHA in PAOs
9	Low hydrogen partial pressure (pH ₂) Acidogenesis
10	High pH ₂ Acidogenesis
11	Lysis of acidogens
12	Acetogenesis
13	Lysis of acetogens
14	Acetoclastic methanogenesis
15	Lysis of acetoclastic methanogens
16	Acetate oxidation (Equation 3-36)
17	Lysis of acetate oxidizing bacteria
18	Hydrogenotrophic methanogenesis
19	Lysis of hydrogenotrophic methanogens

It can be seen from Table 3.7 that the reactions are like the UCTSDM3P model with the exception of reactions (16) and (17) which are meant to represent the newly added metabolic pathway of syntrophic acetate oxidation (SAO) along with the lysis of the associated acetate-oxidizing bacteria.

3.4 THP MODEL

Following the establishment of the influent feed in Section 3.1.3, inputs into excel- and WEST-based THP models were carried out allowing for a comparison of performance between the two models. This sub-section describes the conceptual model, procedures, and equations used in the development of the dynamic and excel-based THP model. Notably, it is assumed that the THP processes occur instantaneously and therefore the procedure applied to the steady state model was used to explicitly highlight the equations used in the THP model.

At elevated temperatures, the increase in temperatures results in increased hydrolysis rates resulting in methanogenesis as the slowest process. The THP model on the other hand, was modelled in accordance with investigations by Wett *et al.*, (2014). Therefore, the THP pre-treatment unit was responsible for pasteurization, solubilization and activation of the waste sludge before being fed into the anaerobic digester at mesophilic conditions.

Pasteurization is the process through which all the organic living matter is decayed and subsequently converted to both biodegradable and unbiodegradable material. In accordance with Wett *et al.*, (2014), 77% is converted to particulate substrate, 20% to endogenous residue and the remaining 3% to soluble inert organics. Solubilization in turn, involves the process through which a characteristic range of 25-45% of the biodegradable particulate (BPO) material is converted into fermentable soluble organics (60% of the converted BPO) (e.g., amino acids and sugars) and volatile fatty acids (VFAs) (remaining 40% of converted BPO) (Flores-Alsina *et al.*, 2021). Lastly, activation is the process by which a fraction of the unbiodegradable particulate organics is converted to biodegradable particulate organics as a result of breakdown due to increased temperature and pressure.

Following investigations by Wett *et al.*, (2014), the pre-treatment processes were modelled based on the set process temperatures as opposed to the process period. The THP process was therefore modelled for temperatures ranging from 150°C to 180°C. Accordingly, considering pasteurization at 150°C the fraction of biomass converted to inert soluble organics increased from 3% to 9% decreasing the fraction converted to biodegradable particulate organics from 77% to 71%. For solubilization at 150°C, 25% of the biodegradable particulate material is solubilized to simple organics whereas at 180°C, 45% of the biodegradable particulate material is solubilized.

As for activation and in accordance with Wett *et al.*, (2014), at 150°C, barely any endogenous residue conversion occurs while at 180°C, almost complete conversion occurs and soluble inert production increases from 3% to 9%.

The parameters involved in the development of the THP model are as shown in the following Table 3.7.

Table 3.7: THP Model Parameters

Parameters		
Temperature		
Tmin	150	Lower limit for temperature dependence
Tmax	180	Upper limit for temperature dependence
Pasteurization		
f_pasteur_BP_tmin	0.77	Fraction of biomass to X_B_Org at Tmin
f_pasteur_BP_tmax	0.71	Fraction of biomass to X_B_Org at Tmax
f_pasteur_UP_tmin	0.2	Fraction of biomass to X_U_Org at Tmin
f_pasteur_UP_tmax	0.2	Fraction of biomass to X_U_Org at Tmax
f_pasteur_US_tmin	0.03	Fraction of biomass to S_U at Tmin
f_pasteur_US_tmax	0.09	Fraction of biomass to S_U at Tmax
Solubilisation		
f_sol_BP_tmin	0.25	Fraction of BP solubilized at Tmin
f_sol_BP_tmax	0.45	Fraction of BP solubilized at Tmax
f_sol_PS_tmin	0.25	Fraction of primary sludge BP solubilized at Tmin
f_sol_PS_tmax	0.45	Fraction of primary sludge solubilized at Tmax
f_sol_BP_Ac	0.4	Fraction of BP solubilized and converted to acetate
f_sol_BP_SF	0.6	Fraction of BP solubilized and converted to S_F
f_sol_PS_Ac	0.4	Fraction of primary sludge BP solubilized and converted to acetate
f_sol_PS_SF	0.6	Fraction of primary sludge BP solubilized and converted to S_F
Activation		

f_act_UPS_tmin	0	Fraction of X_U_Inf converted to X_B_Org at Tmin
f_act_UP_tmin	0	Fraction of X_U_Org converted to X_B_Org at Tmin
f_act_UPS_tmax	1	Fraction of X_U_Inf converted to X_B_Org at Tmax
f_act_UP_tmax	1	Fraction of X_U_Org converted to X_B_Org at Tmax
f_act_UP	0	Fraction of X_U_Org converted to X_B_Org
f_act_UPS	0	Fraction of X_U_Inf converted to X_B_Org

Following the identification of the parameters, the mass of products as output from the THP-model could be calculated through the stoichiometry of the processes, which is known from the selected elemental compositions. The THP model kinetics which are assumed to be relatively instantaneous and therefore only dependent on the extent, is dictated by the selected THP temperature and the boundaries as prescribed by the parameters in the Table 3.7 above.

3.4.1 Pasteurization

As has been discussed, pasteurization is the process through which organic material is broken down and subsequently converted into biodegradable and unbiodegradable material. A linear progression was assumed for temperature values within the prescribed lower limit of 150°C and upper limit of 180°C. This linear relationship was assigned to a variable F_Temp where the value varied between 0 and 1, with 0 being the F_Temp value at a temperature of 150°C and below, and 1 the value at a temperature of 180°C and above. The value of F_Temp between 150 and 180°C was calculated as follows in Equation (3-27):

$$F_{Temp} = \frac{THP_{temp} - 150}{180 - 150} \quad (3 - 27)$$

Where THP_{temp} refers to the selected THP operational temperature.

Assuming a THP temperature of 180°C, the F_Temp was established to be 1 and therefore the fraction of biomass that was pasteurized to biodegradable particulate material (f_pasteur_BP) was calculated to be 0.71. The fraction pasteurized to inert soluble (f_pasteur_US) was calculated to be 0.09 and that to unbiodegradable particulate (f_pasteur_UP) remained constant at 0.20. Once the fractions were established, the kinetics could be calculated.

For the stoichiometric part of the model, the electron donating capacity (EDC) of the respective components first had to be computed. Using the COD quantities that were as calculated in the previous Section 3.3.2 the electron donating capacities were calculated by dividing the respective COD quantities by 8 which is the weight of 1 atom of oxygen. The respective EDCs are as shown in Table 3.8.

Table 3.8: Electron Donating Capacities

Electron Donating Capacity	
gam_o	4.221
gam_f	4.529
gam_e	4.309
gam_bp	4.221
gam_us	4.374
gam_up	4.309
gam_bps	4.7396
gam_vfa	7.9995

Where:

gam_o is the EDC of organisms in the wastewater

gam_f the EDC of fermentable soluble organics

gam_e the EDC of endogenous residue

gam_bp the EDC of biodegradable particulate organics

gam_us the EDC of unbiodegradable soluble organics

gam_up the EDC of unbiodegradable particulate organics

gam_bps the EDC of biodegradable particulate organics in the primary sludge

and

gam_vfa the EDC of the volatile fatty acids

With the EDCs computed, the stoichiometric calculations for the pasteurization of the various wastewater compositions were calculated as shown in Table 3.9. Likewise, using the mass of

biomass (Biomass_in) compiled from computing the influent feed in the previous step, the kinetic calculation for the fraction pasteurized to biodegradable material is as follows in Table 3.9.

Table 3.9: Pasteurization Kinetic and Stoichiometric Equations

Kinetics	
<i>Pasteurisation_BP</i>	$\frac{f_pasteur_BP * Biomass_in}{MM \text{ of organism component}}$
<i>Pasteurization_UP</i>	$\frac{f_pasteur_UP * Biomass_in}{MM \text{ of organism component}}$
<i>Pasteurization_US</i>	$\frac{f_pasteur_US * Biomass_in}{MM \text{ of organism component}}$
Stoichiometry	
$[Pasteurisation_BP][X_B_Org]$	$\frac{gam_o}{gam_{bp}} * MM \text{ of } X_B_Org$
$[Pasteurisation_UP][X_U_Org]$	$\frac{gam_o}{gam_{up}} * MM \text{ of } X_U_Org$
$[Pasteurisation_US][S_U]$	$\frac{gam_o}{gam_{us}} * MM \text{ of } SU$

Where:

- *Biomass_in* refers to the mass of biomass compiled from the influent feed
- MM refers to the molar mass of the respective component as was selected and shown in the table above in the previous sub-section
- *Pasteurisation_BP* refers to the reaction where a fraction of organism mass is converted into biodegradable particulate organics
- *Pasteurisation_UP* refers to the reaction where a fraction of organism mass is converted into unbiodegradable particulate organics
- *Pasteurisation_US* refers to the reaction where a fraction of organism mass is converted into unbiodegradable soluble organics

These kinetic calculations yield a value expressed as amount of moles.

The product of this stoichiometric calculations is expressed as grams per mole (g/mol). With the stoichiometric and kinetic calculations computed, the mass of material pasteurized in this example was obtained by the product of the stoichiometric and kinetic calculations. The mass of

biomass pasteurized, denoted as *BP_Pasteur*, and converted to biodegradable particulate material was computed as shown in Table 3.10.

Table 3.10: Pasteurization Resultant Masses

Resultant masses	
<i>Biomass converted to X_B_Org</i>	$[Pasteurisation_BP][X_B_Org] * Pasteurisation_BP$
<i>Biomass converted to X_U_Org</i>	$[Pasteurisation_UP][X_U_Org] * Pasteurisation_UP$
<i>Biomass converted to SU</i>	$[Pasteurisation_US][S_U] * Pasteurisation_US$

The product of this operation yields a value expressed as grams which is the appropriate unit for this reaction.

3.4.2 Activation

Activation is the process through which the endogenous unbiodegradable (X_U_Org) fraction of organics is converted to particulate substrate (X_B_Org). Investigations by Wett *et al.*, (2014) set the conversion of endogenous unbiodegradable fraction of organics (*f_act_UP*) at 0% for the lower limit THP temperature of 150°C and complete conversion (100%) at the upper limit THP temperature of 180°C with a linear relationship assumed between the two limits. With the fraction of organics activated known, the mass of endogenous unbiodegradable organics was computed using the kinetic and stoichiometric product calculations as was done in the pasteurization process. Given the endogenous unbiodegradable fraction is contained in both the PS and WAS, the kinetic and stoichiometric calculations for the activation process were computed for both as follows in Table 3.11.

Table 3.11: Activation Kinetic and Stoichiometric Equations

Kinetics	
<i>Activation_UP_BP</i>	$f_act_UP * \frac{(UP_{in} + UP_{pasteur})}{MM \text{ of endogenous unbiodegradable particulate component}}$
<i>Activation_UPS_BP</i>	$f_act_UPS * \frac{(UPS_{in})}{MM \text{ of endogenous unbiodegradable particulate component}}$
Stoichiometry	
$[Activation_UP_BP][X_B_Org]$	$\frac{gam_e}{gam_{bp}} * MM \text{ of } X_B_Org$
$[Activation_UPS_BP][X_B_Org]$	$\frac{gam_{up}}{gam_{bp}} * MM \text{ of } X_B_Org$

$[Activation_UP_BP][X_U_Org]$	$(-1) * MM\ of\ X_U_Org$
$[Activation_UPS_BP][X_U_Inf]$	$= (-1) * MM\ of\ X_U_Inf$

Where:

- *Activation_UP_BP* refers to the reaction where a fraction of the endogenous unbiodegradable particulate organics in WAS is converted to biodegradable particulate substrate.
- *Activation_UPS_BP* refers to the reaction where a fraction of the endogenous unbiodegradable particulate organics in PS is converted to biodegradable particulate substrate.
- *UP_{in}* refers to the mass of the endogenous unbiodegradable particulate organics found in WAS
- *UP_{Pasteur}* refers to the mass of the endogenous unbiodegradable particulate organics in WAS as a result of the pasteurization process
- *UPS_{in}* refers to the mass of the endogenous unbiodegradable particulate organics found in PS

With the kinetic and stoichiometric calculations computed, the mass of endogenous unbiodegradable particulate organics converted to biodegradable particulate substrate through activation was calculated as follows in Table 3.12.

Table 3.12: Activation Resultant Masses

Remaining Mass	
Mass of BPO from WAS UPO activation	$[Activation_UP_BP][X_B_Org] * Activation_UP_BP$
Mass of BPO from PS UPO activation	$[Activation_UPS_BP][X_B_Org] * Activation_UPS_BP$
Mass of WAS UPO activated	$[Activation_UP_BP][X_U_Org] * Activation_UP_BP$
Mass of PS UPO activated	$[Activation_UPS_BP][X_B_Inf] * Activation_UP_BP$

3.4.3 Solubilization

Solubilization refers to the process where a fraction of biodegradable particulate organics both in PS and WAS are converted to soluble organics either in the form of acetate (VFAs) or fermentable soluble organics (FBSOs). According to work carried out by Wett *et al.*, (2014) the

range of solubilization ranges from 25% at the lower temperature limit of 150°C to 45% at the higher temperature limit of 180°C. Additionally, of the amount that is solubilized, 40% is converted to acetate and the remaining 60% to fermentable soluble organics.

Assuming a THP temperature of 180°C, the fraction of biodegradable particulate organics solubilized (f_{sol_BP}) was calculated to be 0.45. Of this solubilized fraction, the fraction converted to acetate ($f_{sol_BP_Ac}$) was calculated to be 0.40 and that solubilized to fermentable soluble organics ($f_{sol_BP_SF}$) was calculated to be 0.60. Just as has been done for all the THP processes above, calculation of the amount solubilized requires computation of both the stoichiometry and kinetics. Given the biodegradable particulates are contained both in the WAS and PS, calculations were done for both. The kinetic and stoichiometric calculations for the solubilization of biodegradable particulate organics in the PS and WAS were computed as depicted in Table 3.13.

Table 3.13: Solubilization Kinetic and Stoichiometric Equations

Kinetics	
$Solubilization_BP_Ac$	$f_{sol_BP} * f_{sol_BP_Ac} * \frac{(BP_{in} + BP_{pasteur} + BP_{activated})}{MM \text{ of biodegradable particulate component}}$
$Solubilization_BP_SF$	$f_{sol_BP} * f_{sol_BP_SF} * \frac{(BP_{in} + BP_{pasteur} + BP_{activated})}{MM \text{ of biodegradable particulate component}}$
$Solubilization_PS_SF$	$f_{sol_BP} * f_{sol_BP_SF} * \frac{PS_{in}}{MM \text{ of biodegradable particulate component}}$
$Solubilization_PS_Ac$	$f_{sol_BP} * f_{sol_BP_Ac} * \frac{PS_{in}}{MM \text{ of biodegradable particulate component}}$
Stoichiometry	
$[Solubilisation_BP_Ac][S_VFA]$	$\left((0.125 * f_h) - (0.325 * f_n) - (0.25 * f_o) + (0.625 * f_p) + 0.5 \right) * MM \text{ of VFA}$

$[Solubilisation_BP_Ac][X_B_Org]$	$(-1) * MM\ of\ X_B_Org$
$[Solubilisation_BP_Ac][S_F]$	$\frac{gam_{bp}}{gam_f} * MM\ of\ Fermentable\ soluble\ organics\ S_F$
$[Solubilisation_BP_SF][X_B_Org]$	$(-1) * MM\ of\ X_B_Org$
$[Solubilisation_PS_Ac][S_VFA]$	$\left((0.125 * f_h) - (0.325 * f_n) - (0.25 * f_o) + (0.625 * f_p) + 0.5 \right) * MM\ of\ VFA$
$[Solubilisation_PS_Ac][X_B_Inf]$	$(-1) * MM\ of\ X_B_Inf$
$[Solubilisation_PS_Ac][S_F]$	$\frac{gam_{bps}}{gam_f} * MM\ of\ Fermentable\ soluble\ organics\ S_F$
$[Solubilisation_PS_SF][X_B_Inf]$	$(-1) * MM\ of\ X_B_Inf$

Where:

- *Solubilization_BP_Ac* refers to the reaction where a fraction of the biodegradable particulate organics is converted to acetate
- *Solubilization_BP_SF* refers to the reaction where a fraction of the biodegradable particulate organics is converted to fermentable soluble organics
- *Solubilization_PS_Ac* refers to the reaction where a fraction of the Primary Sludge (PS) biodegradable particulate organics is converted to acetate
- *Solubilization_PS_SF* refers to the reaction where a fraction of PS biodegradable particulate organics is converted to fermentable soluble organics
- BP_{in} is the mass of biodegradable particulate organics contained in the influent feed mixture
- $BP_{Pasteur}$ is the mass of biodegradable particulate organics from the pasteurization process
- $BP_{Activated}$ is the mass of biodegradable particulate organics from the activation process

With the stoichiometric and kinetic calculations computed, the mass of material solubilized was obtained by the product of the stoichiometric and kinetic calculations. Therefore, the mass of biodegradable particulate organics in WAS solubilized and converted to biodegradable soluble organic material such as acetate and fermentable soluble organics was computed as follows in Table 3.14.

Table 3.14: Solubilization Resultant Masses

Remaining Mass	
<i>WAS BPO solubilized to Acetate</i>	$[Solubilisation_{BP_Ac}][Ac]$ $* Solubilisation_{BP_Ac}$
<i>WAS BPO solubilized to S_F</i>	$[Solubilisation_{BP_SF}][SF]$ $* Solubilisation_{BP_SF}$
<i>WAS BPO solubilized to Acetate</i>	$[Solubilisation_{BP_Ac}][X_B_Org]$ $* Solubilisation_{BP_Ac}$
<i>WAS BPO solubilized to S_F</i>	$[Solubilisation_{BP_SF}][X_B_Org]$ $* Solubilisation_{BP_SF}$
<i>Mass of PS BPO solubilized to Acetate</i>	$[Solubilisation_{PS_Ac}][Ac]$ $* Solubilisation_{PS_Ac}$
<i>Mass of PS BPO solubilized to S_F</i>	$[Solubilisation_{PS_SF}][SF]$ $* Solubilisation_{PS_SF}$
<i>Mass of PS BPO solubilized to Acetate</i>	$[Solubilisation_{PS_Ac}][X_B_Inf]$ $* Solubilisation_{PS_Ac}$
<i>Mass of PS BPO solubilized to S_F</i>	$[Solubilisation_{PS_SF}][X_B_Inf]$ $* Solubilisation_{PS_SF}$

Once the masses as a result of the THP processes were computed, a summed conversion of the respective component masses were computed where the respective outflow resultant masses were added to their initial concentrations. For instance, the final fermentable soluble organics (S_F) was computed as follows:

$$Final\ mass\ of\ S_F = [Solubilisation_{BP_SF}][S_F] * [Solubilisation_{PS_SF}][S_F] + Initial\ mass\ of\ S_F$$

The same was done for all the other components (Organisms, Endogenous residue, volatile fatty acids, unbiodegradable soluble organics, PS biodegradable particulate organics and biodegradable and unbiodegradable particulate organics and the calculations were as follows in Table 3.15.

Table 3.15: Final THP component masses

Final masses	Equation
<i>Final mass of X_BOrg</i>	$= [Pasteurisation_{BP}][X_{B_Org}]$ $+ [Solubilisation_{BP_Ac}][X_{B_Org}]$ $+ [Solubilisation_{BP_SF}][X_{B_Org}]$ $+ [Activation_{UP_BP}][X_{B_Org}]$ $+ [Activation_{UPS_BP}][X_{B_Org}]$ $+ Initial\ mass\ of\ X_{B_Org}$
<i>Final mass of X_UOrg</i>	$= [Pasteurisation_{BP}][X_{U_Org}]$ $+ [Activation_{UP_BP}][X_{U_Org}]$ $+ Initial\ mass\ of\ X_{U_Org}$
<i>Final mass of S_U</i>	$= [Pasteurisation_{US}][S_U] + initial\ mass\ of\ S_U$
<i>Final mass of S_{VFA}</i>	$= [Solubilisation_{BP_Ac}][S_{VFA}]$ $+ [Solubilisation_{PS_Ac}][S_{VFA}]$ $+ Initial\ mass\ of\ S_{VFA}$
<i>Final mass of X_BInf</i>	$= [Solubilisation_{PS_Ac}][X_{B_Inf}]$ $+ [Solubilisation_{PS_SF}][X_{B_inf}]$ $+ initial\ mass\ of\ X_{B_Inf}$
<i>Final mass of X_UInf</i>	$= [Activation_{UPS_BP}][X_{U_Inf}]$ $+ Initial\ mass\ of\ X_{U_Inf}$

As a result of the high temperatures involved, some water is lost in the process. The mass of water lost was calculated for every process using the stoichiometric and kinetic computations similar to the other components. This mass of water was subtracted from the initial flux of water in order to obtain the outflow mass of water. This was used to divide the components masses and get the final concentrations.

3.5 ANALYTICAL PROCEDURES

In order to evaluate and compare the performance of both the steady state and dynamic models, analytical procedures were laid out. These were the fraction of COD removed, the amount of

struvite precipitated, and the fraction of OP and FSA released. The amount of struvite precipitated was calculated as explained in Section 3.2.4.1. The percentage of COD removed, and OP and FSA released was calculated as shown in Equations (3-28)-(3-30):

$$\%COD\ Removed = \frac{(S_{Bpi} + S_{asi} + S_{bsfi}) - (S_{Bpe} + S_{ase} + S_{bsfe})}{(S_{Bpi} + S_{asi} + S_{bsfi})} * 100 \quad (3 - 28)$$

Where:

S_{Bp} is the biodegradable particulate organic concentration

S_{asi} is the volatile fatty acids (VFA)

S_{bsfi} is the fermentable soluble organics

And the subscript 'i' refers to the influent and 'e' to the effluent components.

$$\%FSA\ released = \frac{Effluent\ FSA - Influent\ FSA}{Influent\ TKN} * 100 \quad (3 - 29)$$

$$\%OP\ released = \frac{Effluent\ OP - Influent\ OP}{Influent\ TP} * 100 \quad (3 - 30)$$

3.6 MODEL EVALUATION

The steady state model was evaluated by performing a mass balance on the influent and effluent components of the wastewater (i.e., COD, carbon, hydrogen, nitrogen, oxygen, phosphorus, and metals). The explicit nature of the stoichiometric equations used in the steady state model allow for an intuitive understanding of the parameters used and the effect they have relative to the model outputs.

The dynamic model on the other hand required a more thorough sensitivity analysis to determine the effects of the variables and parameters on the outputs from the model. The AD model used in this project was adopted from the AD model by Ghooor (2020) where they calibrated the model using the Standard Regression Coefficient (SRC) analysis, Morris Screening and Extended-FAST methods to identify the important parameters. The model was therefore not re-calibrated but rather taken through a model verification process whereby the stoichiometric equations for the processes were checked for internal consistency by performing a COD, CHONP, Mg, K, Ca and

charge balance as described by Hauduc *et al.*, (2010). Additionally, the THP part of the model was also checked for internal consistency to ensure a mass balance was obtained in the THP model. The mass balance verification spreadsheets have been included in Appendix 7.2 at the end of this report for further review by the reader.

3.7 CLOSURE

Through a description of the components, their characterization and elemental formulations, the stoichiometric and kinetic descriptions of both the (Steady state and dynamic) THP and extended AD models were obtained as detailed in this Chapter. Chapter 3 therefore details the methodology followed in developing the respective models. Additionally, in order to ensure a fair comparison between the steady state and dynamic models, uniform influent feed was compiled for both the steady state and dynamic models. Once the feed and models were established, some analytical procedures to measure the performances from the different configurations were employed. The results from the analytical procedures discussed in this Chapter will be displayed and discussed in the subsequent Chapter (Chapter 4).

4 RESULTS AND DISCUSSIONS

The steady state and dynamic integrated thermal hydrolysis process – anaerobic digestion (THPAD) model was developed in Microsoft Excel and in WEST® (Vanhooren *et al.*, 2003; a WWTP simulation platform provided within MikebyDHI software) as described in Chapter 3. In order to evaluate the model, the Cape Flats wastewater treatment works (CFWWTW) anaerobic digestion (AD) system was simulated both in an excel-based steady state AD model and the dynamic model (Extended-UCTSDM3P model) developed in WEST®. This section compares and discusses the performance of both the steady state and the dynamic models in predicting COD removal, the associated nutrient (N and P) and metallic ion (Mg, K and Ca) release, and struvite precipitation as well as the observed virtual AD system performance with and without a THP unit.

The excel-based steady state AD model developed was based on the AD model of Sötemann *et al.*, (2005), with the incorporated changes associated with hydrolysis kinetics, stoichiometry, struvite precipitation and weak acid/base chemistry. This model was also inclusive of the phosphorus (P) element that allowed for the AD of waste activated sludge containing PAOs, in accordance with Ikumi (2011) and Harding (2009). The kinetic equations used for the various processes can be obtained from the literature (Ikumi, 2020; Ghoor, 2020) and remain relevant as the AD unit proceeding the THP unit was operated at the conventional AD temperature of 35°C. The modelled THP unit on the other hand was based on the work by Wett *et al.*, (2014), as discussed in the literature review Section 2.3.1.2, with the stoichiometric reactions coded into both the dynamic WEST® model and the excel-based steady state model as was described in Section 3.4.

4.1 INFLUENT COMPOSITION

The procedure followed to obtain the influent wastewater composition that was used for both models was explained in Section 3.1.3. Following those steps and the selection of molar fractions from experiments done by (Ikumi, 2011), the influent wastewater component concentrations for the configurations with and without THP were as shown in Table 4.1 below.

Table 4.1: Influent Component Compositions

Influent component concentrations (in mg/l)										
	VSS		COD		N		P		C	
Components	Without THP	With THP	Without THP	With THP	Without THP	With THP	Without THP	With THP	Without THP	With THP
UPO	16552	38699	24474	57219	1658	2596	420	981	8567	20029
BPO	19406	45460	28877	67645	1161	3968	349	817	9966	23346
FBSO	0	0	46	46	0.53	0.53	0.31	0.31	15.25	15.25
VFA	0	0	20	20	0	0	0	0	7.51	7.51
USO	0	-	47	47	1.62	1.62	0	0	16.13	16.13
Inorganic	0	0	0	0	40	40	7.3	7.3	5	5
Sum	35959	84159	53463	124976	2862	6638	776	1806	18577	43419

As can be seen from the table above, the wastewater comprised primarily of particulate components (UPO and BPO) with relatively negligible amounts of soluble components (FBSO, VFA and USO) present in the influent. The disparity in the influent composition concentration values between the two configurations (with and without THP) was as a result of the thickening process that precedes the THP unit. Due to the high temperature and pressure processes that take place in the THP unit, it has the capacity to break down a relatively higher mass of organic material because of the decreased viscosity. Consequently, while the configuration without THP received an influent solids concentration of 4.7% (4700 g/m³), the setup with a THP unit received an influent solids concentration of 11% (11000 g/m³) which is 2.3 times more solid sludge than the conventional setup. Hence the notable increase in the particulate concentrations while the soluble concentrations remained the same as they were unaffected by the thickening process before the THP unit.

4.2 THP MODEL RESULTS

For the THP configuration, as described in section 3.4, the thickened influent wastewater was subjected to THP processes at set temperatures of 150 °C, 165°C and 180°C. The following graphs show the changes that occurred to the influent wastewater component concentrations before THP as has been discussed above, and at the different set temperatures of 150 °C, 165°C and 180°C.

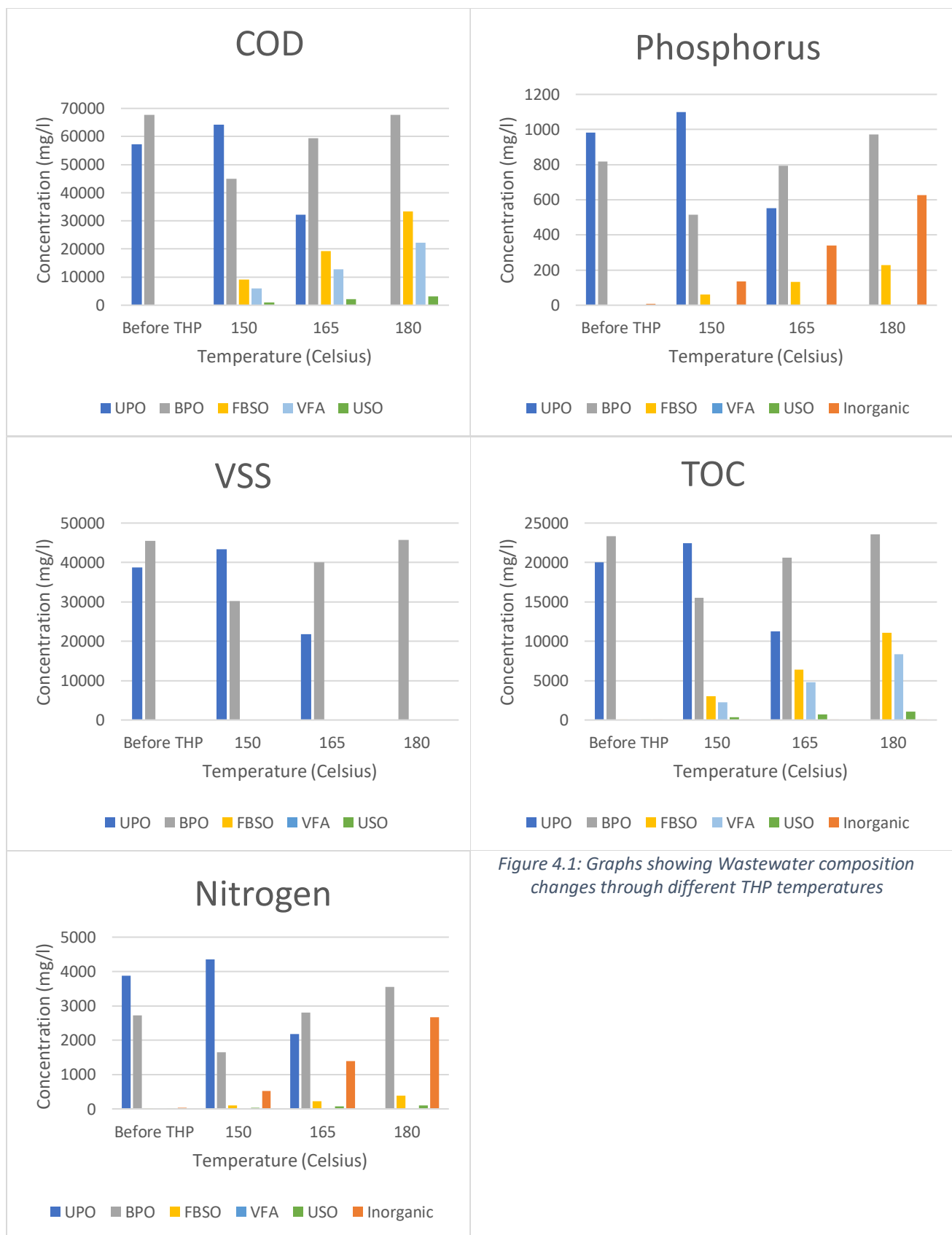


Figure 4.1: Graphs showing Wastewater composition changes through different THP temperatures

From the graphs of the influent concentrations above, we see a common trend in the particulate components. Before the THP unit, the wastewater comprised primarily of biodegradable and unbiodegradable particulate organics (BPO and UPO, respectively) with the former being the higher concentration. Upon thermal hydrolysis process pre-treatment, it was observed that the UPO increased in concentration and was now higher than the BPO concentration which was reduced relative to the influent wastewater BPO composition before the THP unit. The reason for the decrease in BPO concentration can be attributed partly to the breakdown of the organics under high pressure and temperature in a process known as hydrolysis where the particulate components are broken down to smaller monomers such as VFA and FBSO and partly due to the pasteurization process where 20% of the biomass was converted to unbiodegradable particulate organics (X_U_Org) (Wett *et al.*, 2014).

For all the wastewater material measurements (COD, VSS, TOC, TKN and TP), we see a progressive increase in the BPO concentration from the lower THP temperature limit of 150°C to the upper limit of 180°C. In contrast, we see a progressive decrease in the UPO concentration with the same increase in thermophilic temperature. These changes in the BPO and UPO concentrations are as a result of the physical processes that take place in the THP, namely pasteurization and activation. With increase in the THP temperature, the fraction of UPO converted to BPO (i.e., activation) increases from 0% at 150°C to 100% at 180°C hence the complete utilization of the unbiodegradable particulate component (i.e., X_U_Org) at 180°C. Additionally, due to pasteurization the endogenous residue associated with the biomass is converted to particulate substrate (X_B_Org) and contributes to further increase in the BPO concentration.

From the COD, TOC, TKN and TP graphs, it was observed that the soluble portion of the wastewater comprised of volatile fatty acids (VFAs), fermentable soluble biodegradable organics (F-BSO) and unbiodegradable soluble organics (USO). From the graphs above, a progressive increase in the concentration of soluble organics coming out of the THP with an increase in the THP operating temperature was observed. This increase in concentration of soluble components was as a result of an increase in the solubilization rate with increase in THP temperature. At the lower limit of 150°C, 25% of the biodegradable particulate organics were converted to acetate (VFAs) and fermentable soluble organics (FBSO) while at the upper limit of 180°C this fraction

increased from 25% to 45%. Additionally, with increase in the THP operating temperature from 150°C to 180°C, the amount of biomass pasteurized into soluble inert components increased from 3% to 9% respectively, accounting for the slight increase in unbiodegradable soluble organics (USOs) with increase in THP temperature. As for the TKN and TP soluble components, with an increase in THP temperatures and subsequently the solubilization rates, the organically bound N and P components were released as ammonia and phosphate, respectively, contributing to the increased soluble components from the THP unit.

For the TKN and TP components of the wastewater, upon solubilization of the particulate substrate, the N and P components of the wastewater were released as ammonia and phosphates (Wett *et al.*, 2014). As a result, we see an increase in the phosphorus inorganics present in the wastewater with increase in thermophilic temperature. Similarly, from the graph displaying nitrogen, we see a progressive increase in the nitrogen inorganics concentration with increase in the thermophilic temperature. This was in line with investigations that showed the THPAD setup leading to an increase in the amount of ammonia released into the system (Phothilangka *et al.*, 2008).

4.3 AD MODEL RESULTS

4.3.1 Nutrient removal (and Methane Production)

Having established the output from the THP unit, an evaluation of the AD performance in both the excel-based model and the dynamic model developed in WEST® was carried out. In the steady state excel model, given the known flowrate and reactor volume, a solids retention time of 15 days was calculated and used to evaluate the steady state AD performance (using the simplified spreadsheet model that contains explicit stoichiometric equations). These results were compared to the outputs from the Extended-UCTSDM3P model developed in WEST®. To ensure that the results obtained from the dynamic model had reached steady state, in accordance with Henze *et al.*, (2008), the length of the simulation could be no less than 3 times the sludge age. Hence a 100-day simulation run was selected and deemed to be satisfactory in ensuring the dynamic model had reached a steady state condition.

Once both models were set up as described in Chapter 3, the input and output data were pre- and post-processed, and their virtual performances evaluated following the analytical

procedures described in Section 3.5. The following Table 4.2 summarizes the performances from the virtual simulation of both a steady state and dynamic AD model with and without a THP unit assuming an instance of infinite solubility, whereas Table 4.3 summarizes the performance of these models taking struvite precipitation into account. The performances of these models are tabulated below along with the respective mass balances to evaluate the accuracy of the processes and subsequently the results. The process mass balance verifications have been provided in Appendix 7.2 at the end of this report.

Table 4.2: Steady State and Dynamic AD results with and without THP at infinite solubility

At Infinite solubility	Without THP		With THP	
COD and Nutrient Removal and Mineral ppt	Steady state	Dynamic	Steady state	Dynamic
% FSA Released	19.25	22.09	29.79	36.77
% OP Released	22.23	25.73	38.29	45.14
%COD Removed	54.75	62.92	74.94	79.74
Struvite Precipitated	0.00	0.00	0.00	0.00
ACP Precipitated	0.00	0.00	0.00	0.00
Calcite Precipitated	0.00	0.00	0.00	0.00
pH	6.91	6.97	7.69	7.54
Mass Balances				
COD balance (%)	100.00	100.48	100.00	102.61
Carbon balance (%)	100.00	100.49	100.00	102.65
Nitrogen balance (%)	100.00	100.62	100.00	102.27
Phosphorous balance (%)	100.00	100.70	100.00	102.31
Magnesium balance (%)	100.00	100.41	100.00	102.14
Potassium balance (%)	100.00	100.40	100.00	102.13
Calcium balance (%)	100.00	100.50	100.00	102.22

Table 4.3: Steady State and Dynamic AD Model Results accounting for Struvite Precipitation

COD and Nutrient Removal and Mineral ppt	Without THP		With THP	
	Steady state	Dynamic	Steady state	Dynamic
% FSA Released	17.79	20.07	28.92	35.91
% OP Released	10.30	9.12	31.25	37.90
%COD Removed	54.75	62.93	74.94	79.74
Struvite Precipitated	733.29	1021.77	1017.65	1051.36
ACP Precipitated	0.00	0.00	0.00	0.00
Calcite Precipitated	0.00	0.00	0.00	0.00
pH	6.83	6.93	7.34	7.45
Mass Balances				
COD balance (%)	100.00	100.46	100.00	102.65
Carbon balance (%)	100.00	100.50	100.00	102.70
Nitrogen balance (%)	100.00	100.66	100.00	102.31
Phosphorous balance (%)	100.00	100.71	100.00	102.34
Magnesium balance (%)	100.00	100.33	100.00	102.04
Potassium balance (%)	100.00	100.44	100.00	102.17
Calcium balance (%)	100.00	100.53	100.00	102.26

Comparing the models' outputs for the configurations with and without the THP unit, both models were observed to yield similar results with respect to each other in their respective contexts. This was a good indication that the two models were simulating similar processes. Furthermore, the mass balances for the steady state models were completely balanced whereas the dynamic model mass balances contained relatively small imbalances that were acceptable as they did not exceed 5% (mainly due to errors by the selected simulator, as the model processes were checked to be 100% mass balanced according to the method proposed by Hauduc *et al.*, (2010) and as explained in Section 3.5. This was an indication that the energy within the entire process was satisfactorily accounted for. Knowing that the steady state and dynamic models were simulating similar processes, it was possible to analyze the performance under the different configurations. The % OP released, %FSA released, and % COD removed was observed to be higher in the configuration with a THP system in operation compared to that without. This was an expected outcome as the use of the THP process meant that a higher fraction of the organics was made available for anaerobic digestion. On the other hand, for both configurations, the dynamic model yielded higher amounts of organics broken down and released as OP or FSA. This

could be attributed to the more detailed nature of the dynamic model. The steady state model is a simplification of the processes that take place in the THPAD process. As a result of the simplification, some processes that contribute to the final concentrations may not have been accounted for.

Simulations were run for the instance of infinite solubility and with struvite precipitation and the results obtained were as observed in Tables 4.2 and 4.3 above. For both instances, consistent results were obtained for the concentration of COD removed, and OP and FSA released in the sense that the results obtained were within a 10% difference of each other for both configurations (with and without THP). Furthermore, for both instances, the increase in the concentration of COD removed between the configuration without THP and that with THP was constant at 20% for the steady state model and 17% for the dynamic model. This aligned with the numerous investigations that credited thermal pretreatment with increased organic solids destruction (Li and Noike, 1992; Valo *et al.*, 2004). Additionally, from Tables 4.2 and 4.3 above, the pH ranges for both instances were within acceptable allowances for optimal operations of the AD digesters (i.e., pH between 6.6 and 7.5).

As for methane production, the steady state model provided more conservative results compared to the dynamic model as shown in Table 4.4 below. In the steady state model, the methane production increased by 2.5 times when the THP unit was included in the setup whereas the dynamic model recorded an increase in methane production by 5.7 times. However, regardless of the type of model used, the methane production significantly increased when the THP unit was incorporated which is in accordance with numerous investigations previously carried out. This can be attributed to the fact that as a result of the THP pretreatment process, a higher fraction of biodegradable organics that was previously inaccessible was availed, implying that more organics were available for the methanogenic process and thereby, for conversion to methane.

Table 4.4: Methane production

	Without THP		With THP	
Methane Production	Steady State	Dynamic	Steady State	Dynamic
Gas Production (litres)	12348	14196	31619	79788
CH ₄ produced (l gas/l influent)	5.83	6.69	14.17	38.43
COD of CH ₄ (mgCOD/l feed)	15217	17572	92489	100920
pCO ₂	0.41	0.41	0.44	0.40

5 CONCLUSIONS AND RECOMMENDATIONS

The primary aim of this project was to develop a model capable of simulating the integrated THPAD process. Through a comprehensive literature review, the key processes that take place in a THP and AD unit at elevated temperatures were identified and modelled for both a steady state and dynamic model. Both models were evaluated through a model verification process for both the THP and AD unit to ensure internal consistency.

Using data obtained from the experiments carried out by Ikumi (2011) as the influent wastewater compositions, a comparative desktop case study of the Cape Flats Wastewater Treatment Works (CFWWTW) was conducted whereby the models were used to virtually simulate the conventional anaerobic digestion process as the base scenario in comparison to including the thermal hydrolysis process unit before the anaerobic digester. Comparing their performances, both models provided consistent results in their respective contexts (i.e., the steady state and dynamic models provided similar results for the setup with and without the THP unit). Furthermore, an acceptable mass balance was obtained for both models implying that the energy transfer within the systems was adequately accounted for. While the performances were consistent in their contexts, some discrepancies were observed specifically with the dynamic model configurations (e.g., mass balances). Additionally, the amount of struvite precipitated for the steady state and dynamic model differed alluding to some limitations involved between the models.

From the results obtained and discussed in Chapter 4, thermal hydrolysis process (THP) pre-treatment could be a viable solution to the issue of limited handling capacities in anaerobic digesters with the increase in population and the stricter legislation requirements for disposable sludge. According to the simulation results, incorporation of the THP unit before the anaerobic digesters was observed to allow for 2.3 more times the concentration of sludge to be digested in comparison to the conventional anaerobic digestion process, implying an improved sludge handling capacity at the same AD volume. Additionally, the THPAD configuration showed a significant increase in the amount of methane produced in comparison to the conventional AD setup. Not only did this suggest that the energy generated from the methane could be used to meet some of the heating costs required for the THP unit, but also that the THP unit availed more biodegradable material for conversion to methane.

As was stated in previous sections, no laboratory experiments were conducted. Therefore, many of the outcomes were based on theoretical scenarios and knowledge collected from an extensive literature review. However, the model is detailed and flexible enough to show how the anaerobic digestion process can be improved through the thermal hydrolysis process. The model is therefore a tool that could be used in predicting digester performance when calibrated with accurate meaningful data collected from a pilot or full-scale plant.

A rigorous calibration and validation process is therefore recommended to check the following:

- If the unbiodegradable effluent from an AD operated at a long sludge age (such that there is no more biogas produced) when fed to THP would become biodegradable when fed back to the AD (evidenced by biogas generation)
- A comprehensive characterization of the compounds and weak acid and base species before and after the THP and calibration of the kinetics that allow for the predicted changes in compounds due to THP processes for various sludges fed to THP unit i.e. (a) Primary Sludge, (b) WAS from ND systems, (c) WAS from NDEBPR AS systems (containing PAOs and their stored PP) and (d) WAS from chemical P removal AS systems (containing chemically precipitated P e.g., ferric phosphates)

6 REFERENCES

- Abelleira-Pereira, Perez-Elvira, S., Sanchez-Oneto, J., De la Cruz, R., Portela, J., and Nebot, E. (2015) 'Enhancement of methane production in mesophilic anaerobic digestion of secondary sewage sludge by advanced thermal hydrolysis pretreatment', *Water Research*, 71, pp. 330–340. doi: 10.1016/j.watres.2014.12.027.
- Angelidaki, I. and Ahring, B. K. (1993) 'Thermophilic anaerobic digestion of livestock waste: the effect of ammonia', *Applied microbiology and biotechnology*, 38, pp. 560–564.
- Angelidaki, I., Ellegaard, L. and Ahring, B. K. (1999) 'A comprehensive model of anaerobic bioconversion of complex substrates to biogas', *Biotechnology and Bioengineering*, 63(3), pp. 363–372. doi: 10.1002/(SICI)1097-0290(19990505)63:3<363::AID-BIT13>3.0.CO;2-Z.
- Batstone, D. J., Keller, I., Angelidaki, I., Kalyuzhnyi, S.V., Pavlostathis, S.G., Rozzi, A., Sanders, W.T.M., Siegrist, H. and Vavilin, V.A. (2002) 'The IWA Anaerobic Digestion Model No 1 (ADM1).', *Water science and technology: a journal of the International Association on Water Pollution Research*, 45(10), pp. 65–73. doi: 10.2166/wst.2002.0292.
- Bolzonella, D., Pavan, P., Battistoni, P. and Cecchi, F. (2004) 'Mesophilic anaerobic digestion of waste activated sludge: influence of the solid retention time in the wastewater treatment process', *Process Biochemistry*, 40(3–4), pp. 1453–1460. doi: 10.1016/j.procbio.2004.06.036.
- Bolzonella, D., Pavan, P., Zanette, M. and Cecchi, F. (2007) 'Two-Phase Anaerobic Digestion of Waste Activated Sludge: Effect of an Extreme Thermophilic Prefermentation', *Industrial & Engineering Chemistry Research*, 46(21), pp. 6650–6655. doi: 10.1021/ie061627e.
- Brouckaert, C. J., Ikumi, D. and Ekama, G. (2010) 'Modelling of Anaerobic Digestion for Incorporation Into a Plant-Wide Wastewater Treatment Model', .
- Chen, Y., Cheng, J. J. and Creamer, K. S. (2007) 'Inhibition of anaerobic digestion process: a review.', *Bioresource technology*, 99(10), pp. 4044–64. doi: 10.1016/j.biortech.2007.01.057.
- Choi, J., Han, S. and Lee, C. (2018) 'sludge by thermal hydrolysis pretreatment', *Bioresource Technology*. Elsevier, 259(February), pp. 207–213. doi: 10.1016/j.biortech.2018.02.123.

Corominas, L., Rieger, L., Takacs, I., Ekama, G., Hauduc, H., Vanrolleghem, P.A., Oehmen, A., Gernaey, K.V., Van Loosdrecht, M.C.M. and Comeau, Y. (2010) 'New framework for standardized notation in wastewater treatment modelling', *Water Science and Technology*, 61(4), pp. 841–857. doi: 10.2166/wst.2010.912.

Dold P.L., Ekama G.A. and Marais G.vR. (1980). A general model for the activated sludge process. *Prog. Wat. Technol.*, 12 (Tor) 47-77.

Eastman, J. A. and Ferguson, J. F. (1981) 'Solubilization of particulate organic carbon during the acid phase of anaerobic digestion', *Journal of the Water Pollution Control Federation*, 53(3 I), pp. 352–366.

Ekama, G. A. and Ikumi, D. S. (2019) 'Plantwide modelling – anaerobic digestion of waste sludge from parent nutrient (N and P) removal systems', 45(3), pp. 305–316.

Ekama, G. A., Wentzel, M. C. and Sötemann, S. W. (2006) 'Tracking the inorganic suspended solids through biological treatment units of wastewater treatment plants', *Water Research*, 40(19), pp. 3587–3595. doi: 10.1016/j.watres.2006.05.034.

Elliott, A. and Mahmood, T. (2007) 'Pretreatment technologies for advancing anaerobic digestion of pulp and paper biotreatment residues', *Water Research*, 41(19), pp. 4273–4286. doi: 10.1016/j.watres.2007.06.017.

Flores-Alsina, X., Ramin, E., Ikumi, D., Harding, T., Batstone, D.J., Brouckaert, C., Sotemann, S. and Gernaey, K.V. (2021) 'Assessment of sludge management strategies in wastewater treatment systems using a plant-wide approach', *Water Research*. Elsevier Ltd, 190, p. 116714. doi: 10.1016/j.watres.2020.116714.

Fotidis, I. A., Karakashev, D., Kotsopoulos, T.A., Martzopoulos, G. and Angelidaki, I. (2013) 'Effect of ammonium and acetate on methanogenic pathway and methanogenic community composition', *FEMS Microbiology Ecology*, 83(1), pp. 38–48. doi: 10.1111/j.1574-6941.2012.01456.x.

Gavala, H. K., Yenil, U., Skiadas, I., Westermann, P. and Ahring, B.K. (2003) 'Mesophilic and thermophilic anaerobic digestion of primary and secondary sludge. Effect of pre-treatment at

elevated temperature', *Water Research*, 37(19), pp. 4561–4572. doi: 10.1016/S0043-1354(03)00401-9.

Ge, H., Jensen, P. D. and Batstone, D. J. (2011) 'Temperature phased anaerobic digestion increases apparent hydrolysis rate for waste activated sludge', *Water Research*. Elsevier Ltd, 45(4), pp. 1597–1606. doi: 10.1016/j.watres.2010.11.042.

Gebreeyessus, G. and Jenicek, P. (2016) 'Thermophilic versus Mesophilic Anaerobic Digestion of Sewage Sludge: A Comparative Review', *Bioengineering*, 3(2), p. 15. doi: 10.3390/bioengineering3020015.

Ghoor, T. 2020. Developments in anaerobic digestion modelling. University of Cape Town, Engineering and the Built Environment ,Department of Civil Engineering.

Han, Y. and Dague, R. R. (1997) 'Laboratory studies on the temperature-phased anaerobic digestion of domestic primary sludge', *Water Environment Research*, 69(6), pp. 1139–1143. doi: 10.2175/106143097x125885.

Hansen, K. H., Angelidaki, I. and Ahring, B. K. (1998) 'Anaerobic Digestion of Swine Manure: Inhibition by Ammonia', *Water Research*, 32(1), pp. 5–12. doi: 10.1016/S0043-1354(97)00201-7.

Harding, T., Ikumi, D. and Ekama, G. (2009) *A steady state stoichiometric model describing the anaerobic digestion of biological excess phosphorus removal waste activated sludge*. University of Cape Town.

Hejnfelt, A. and Angelidaki, I. (2009) 'Anaerobic digestion of slaughterhouse by-products', *Biomass and Bioenergy*. Elsevier Ltd, 33(8), pp. 1046–1054. doi: 10.1016/j.biombioe.2009.03.004.

Higgins, M. J., Beightol, S., Mandahar, U., Suzuki, R., Xiao, S., Lu, H., Le, T., Mah, J., Pathak, B., DeClippeleir, H., Novak, J.T., Al-Omari, A. and Murthy, S. (2017) 'Pretreatment of a primary and secondary sludge blend at different thermal hydrolysis temperatures : Impacts on anaerobic digestion , dewatering and filtrate characteristics', *Water Research*. Elsevier Ltd, 122, pp. 557–569. doi: 10.1016/j.watres.2017.06.016.

Ho, D. P., Jensen, P. D. and Batstone, D. J. (2013) 'Methanosarcinaceae and Acetate-Oxidizing

Pathways Dominate in High-Rate Thermophilic Anaerobic Digestion of Waste-Activated Sludge', *Applied and Environmental Microbiology*, 79(20), pp. 6491–6500. doi: 10.1128/aem.01730-13.

Ikumi, D., Harding, T., Vogts, M., Lakay, M.T., Mafungwa, H., Brouckaert, C. and Ekama, G. (2015) *Mass Balances Modelling Over Wastewater Treatment Plants*. Water Research Group, Department of Civil Engineering, University of Cape Town.

Ikumi, D. S. (2011) 'The Development of a Three Phase Plant-Wide Mathematical Model for Sewage Treatment', Water Research Group, Department of Civil Engineering, University of Cape Town.

Ikumi, D. S. (2020) 'Sensitivity analysis on a three-phase plant-wide water and resource recovery facility model for identification of significant parameters', *Water SA*, 46(3), pp. 476–492. doi: 10.17159/wsa/2020.v46.i3.8658.

Ikumi, D. S. and Ekama, G. A. (2019) 'Plantwide modelling – Anaerobic digestion of waste sludge from parent nutrient (N and p) removal systems', *Water SA*, 45(3), pp. 305–316. doi: 10.17159/wsa/2019.v45.i3.6698.

Ikumi, D. S., Harding, T. H. and Ekama, G. A. (2014) 'Biodegradability of wastewater and activated sludge organics in anaerobic digestion', *Water Research*. Elsevier Ltd, 56, pp. 267–279. doi: 10.1016/j.watres.2014.02.008.

Izzett H.B., Wentzel M.C. and Ekama G.A. (1992). The Effect of Thermophilic Heat Treatment on the Anaerobic Digestibility of Primary Sludge. MSc Thesis W76, Dept. of Civil Eng., University of Cape Town, Rondebosch, 7701, Cape, South Africa.

Li, Y.-Y. and Noike, T. (1992) 'Upgrading of anaerobic digestion of waste activated sludge by temperature-phased process with recycle', *Energy*, 87(34), pp. 381–389. doi: 10.1016/j.energy.2015.04.110.

Loewenthal, R. E., Wentzel, M.C., Ekama, G.A. and Marais, G. (1991) *Mixed weak acid/base systems Part 2: Dosing estimation, aqueous phase*. Water SA Vol. 17, No.2. doi: ISSN 0378-4738.

Loewenthal, R. E., Ekama, G. and Marais, G. (1989) *Mixed weak acid/base systems Part 1 - Mixture characterisation*. Water SA Vol. 15. doi: ISSN 0378-4738.

Loewenthal, R. E., Kornmuller, U. R. C. and van Heerden, E. P. (1994) 'Modelling struvite precipitation in anaerobic treatment systems', *Water Science and Technology*. Water Science Techn. Vol. 30, No. 12, 30(12), pp. 107–116.

McCarty P.L. (1975). Stoichiometry of biological reactions. *Progress in Water Technology*, 7 (1), 157-172.

Moosbrugger, R., Wentzel, M.C., Ekama, G. and Marais, G. (1993) 'Mixed weak acid base chemistry and pH in anaerobic digestion - A review', *Water SA*, pp. 1–10.

Musvoto, E. V., Wentzel, M.C. and Ekama, G.A. (2000) 'Integrated chemical-physical processes modelling - I. Development of a kinetic-based model for mixed weak acid/base systems', *Water Research*, 34(6), pp. 1857–1867. doi: 10.1016/S0043-1354(99)00334-6.

Neyens, E. and Baeyens, J. (2003) 'A review of thermal sludge pre-treatment processes to improve dewaterability', *Journal of Hazardous Materials*, 98(1–3), pp. 51–67. doi: 10.1016/S0304-3894(02)00320-5.

Nges, I. A. and Liu, J. (2009) 'Effects of anaerobic pre-treatment on the degradation of dewatered-sewage sludge', *Renewable Energy*. Elsevier Ltd, 34(7), pp. 1795–1800. doi: 10.1016/j.renene.2008.12.001.

Nopens, I., Batstone, D., Copp, J., Jeppsson, U., Volcke, E., Alex, J. and Vanrolleghem, P.A. (2009) 'An ASM/ADM model interface for dynamic plant-wide simulation', *Water Research*. Elsevier Ltd, 43(7), pp. 1913–1923. doi: 10.1016/j.watres.2009.01.012.

Parkin, G. F. and Owen, W. F. (1986) 'Fundamentals of Anaerobic Digestion of Wastewater Sludges', *Journal of Environmental Engineering*, 112(5), pp. 867–920. doi: 10.1061/(asce)0733-9372(1986)112:5(867).

Phothilangka, P., Schoen, M. A. and Wett, B. (2008) 'Benefits and drawbacks of thermal pre-hydrolysis for operational performance of WWTP.pdf', *Water Science and Technology*, 58(8), pp. 1547–1553. doi: Doi 10.2166/Wst.2008.500.

Rajagopal, R., Massé, D. I. and Singh, G. (2013) 'A critical review on inhibition of anaerobic digestion process by excess ammonia', *Bioresource Technology*. Elsevier Ltd, 143, pp. 632–641.

doi: 10.1016/j.biortech.2013.06.030.

Sam-Soon, P. A., Loewenthal, R.E., Wentzel, M.C. and Marais, G. (1991) 'Effect of sulphate on pelletisation in the UASB system with glucose as substrate', *Water SA*, 17(1), pp. 47–56.

Schnurer, A., Houwen, F. P. and Svensson, B. H. (1994) 'Mesophilic syntrophic acetate oxidation during methane formation by a triculture at high ammonium concentration', p. 5.

Sötemann, S. W., Ristow, N.E., Wentzel, M.C. and Ekama, G. (2005) 'A steady state model for anaerobic digestion of sewage sludges', 31(4), pp. 511–516.

Valo, A., Carrère, H. and Delgenès, J. P. (2004) 'Thermal, chemical and thermo-chemical pre-treatment of waste activated sludge for anaerobic digestion', *Journal of Chemical Technology and Biotechnology*, 79(11), pp. 1197–1203. doi: 10.1002/jctb.1106.

Vavilin, V. A., Rytov, S.V., Lokshina, L., Rintala, J. and Lyberatos, G. (2001) 'Simplified hydrolysis models for the optimal design of two-stage anaerobic digestion', *Water Research*, 35(17), pp. 4247–4251. doi: 10.1016/S0043-1354(01)00148-8.

Westerholm, M., Moestedt, J. and Schnürer, A. (2016a) 'Biogas production through syntrophic acetate oxidation and deliberate operating strategies for improved digester performance', *Applied Energy*, 179, pp. 124–135. doi: 10.1016/j.apenergy.2016.06.061.

Westerholm, M., Moestedt, J. and Schnürer, A. (2016b) 'Biogas production through syntrophic acetate oxidation and deliberate operating strategies for improved digester performance', *Applied Energy*. The Authors, 179, pp. 124–135. doi: 10.1016/j.apenergy.2016.06.061.

Wett, B., Murthy, S., Takacs, I., Wilson, C.A., Novak, J., Panter, K. and Bailey, W. (2009) 'Simulation of Thermal Hydrolysis at the Blue Plains AWT: A new toolkit developed for full-plant process design', in *Proceedings of 82nd Annual Water Environment Federation Technical Exhibition and Conference*. Orlando, USA. doi: 10.1017/CBO9781107415324.004.

Wett, B., Takacs, I., Batstone, D., Wilson, C. and Murthy, S. (2014a) 'Anaerobic model for high-solids or high-temperature digestion - Additional pathway of acetate oxidation', *Water Science and Technology*, 69(8), pp. 1634–1640. doi: 10.2166/wst.2014.047.

Wett, B., Takacs, Batstone, D., Wilson, C. and Murthy, S. (2014b) 'Anaerobic model for high-solids

or high-temperature digestion - Additional pathway of acetate oxidation', *Water Science and Technology*, 69(8), pp. 1634–1640. doi: 10.2166/wst.2014.047.

Williamson, K. and McCarty, P. L. (1976) 'A model of substrate utilization by bacterial films', *Journal of the Water Pollution Control Federation*, 48(1), pp. 9–24.

Wilson, C. A., Murthy, S.M., Fang, Y. and Novak, J.T. (2008) 'The effect of temperature on the performance and stability of thermophilic anaerobic digestion', *Water Science and Technology*, 57(2), pp. 297–304. doi: 10.2166/wst.2008.027.

Zinder, S. H. and Koch, M. (1984) 'Non-aceticlastic methanogenesis from acetate: acetate oxidation by a thermophilic syntrophic coculture', *Archives of Microbiology*, 138(3), pp. 263–272. doi: 10.1007/BF00402133.

7 APPENDIX

7.1 INFLUENT COMPONENT COMPOSITION

In order to calculate the influent component compositions, it was imperative to obtain the context of their applications. Given the study was meant to virtually simulate the Cape Flats Wastewater Treatment Works (CFWWTW), the following Table A.1 illustrate the characteristics of the CFWWTW anaerobic digester.

Table A.2: Cape Flats Anaerobic Digester Design Parameters

AD Design Parameters		
	Conventional	THP
WAS in Feed (%)	60	60
PS in Feed (%)	40	40
Sludge age (days)	15	15
Flowrate (m ³ /d)	1257	1257
Solid Concentration TSS g/l	47	110
Solid Concentration VSS g/l	36.0	84.2
Solid Concentration ISS g/l	11.0	25.8
Loading Rate	2.4	5.6
Reactor Volume (m ³)	18850	18850

Once the operational parameters were selected, the primary sludge (PS) and waste activated sludge (WAS) characteristics were broadly specified as shown in the following Table A.2.

Table A.3: PS and WAS characteristics for conventional AD and just before THP pre-treatment

	Conventional AD		Before THP	
	PS	WAS	PS	WAS
Solid Concentration TSS g/l	47	47	110	110
VSS/TSS	0.81	0.74	0.81	0.74
Solid Concentration VSS g/l	38	35	89	81
ISS	9	12	21	29
fs'up	0.36	0.53	0.36	0.53

The conventional AD total solids concentration (TSS) of 4.7% was obtained from typical TSS values measured in the current CFWWTW facilities. The value of 11% for the THPAD configuration, was obtained from literature values of the increased solid rates that a THPAD unit was determined to

handle which was about 2 times more than the conventional configuration. The VSS/TSS ratios as well as the $f_{s'up}$ values were obtained from experiments carried out by Ikumi (2011).

A brief description of the influent wastewater was as described in Section 3.3.2 on feed. The following Table A.3 summarizes the characteristics of the wastewater components as investigated by Ikumi (2020) and as described in section 3.3.2.

Table A.4: Elemental Wastewater Component Characteristics and their mass ratios

Composition	C	H	O	N	P	COD per mol	Molar mass per mol	fcv	fc	fn	fp	fo	fh	Check
PS UPO	1	1.534	0.421	0.166	0.019	34.31	23.20	1.479	0.51	0.100	0.025	0.29	0.07	1.00
PS BPO	1	1.623	0.577	0.032	0.008	35.30	23.57	1.498	0.51	0.019	0.011	0.39	0.07	1.00
WAS UPO	1	1.534	0.421	0.166	0.019	34.31	23.21	1.479	0.52	0.100	0.025	0.29	0.07	1.00
WAS BPO	1	1.534	0.421	0.166	0.019	34.31	23.21	1.479	0.52	0.100	0.025	0.29	0.07	1.00
SF	1	1.942	0.681	0.03	0.008	36.24	25.53	1.419	0.47	0.016	0.009	0.43	0.08	1.00
SU	1	1.833	0.6	0.086	0	35	24.66	1.419	0.49	0.048	0	0.39	0.07	1.00
VFA	2	3	2	0	0	63.99	59.04	1.083	0.41	0	0	0.54	0.05	1.00

Once these characteristics were established, it was possible to fractionate the wastewater into the respective primary sludge and waste activated sludge component concentrations as well as the blend for the conventional AD setup and before the THP unit (after thickening) as was described in Section 3.3.2. The results obtained are as shown in Tables A.4 – A.10. It should be noted that the VFA, and USO COD, as well as the inorganic concentrations were obtained directly from experiments carried out by Ikumi (2011).

Table A.5: Conventional AD Primary Sludge Component Concentrations

Conventional AD Configuration							
PS (mg/l)							
Influent feed	PS UPO	PS BPO	FBSO	VFA	USO	Inorganic	Total
VSS	13827.81	24127.23	0	0	0	0	37955.036
COD	20445.24	36132.10	115	50	50	0	56792.346
N	1385.47	458.74	1.33	0	1.720	40	1887.270
P	350.67	253.60	0.786	0	0	7.3	612.359
C	7156.91	12292.73	38.114	18.768	17.159	5	19528.683

Table A.6: Conventional AD Waste Activated Sludge Component Concentrations

Conventional AD Configuration							
WAS (mg/l)							
Influent feed	WAS UPO	WAS BPO	FBSO	VFA	USO	Inorganic	Total
VSS	18368.854	16258.927	0	0	0	0	34627.782
COD	27159.451	24039.796	0	0	45	0	51244.247
N	1840.468	1629.063	0	0	1.549	40	3511.080
P	465.828	412.321	0	0	0	7.3	885.449
C	9507.233	8415.190	0	0	15.443	5	17942.865

Table A.7: Conventional AD Blended Sludge Component Concentrations

Conventional AD Configuration							
Blended sludge (mg/l)							
Blend	UPO	BPO	FBSO	VFA	USO	Inorganic	Sum
VSS	16552	19406	0	0	0	0	35959
COD	24474	28877	46	20	47	0	53463
N	1658	1161	1	0	2	40	2862
P	420	349	0	0	0	7	776
C	8567	9966	15	8	16	5	18577

With the blended sludge components obtained, these were further subdivided into a pre-processor that fractionated the wastewater into components suitable for input into the dynamic model. These component concentrations were obtained as shown in Table A.7.

Table A.8: Conventional AD Blended Sludge Pre-processed Component Concentrations

Inputs for Pre-Processor		
Components	VSS (mg/l)	COD (mg/l)
[X_OHO]	5365.44584	7933.132692
[X_PAO]	4389.91023	6490.74493
[X_AD]	0	0
[X_AC]	0	0
[X_AM]	0	0
[X_HM]	0	0
[X_ANO]	0	0
[X_B_Org]	0	0
[X_U_Org]	11021.3129	16295.67051

[X_B_Inf]	9650.89034	14452.84061
[X_U_Inf]	5531.12405	8178.097844
[S_F]	32.4077398	46
[S_U]	33.1181911	47
[S_VFA]	18.4523095	20
[X_PAO_PP]	0	0
Sum	36042.6616	53463.4866

Table A.9: PS Component Concentrations prior to THP pre-treatment

Before THP Pretreatment							
PS (mg/l)							
Influent feed	PS UPO	PS BPO	FBSO	VFA	USO	Inorganic	Total
VSS	32293.11	56537.821	0	0	0	0	88830.93
COD	47747.301	84669.091	115	50	50	0	132631.39
N	3235.609	1074.970	1.333	0	1.721	40	4353.63
P	818.943	594.276	0.786	0	0	7.3	1421.31
C	16714.060	28805.814	38.114	18.768	17.159	5	45598.92

Table A.10: WAS Component Concentrations prior to THP Pre-treatment

Before THP Pretreatment							
WAS (mg/l)							
Influent feed	WAS UPO	WAS BPO	FBSO	VFA	USO	Inorganic	Total
VSS	42969.315	38074.429	0	0	0	0	81043.74
COD	63532.703	56295.322	0	0	45	0	119873.03
N	4305.311	3814.868	0	0	1.549	40	8161.73
P	1089.688	965.556	0	0	0	7.3	2062.54
C	22239.779	19706.316	0	0	15.443	5	41966.54

Table A.11: Blended Sludge Component Concentrations prior to THP Pre-treatment

Before THP Pretreatment							
Blended sludge (mg/l)							
Blend	UPO	BPO	FBSO	VFA	USO	Inorganic	Sum
VSS	38699	45460	0	0	-	0	84159
COD	57219	67645	46	20	47	0	124976
N	3877	2719	0.53	0.00	1.62	40	6638
P	981	817	0.31	0.00	0.00	7.3	1806
C	20029	23346	15.25	7.51	16.13	5	43419

Once the influent wastewater component concentrations were obtained, these values were fractionated into the dynamic organic components for input into the THP preprocessor as shown in Table A.11. It should be noted that the BPO concentration was divided into the [X_OHO] and [X_PAO] components as described in Section 3.3.2.

Table A.12: Input THP AD Blended Sludge Pre-processed Component Concentrations

Inputs for Pre-Processor				
Temperature	180			
Inflow (l/d)	1256640000			
Components	VSS (mg)	VSS (mg/l)	COD (mg)	COD (mg/l)
[X_OHO]	15789130.7	12564.56163	23345174.46	18577.45612
[X_PAO]	12918379.7	10280.09588	19100597.28	15199.73682
[X_AD]	0	0	0	0
[X_AC]	0	0	0	0
[X_AM]	0	0	0	0
[X_HM]	0	0	0	0
[X_ANO]	0	0	0	0
[X_B_Org]	0	0	0	0
[X_U_Org]	32398176	25781.58897	47902641.58	38119.62183
[X_B_Inf]	28419075	22615.12843	42559426.83	33867.63658
[X_U_Inf]	16232327.6	12917.24567	24000467.55	19098.92058
[S_F]	40724.8621	32.40773976	57805.44	46
[S_U]	41617.6436	33.11819105	59062.08	47
[S_VFA]	23187.9102	18.45230952	25132.8	20
[S_PO4]	28116.3037	0	0	0
[X_PAO_PP]	0	0	0	0

Sum	105890736	84242.5988	157050308	124976.372
-----	-----------	------------	-----------	------------

These components were input into the THP model as described in Section 3.4 to obtain the output concentrations that were reconverted back to the wastewater component concentrations. The THP output concentrations and the reconverted component concentrations obtained are as shown in Tables A.12 and A.13.

Table A.13:Output THP AD Blended Sludge Pre-processed Component Concentrations

Outputs from Pre-Processor				
Outflow	1242041324	1242.041324		
Components	VSS (mg)	VSS (mg/l)	COD (mg)	COD (mg/l)
[X_OHO]	0	0	0	0
[X_PAO]	0	0	0	0
[X_AD]	0	0	0	0
[X_AC]	0	0	0	0
[X_AM]	0	0	0	0
[X_HM]	0	0	0	0
[X_ANO]	0	0	0	0
[X_B_Org]	41114885.9	33102.6715	60790818.8	48944.2804
[X_U_Org]	0	0	0	0
[X_B_Inf]	15630491.2	12584.5179	23407684.8	18846.1401
[X_U_Inf]	0	0	0	0
[S_F]	29161059.3	23478.3326	41391616.3	33325.4743
[S_U]	2733435.64	2200.76063	3879181.54	3123.23065
[S_VFA]	25445074.6	20486.496	27579284.4	22204.8042
[S_PO4]				
[X_PAO_PP]	0	0	0	0
Sum	114113055	91875.4089	157048586	126443.93

Table A.14: Blended Sludge Component Concentrations after THP Pre-treatment

After THP Pretreatment							
Blended sludge (mg/l)							
Blend	UPO	BPO	FBSO	VFA	USO	Inorganic	Sum
VSS	0	45687	0	0	0	0	45687
COD	0	67790	33325	22205	3123	0	126444
N	0	3556	386	0	107	2667	6717
P	0	972	228	0	0	628	1827
C	0	23545	11045	8335	1072	5	44002




The Inorganic N and P components were obtained through the summation of the respective N and P masses of the outputs from the THP model and subsequent subtraction of this summation from the initial total mass into the THP model. The N and P component concentrations were obtained with the use of the N and P mass ratios (f_n and f_p).

With the pre-processed values from the influent conventional AD wastewater and THP output, the influent files into the dynamic model for both setups could be determined.

7.2 MASS BALANCE VERIFICATION SPREADSHEETS

THP Model Verification

Following the input of the pre-processed wastewater component concentrations into the THP model and the THP processes as described in Section 3.4 of this report, a mass balance was carried after every process and the results obtained as shown in Figure B.1.

COD Balancing					
Pasteurisation	Mass	mMols	e-	COD (mMol)	COD(VSS)
Biomass	28707510.41	1237053.268	5305721.47	42445771.7	42445771.7
					
[X_B_Org]	20382332.39	878307.8205	3767062.24	30136497.9	30136497.9
[X_U_Org]	5741502.082	247410.6537	1061144.29	8489154.35	8489154.35
[S_U]	2691818	109146.2702	477514.932	3820119.46	3820119.46
	28815652.47	1234864.744	5305721.47	42445771.7	42445771.7
Balance	100.376703	99.82308571	100	100	100
Activation	Mass	mMols	e-	COD (mMol)	COD(VSS)
[X_U_Inf]	16232327.6	699477.371	3000058.44	24000467.6	24000467.6
					
[X_B_Org]	16232327.6	699477.371	3000058.44	24000467.6	24000467.6
[X_U_Inf]	0	0	0	0	0
	16232327.6	699477.371	3000058.44	24000467.6	24000467.6
Balance	100	100	100	100	100
Solubilisation	Mass	mMols	e-	COD (mMol)	COD(VSS)
[X_B_Inf]	28419074.99	1205512.883	5319928.35	42559426.8	42559426.8
					
[S_VFA]	7067435.71	119705.8696	957587.104	7660696.83	7660218.04
[S_F]	8095626.17	317081.8224	1436380.66	11491045.2	11491045.2
[X_B_Inf]	15630491.24	663032.0858	2925960.59	23407684.8	23407684.8
	30793553.12	1099819.778	5319928.35	42559426.8	42558948
Balance	108.3552267	91.23251962	100	100	99.998875



Activation	Mass	mMols	e-	COD (mMol)	COD(VSS)
[X_U_Org]	38139678	1643500.7	7048974.49	56391795.9	56391795.9
					
[X_B_Org]	38139678	1643500.7	7048974.49	56391795.9	56391795.9
[X_U_Org]	0	0	0	0	0
	38139678	1643500.7	7048974.49	56391795.9	56391795.9
Balance	100	100	100	100	100
Solubilisation	Mass	mMols	e-	COD (mMol)	COD(VSS)
[X_B_Org]	74754338	3221285.89	13816095.2	110528761	110528761
					
[S_VFA]	18354451	310881.572	2486897.13	19895177.1	19893933.6
[S_F]	21024708.3	823475.871	3730345.7	29842765.6	29842765.6
[X_B_Org]	41114885.9	1771707.24	7598852.35	60790818.8	60790818.8
	80494045.2	2906064.68	13816095.2	110528761	110527518
Balance	107.678092	90.2144293	100	100	99.998875

Figure B.4: THP Processes Mass Balance

It was apparent that an electron and COD mass balance was obtained after every process ascertaining that the energy was accordingly accounted for throughout the THP model.

Extended-UCTSDM3P Model Verification

Once simulations were run in the WEST® model, the influent and effluent mass concentrations were exported to excel and run through a post-processor in order to re-convert the mass concentrations into elemental concentrations. The post process involved first obtaining the weight of the different elements in each model component and multiplying these by the respective component mass concentration. Tables B.1 and B.2 display the values obtained.

Table B.1: Elemental masses per component unit mole

Component values per unit mol									
Molecular weight		COD		C	H	O	N	P	Charge
MW [H2O]	18.0148	COD_per_mol[H2O]	0	0	2.0158	15.999	0	0	0
MW [S H]	1.0079	COD_per_mol[S H]	0	0	1.0079		0	0	1
MW [S Na]	22.99	COD_per_mol[S Na]	0	0			0	0	2
MW [S K]	39.098	COD_per_mol[S K]	0	0			0	0	1
MW [S Ca]	40.078	COD_per_mol[S Ca]	0	0			0	0	2
MW [S Mg]	24.305	COD_per_mol[S Mg]	0	0			0	0	2
MW [S NHx]	18.0386	COD_per_mol[S NHx]	0	0	4.0316		14.007	0	1
MW [S Cl]	35.453	COD_per_mol[S Cl]	0	0			0	0	-2
MW [S VFA]	59.0437	COD_per_mol[S VFA]	63.996	24.022	3.0237	31.998	0	0	-1
MW [S Pr]	73.0705	COD_per_mol[S Pr]	111.993	36.033	5.0395	31.998	0	0	-1
MW [S CO3]	60.008	COD_per_mol[S CO3]	0	12.011		47.997	0	0	-2
MW [S SO4]	96.062	COD_per_mol[S SO4]	0				0	0	-2
MW [S PO4]	94.97	COD_per_mol[S PO4]	0			63.996	0	30.974	-3
MW [S H2]	2.0158	COD_per_mol[S H2]	15.999		2.0158		0	0	0
MW [S U]	24.66248	COD_per_mol[S U]	34.9978125	12.011	1.847481	9.5994	1.204602	0	0
MW [S F]	25.53166	COD_per_mol[S F]	36.237735	12.011	1.957342	10.89532	0.42021	0.247792	0
MW [S Glu]	180.1548	COD_per_mol[S Glu]	191.988	72.066	12.0948	95.994	0	0	0
MW [S O]	31.998	COD_per_mol[S O]	-31.998			31.998	0	0	0
MW [S NOx]	62.004	COD_per_mol[S NOx]	-64			47.997	14.007	0	-1
MW [S N2]	28.014	COD_per_mol[S N2]	-48				28.014	0	0
MW [X U Inf]	23.20637	COD_per_mol[X U Inf]	34.3098555	12.011	1.546119	6.735579	2.325162	0.588506	0
MW [X B Org]	23.20637	COD_per_mol[X B Org]	34.3098555	12.011	1.546119	6.735579	2.325162	0.588506	0
MW [X PAO_PP]	100.5122	COD_per_mol[X PAO_PP]	0			47.997	0	30.974	0
MW [X PAO Stor]	86.0894	COD_per_mol[X PAO Stor]	143.991	48.044	6.0474	31.998	0	0	0
MW [X Str NH4]	245.4024	COD_per_mol[X Str NH4]	0		16.1264	159.99	14.007	30.974	0
MW [X ACP]	310.174	COD_per_mol[X ACP]	0			127.992	0	61.948	0
MW [X Str K]	266.4618	COD_per_mol[X Str K]	0		12.0948	159.99	0	30.974	0
MW [X Cal]	100.086	COD_per_mol[X Cal]	0	12.011		47.997	0	0	0
MW [X Mag]	84.313	COD_per_mol[X Mag]	0	12.011		47.997	0	0	0
MW [X Newb]	174.3273	COD_per_mol[X Newb]	0		7.0553	111.993	0	30.974	0
MW [X OHO]	23.20637	COD_per_mol[X OHO]	34.3098555	12.011	1.546119	6.735579	2.325162	0.588506	0

MW [X_PAO]	23.20637	COD_per_mol[X_PAO]	34.3098555	12.011	1.546119	6.735579	2.325162	0.588506	0
MW [X_AD]	23.20637	COD_per_mol[X_AD]	34.3098555	12.011	1.546119	6.735579	2.325162	0.588506	0
MW [X_AC]	23.20637	COD_per_mol[X_AC]	34.3098555	12.011	1.546119	6.735579	2.325162	0.588506	0
MW [X_AM]	23.20637	COD_per_mol[X_AM]	34.3098555	12.011	1.546119	6.735579	2.325162	0.588506	0
MW [X_OB]	23.20637	COD_per_mol[X_OB]	34.3098555	12.011	1.546119	6.735579	2.325162	0.588506	0
MW [X_HM]	23.20637	COD_per_mol[X_HM]	34.3098555	12.011	1.546119	6.735579	2.325162	0.588506	0
MW [X_U_Org]	23.20637	COD_per_mol[X_U_Org]	34.3098555	12.011	1.546119	6.735579	2.325162	0.588506	0
MW [X_B_Inf]	23.57426	COD_per_mol[X_B_Inf]	35.3017935	12.011	1.635822	9.231423	0.448224	0.247792	0
MW [X_ISS]	100	COD_per_mol[X_ISS]	0				0	0	0
MW [X_ANO]	23.20637	COD_per_mol[X_ANO]	34.3098555	12.011	1.546119	6.735579	2.325162	0.588506	0
MW [G_CO2]	44.009	COD_per_mol[G_CO2]	0	12.011		31.998	0	0	0
MW [G_CH4]	16.0426	COD_per_mol[G_CH4]	63.996	12.011	4.0316		0	0	0

Table B.2: Elemental molar fractions for dynamic model components

Composition Matrix - Balance Check								
	COD	C	H	O	N	P	Charge	Mass
H2O	0	0	0.111896885	0.888103115	0	0	0	1
S_H	0	0	1	0	0	0	0.992161921	1
S_Na	0	0	0	0	0	0	0.086994345	1
S_K	0	0	0	0	0	0	0.025576756	1
S_Ca	0	0	0	0	0	0	0.04990269	1
S_Mg	0	0	0	0	0	0	0.082287595	1
S_NHx	0	0	0.223498498	0	0.776501502	0	0.055436675	1
S_Cl	0	0	0	0	0	0	-0.056412715	1
S_VFA	1.083875164	0.406851197	0.051211222	0.541937582	0	0	-0.016936608	1
S_Pr	1.532670503	0.493126501	0.068967641	0.437905858	0	0	-0.013685413	1
S_CO3	0	0.200156646	0	0.799843354	0	0	-0.033328889	1
S_SO4	0	0	0	0	0	0	-0.020819887	1
S_PO4	0	0	0	0.673854902	0	0.326145098	-0.031588923	1
S_H2	7.936799286	0	1	0	0	0	0	1
S_U	1.41907094	0.48701504	0.074910573	0.389230886	0.048843501	0	0	1
S_F	1.419325301	0.470435478	0.076663311	0.426737541	0.016458388	0.009705282	0	1
S_Glu	1.065683512	0.400022647	0.067135597	0.532841756	0	0	0	1

S_O	-1	0	0	1	0	0	0	1
S_NOx	-1.032191472	0	0	0.77409522	0.22590478	0	-0.016127992	1
S_N2	-1.713429	0	0	0	1	0	0	1
X_U_Inf	1.478467421	0.517573506	0.066624763	0.290247043	0.100195009	0.02535968	0	1
X_B_Org	1.478467421	0.517573506	0.066624763	0.290247043	0.100195009	0.02535968	0	1
X_PAO_PP	0	0	0	0.477524218	0	0.308161659	0	1
X_PAO_Stor	1.672575253	0.558071028	0.070245582	0.37168339	0	0	0	1
X_Str_NH4	0	0	0.065714109	0.651949614	0.057077681	0.126217185	0	1
X_ACP	0	0	0	0.412645805	0	0.199720157	0	1
X_Str_K	0	0	0.045390371	0.600423776	0	0.116241803	0	1
X_Cal	0	0.120006794	0	0.47955758	0	0	0	1
X_Mag	0	0.142457272	0	0.569271643	0	0	0	1
X_Newb	0	0	0.040471573	0.642429499	0	0.177677277	0	1
X_OHO	1.478467421	0.517573506	0.066624763	0.290247043	0.100195009	0.02535968	0	1
X_PAO	1.478467421	0.517573506	0.066624763	0.290247043	0.100195009	0.02535968	0	1
X_AD	1.478467421	0.517573506	0.066624763	0.290247043	0.100195009	0.02535968	0	1
X_AC	1.478467421	0.517573506	0.066624763	0.290247043	0.100195009	0.02535968	0	1
X_AM	1.478467421	0.517573506	0.066624763	0.290247043	0.100195009	0.02535968	0	1
X_OB	1.478467421	0.517573506	0.066624763	0.290247043	0.100195009	0.02535968	0	1
X_HM	1.478467421	0.517573506	0.066624763	0.290247043	0.100195009	0.02535968	0	1
X_U_Org	1.478467421	0.517573506	0.066624763	0.290247043	0.100195009	0.02535968	0	1
X_B_Inf	1.497471923	0.509496359	0.069390159	0.391589077	0.019013279	0.010511125	0	1
X_ISS	0	0	0	0	0	0	0	1
X_ANO	1.478467421	0.517573506	0.066624763	0.290247043	0.100195009	0.02535968	0	1
G_CO2	0	0.272921448	0	0.727078552	0	0	0	1
G_CH4	3.989128944	0.748694102	0.251305898	0	0	0	0	1

Once the elemental mass per mol for the different components were obtained, the values were multiplied by the respective component influent and effluent mass concentrations obtained from the WEST® model and these were summed (i.e., Summation of total influent COD, C, H, O, N, and P elemental mass concentrations for the respective components). The model was then verified by

checking that the summation of the influent and effluent mass values were within a 100% balance. The following Table B.3 is an instance of the model verification for the THPAD configuration.

Table B.3: Extended-UCTSDM3P model verification for THPAD configuration

Element	COD	C	H	O	N	P
Influent (g/d)	157040153.197	54694296.092	147778570.501	1150215883.827	8342170.303	2269690.760
Effluent (g/d)	-157069893.540	-54716022.247	-147401259.925	-1147266767.554	-8340812.250	-2269938.553
Mass Balance (%)	100.018	100.040	99.745	99.744	99.984	100.011

7.3 DYNAMIC MODEL DESCRIPTION

Terminology

In order to provide an appropriate description of the model, a brief overview of terminologies often used in modelling is described in this section (I.e., Components, Parameters and Variables). The nomenclature developed by Corominas *et al.*, (2010) is adopted in the development of this model for ease of understanding between model developers.

Components

Components are specific combinations of elements and charge. They specialize the stoichiometry for a system and are subject to the material content of the system. It is therefore important to note that components do not refer to a specific compound or value but rather a group of defined names. For example, the component labelled CO_3 on the model represents the compounds H_2CO_3 , HCO_3^- , CO_3^{2-} and other carbonate complexes present in the system such as $MgCO_3$.

For this THPAD model just as in the predecessor (ADM-3P), it is intended to be adopted for the plant-wide model, the components were therefore selected such that all unit operations across the resource recovery facility are represented in line with the supermodel approach of Jones and Takacs (2004) with each component parameterized based on its COD and molar concentrations.

The following table C.1 shows the components applied to the Extended-UCTSDM3P model. Of note is that the components used are similar to those used for the UCTSDM3P model developed by Ikumi (2011) and modified to include the organism mass as a result of the included acetate oxidizing bacteria (Z_OB).

Table C.1: Components used in the Extended-UCTSDM3P model

	Component Name	Empirical formula	Notation
Total Dissolved Ionic Concentration	Water	H ₂ O	H ₂ O
	Hydrogen ion	H ⁺	H
	Sodium	Na ⁺	Na
	Potassium	K ⁺	K
	Calcium	Ca ²⁺	Ca
	Magnesium	Mg ²⁺	Mg
	Ammonium	NH ₄ ⁺	NH ₄
	Chloride	Cl ⁻	Cl
	Acetate	CH ₃ COO ⁻	Ac
	Propionate	CH ₃ CH ₂ COO ⁻	Pr
	Carbonate	CO ₃ ²⁻	CO ₃
	Sulphate	SO ₄ ²⁻	SO ₄
	Phosphate	PO ₄ ³⁻	PO ₄
	Nitrate	NO ₃ ⁻	NO ₃
Soluble Organics	Dissolved hydrogen	H ₂	H ₂
	Dissolved oxygen	O ₂	O ₂
	Unbiodegradable Soluble Organics	CH _{Yu} O _{Zu} N _{Au} P _{Bu}	USO

	Fermentable Biodegradable Soluble Organics	$CH_{Yf}O_{Zf}N_{Af}P_{Bf}$	FBSO
	Glucose		GLU
Particulates	Unbiodegradable Particulate Organics	$CH_{Yup}O_{Zup}N_{Aup}P_{Bup}$	UPO
	Biodegradable Particulate Organics	$CH_{Ybp}O_{Zbp}N_{Abp}P_{Bbp}$	BPO
	PS biodegradable particulate organics	$CH_{Ybps}O_{Zbps}N_{Abps}P_{Bbps}$	BPO _{PS}
	Polyphosphate	$K_{kp}Mg_{mp}Ca_{cp}PO_3$	PP
	Poly-hydroxy-alkanoate	$C_4H_{12}O_2$	PHA
	Struvite	$MgKPO_4 \cdot 6H_2O$	Struv
	Calcium Phosphate	$Ca_3(PO_4)_2$	ACP
	K-struvite	$MgNH_4PO_4 \cdot 6H_2O$	MgKP
Microorganism Biomass	Ordinary heterotrophic organisms	$CH_{Y0}O_{Z0}N_{A0}P_{B0}$	OHO
	Phosphate accumulating organisms	$CH_{Y0}O_{Z0}N_{A0}P_{B0}$	PAO
	Autotrophic nitrifying organisms	$CH_{Y0}O_{Z0}N_{A0}P_{B0}$	ANO
	Acidogens	$CH_{Y0}O_{Z0}N_{A0}P_{B0}$	Z _{AD}
	Acetogens	$CH_{Y0}O_{Z0}N_{A0}P_{B0}$	Z _{AC}
	Acetoclastic methanogens	$CH_{Y0}O_{Z0}N_{A0}P_{B0}$	Z _{AM}
	Acetate oxidizing methanogens	$CH_{Y0}O_{Z0}N_{A0}P_{B0}$	Z _{OB}
	Hydrogenotrophic methanogens	$CH_{Y0}O_{Z0}N_{A0}P_{B0}$	Z _{HM}
	Endogenous residue	$CH_{Ye}O_{Ze}N_{Ae}P_{Be}$	ER
	Inorganic Settleable Solids		ISS
Gases	Carbon dioxide	CO_2	CO_2
	Methane	CH_4	CH_4

Parameters

Parameters refer to the model constants that define components. These are specific to a context and can be determined from literature, calibration through a model, or experimentally determined values. Parameters are defined prior to a simulation run and remain constant during the simulation. This is the main difference between parameters and variables as

the latter change as the simulation runs. Examples of parameters include temperature, volume of the reactor, wastewater composition fractions, kinetic rate constants and yield coefficients. The following tables C.2 and C.3 show the parameters implemented in this model for both the kinetic and stoichiometric constants.

Table C.2: Kinetic parameters for the Extended-UCTSDM3P model.

	Parameter	Description	Value	Unit
	K_I_H_AO	H ⁺ inhibition factor for acetate oxidizing bacteria	0.001	
Kinetic parameters	K_I_H_AD	H ⁺ inhibition for acidogens	0.0155	
	K_I_NH3	NH ₃ Inhibition for AD organisms	0.0018	
	KS_fPP_PAO_PHAstor	Saturation coeff for polyphosphate	0.01	-
	K_O2	Saturation/inhibition coeff for oxygen	20	-
	K_S_ALK	Saturation coeff for alkalinity (HCO ₃ ⁻)	0.0001	-
	K_S_NHx	Saturation coeff for Ammonia (nutrient)	0.0001	gNH ₃ -N/m ³
	K_S_PO4	Saturation coeff for phosphorus (nutrient)	0.0001	-
	K_S_VFA	Saturation coeff for Acetate	10	-
	KS_AC	Half Sat coeff for acetogens	0.089	g/m ³
	KS_AD	Half Sat coeff for acidogens	0.78	g/m ³
	KS_AM	Half Sat coeff for acetoclastic methanogens	0.013	g/m ³
	KS_BInf_AD_hyd	Half sat coeff for BPO_PS (for sewage organics)	10.124	gCOD/gCOD
	KS_BOrg_AD_hyd	Half sat coeff for BPO (for organics from biomass death)	10.37	gCOD/gCOD
	KS_AO	Half Sat coeff for acetate oxidizing bacteria		g/m ³

KS_HM	Half Sat coeff for hydrogenotrophic methanogens	0.156	g/m3
K_CO2	Rate constant for CO2 exchange in AD	0.1	
K_CO2_eq	equilibrium constant for CO2 liquid - gas phase exchange	1.21E-08	
K_I_H2	Inhibition coefficient for H2 in acidogenesis	1.25	g/m3
K_I_H_AM	H+ inhibition for acetoclastic methanogens	0.00000115	Mol.kg-1
K_I_H_AO	H+ inhibition for acetate oxidizing bacteria	0.00053	Mol.kg-2
K_I_H_HM	H+ inhibition for hydrogenotrophic methanogens	0.00053	Mol.kg-1
TempCoeff	Rate temperature coefficient	0.0667	-
Temperature	System Temperature	35	degC
Tref	Reference temperature for kinetics	35	degC
b_AC	Decay rate constant for Xac	0.015	1/d
b_AD	Decay rate constant for Xad	0.041	1/d
b_AM	Decay rate constant for Xam	0.037	1/d
b_OB	Decay rate constant for Xob	0.037	1/d
b_HM	Decay rate constant for Xhm	0.01	1/d
b_OHO_AD	Decay rate constant for X_OHO in AD	20	1/d
b_PAO_AD	Decay rate constant for X_PAO in AD	20	1/d
kH_F_AD_hyd	Hydrolysis rate constant for FSO	0.5	1/d
kH_PHA_AD_hyd	Hydrolysis rate constant for PHA	5	1/d
kH_PP_AD_hyd	Hydrolysis rate constant for PP	1	1/d
kM_BInf_AD_hyd	Hydrolysis rate constant for BPO_PS	0.14109	1/d
kM_BOrg_AD_hyd	Hydrolysis rate constant for BPO	0.059665	1/d

	kM_fPP_PAO_PHAstor	maximum rate for PP release with anaerobic PHA storage	0.03	1/d
	kdis_cal	Dissolution/ precipitation/ precipitation of calcite	0.5	
	kdis_cap	Dissolution/ precipitation of calcium phosphate	150	
	kdis_mag	Dissolution/ precipitation of magnesite	50	
	kdis_mgkp	Dissolution/ precipitation of K-struvite	100	
	kdis_newb	Dissolution/ precipitation of newberyite	0.05	
	kdis_stru	Dissolution/ precipitation of struvite	300	
	mu_AC	Max specific growth rate for acetogens	1.15	1/d
	mu_AD	Max specific growth rate for acidogens	0.8	1/d
	mu_AM	Max specific growth rate for acetoclastic methanogens	4.39	1/d
	mu_OB	Max specific growth rate for acetate oxidizing bacteria	3.25	1/d
	mu_HM	Max specific growth rate for hydrogenotrophic methanogens	1.2	1/d

Table C.3: Stoichiometric parameters for the proposed model

	f_SU_SF	Inert Fraction in Fermentable Soluble Organics	0	-
Stoichiometric parameters	f_XU_Bio_lysis	Unbiodegradable fraction of biomass that accumulates on lysis with death regeneration model	0.08	-
	ISS_BM	ISS to biomass for OHO and PAO	0.15	g/gCOD
	i_Ca_PP_mol_perP	Molar fraction of Ca/P in polyphosphate	0.0301	
	i_K_PP_mol_perP	Molar fraction of K/P in polyphosphate	0.3308	
	i_Mg_PP_mol_perP	Molar fraction of Mg/P in polyphosphate	0.3045	
	i_H_Org_mol_perC	H/C : organisms	1.4485	dUnit/dUnit
	i_H_SF_mol_perC	H/C : fermentable soluble	1.9836	dUnit/dUnit
	i_H_SU_mol_perC	H/C: unbiodegradable soluble	1.8601	dUnit/dUnit
	i_H_XBInf_mol_perC	H/C: PS biodegradable particulate	2.19	dUnit/dUnit
	i_H_XBOrg_mol_perC	H/C: biodegradable particulate	1.4485	dUnit/dUnit
	i_H_XUInf_mol_perC	H/C: unbiodegradable particulate	1.3372	dUnit/dUnit
	i_H_XUOrg_mol_perC	H/C: endogenous residue	1.4156	dUnit/dUnit
	i_N_Org_mol_perC	N/C : organisms	0.2116	dUnit/dUnit
	i_N_SF_mol_perC	N/C: fermentable soluble	0.0854	dUnit/dUnit
	i_N_SU_mol_perC	N/C: unbiodegradable soluble	0.0629	dUnit/dUnit
	i_N_XBInf_mol_perC	N/C: PS biodegradable particulate	0.06	dUnit/dUnit
	i_N_XBOrg_mol_perC	N/C: biodegradable particulate	0.2116	dUnit/dUnit

i_N_XUInf_mol_perC	N/C: unbiodegradable particulate	0.0916	dUnit/dUnit
i_N_XUOrg_mol_perC	N/C: endogenous residue	0.0677	dUnit/dUnit
i_O_Org_mol_perC	O/C : organisms	0.3808	dUnit/dUnit
i_O_SF_mol_perC	O/C : fermentable soluble	0.6257	dUnit/dUnit
i_O_SU_mol_perC	O/C: unbiodegradable soluble	0.5858	dUnit/dUnit
i_O_XBInf_mol_perC	O/C: PS biodegradable particulate	0.65	dUnit/dUnit
i_O_XBOrg_mol_perC	O/C: biodegradable particulate	0.3808	dUnit/dUnit
i_O_XUInf_mol_perC	O/C: unbiodegradable particulate	0.4528	dUnit/dUnit
i_O_XUOrg_mol_perC	O/C: endogenous residue	0.531	dUnit/dUnit
i_P_Org_mol_perC	P/C : organisms	0.0276	dUnit/dUnit
i_P_SF_mol_perC	P/C: fermentable soluble	0.0091	dUnit/dUnit
i_P_SU_mol_perC	P/C: unbiodegradable soluble	0.0	dUnit/dUnit
i_P_XBInf_mol_perC	P/C: PS biodegradable particulate	0.01	dUnit/dUnit
i_P_XBOrg_mol_perC	P/C: biodegradable particulate	0.0276	dUnit/dUnit
i_P_XUInf_mol_perC	P/C: unbiodegradable particulate	0.0366	dUnit/dUnit
i_P_XUOrg_mol_perC	P/C: endogenous residue	0.0113	dUnit/dUnit
Y_AC	Acetogenesis yield (COD/COD)	0.039714	-
Y_AD	Lo H2 Acetogenesis yield (COD/COD)	0.0895	-
Y_AH	Hi H2 Acetogenesis yield (COD/COD)	0.0895	-
Y_AM	Acetoclastic Methanogenesis yield (COD/COD)	0.03925	-
Y_OB	Acetate Oxidizing Bacteria yield [COD/COD]	0.104	-

	Y_HM	Hydrogenotrophic Methanogenesis yield (COD/COD)	0.04	-
	Y_f_PP_VFA	fraction of P released from PP per VFA used in PHA storage	0.5	
	Y_gly_VFA	Molar ratio of glycogen to acetate used in PHA storage	0.125	

Variables

These refer to components or species which change at every time-step in the simulation. These are classified into various categories within WEST® namely, algebraic variables, derived variables, input variables and output variables.

Derived variables refer to the masses of the components involved. This category contains a segment where the initial masses in the reactor were specified. These initial masses allowed the initial component and species concentrations to be calculated which were then fed into kinetic expressions to determine the component compositions at subsequent time steps (Ghoor, 2020). These initial masses are an important initialization step as their appropriate selection alleviates the model stiffness during simulation runs.

Algebraic variables on the other hand, refer to the component concentrations in the reactor. From the initial masses and the algebraic relationships described in the model editor, the WEST® software computes the components concentrations as well as their respective COD values.

The input and output variables as their names suggest, refer to the components influent and effluent flux values. The influent values may be manually specified however, for this model, they were linked to the municipal wastewater block into which a text file with the influent values expressed as masses calculated in an excel sheet pre-processor

were loaded. The output variables refer to the various component effluent flux values as well as the COD concentrations and the gaseous compositions. Following the completion of a simulation, the variables were exported into an excel file after which they were coded into a post-processor in order to obtain the values as concentrations.